DISSERTATION

THE NUCLEOSOME ASSEMBLY PROTEIN 1: ELUCIDATION OF THE HISTONE BINDING PREFERENCE AND THE MECHANISM OF SELF-ASSOCIATION

Submitted by

Steven J. McBryant

Department of Biochemistry and Molecular Biology

In partial fulfillment of the requirements

for the degree of Doctor of Philosophy

Colorado State University

Fort Collins, Colorado

Summer, 2003

ProQuest Information and Learning Company
300 North Zeeb Road
P.O. Box 1346
Ann Arbor, MI 48106-1346

COLORADO STATE UNIVERSITY

June 20, 2003

WE HEREBY RECOMMEND THAT THE DISSERTATION PREPARED UNDER OUR SUPERVISION BY STEVEN J. MCBRYANT ENTITLED *THE NUCLEOSOME ASSEMBLY PROTEIN 1: ELUCIDATION OF THE HISTONE BINDING PREFERENCE AND THE MECHANISM OF SELF-ASSOCIATION* BE ACCEPTED AS FULFILLING IN PART THE REQUIREMENTS FOR THE DEGREE OF DOCTOR OF PHILOSOPHY.

Committee on Graduate Work

Advisor

Department Head

ABSTRACT OF DISSERTATION

YEAST NUCLEOSOME ASSEMBLY PROTEIN 1: ELUCIDATION OF THE HISTONE BINDING PREFERENCE AND THE MECHANISM OF SELF-ASSOCIATION

The nucleosome assembly protein 1 (NAP1) is a member of the histone chaperone family of proteins, and is thought to function in the deposition of the histone (H2A-H2B) dimer complex onto DNA during chromatin assembly. However, NAP1 is also involved in the nuclear import of (H2A-H2B), the regulation of cell cycle events involving the onset of DNA replication, and the transient disruption of intact nucleosomes that facilitates transcription within a chromatin context.

Though NAP1 is a common laboratory 'tool' used to assemble nucleosomes onto plasmid DNA in order to study chromatin transcription *in vitro*, there remains great uncertainty as to the mechanism with which yeast NAP1 assembles both the $(H3\text{-}H4)_2$ tetramer and the (H2A-H2B) dimer onto plasmid DNA. In this study, direct binding assays and native gel electrophoresis were used to determine that, in contrast to finding in past investigations, yNAP1 shows a clear preference for the tetramer over the dimer. Further, using select deletion mutants of yNAP1 and histones devoid of their N-terminal tails, it was determined that the mechanism for the preference lies in the binding of yNAP1 to the N-terminal tails of histones H3 and H4, but not H2A or H2B. Finally, it was shown that the most acidic portion

of yNAP1, previously shown to be dispensable for chromatin assembly, appears to be a non-specific binding platform for basic proteins.

Native gel electrophoresis of yNAP1 revealed more than one band, thus it was hypothesized that yNAP1 self-associates. The self-association of yNAP1 was studied using biochemical, hydrodynamic and thermodynamic methods. yNAP1 was revealed to be an obligate dimer, in that it likely does not exist in the monomeric state at physiological conditions or concentrations. The monomeric form of yNAP1 was only revealed in the presence of moderate levels of denaturant. Further, we observe that yNAP1 oligomerizes into tetramers and hexamers, and this oligomerization is regulated by counteracting the high electrostatic charge on yNAP1 with high ionic strength. The dimerization of yNAP1 likely plays a role in chromatin assembly, as the histone complexes also exhibit a two-fold symmetry.

Steven J. McBryant
Department of Biochemistry
and Molecular Biology
Colorado State University
Fort Collins, CO 80523
Summer, 2003

ACKNOWLEDGEMENTS

This will likely be the longest section of my dissertation, as my graduate research has been unique for its high level of collaboration, and thus expressing my appreciation to those who have contributed will require considerable space.

I would like to thank Dr. Karolyn Luger for stepping in as my advisor and for her continual interest in my research. Her work ethic served an excellent example for my own. She accepted my mistakes and helped me to be a better scientist and collaborator.

I would also like to thank Dr. Norm Curthoys, Dr. Paul Laybourn, Dr. Olve Peersen, and Dr. Carol Blair for serving on my graduate committee. Each of these individuals invested significant time and effort towards the success of my research and graduate career, and their dedication to graduate research is commendable.

Specifically, I would like to thank Dr. Laybourn for his intellectual input; his knowledge of the literature and willingness to discuss the details of methods and hypotheses was instrumental in my success. I also would like to thank Dr. Curthoys for standing by me when I struggled, made mistakes, and needed counsel. He truly epitomizes the adage of walking softly and carrying a big stick. The department is fortunate to have him as its leader and ambassador. I appreciate that Dr. Blair was willing to step out of her element and open herself up to new ideas, and always managed to contribute despite our (regrettably) limited interaction. Additionally, I would like to thank Dr. Peersen,

as together we unraveled the mysteries of the XL-I, and came to recognize its power and promise. Though his interests lie elsewhere, Dr. Peersen recognized the benefits of a broad scientific approach and diverse methodologies. His friendship and comradery and mentorship will serve as a model for me in my scientific and personal future. I would be remiss if I did not acknowledge the contribution of Dr. Robert Woody. He was always willing to discuss the acquisition and interpretation of results, and to pull a weathered, though useful, text from his library in order to enlighten me.

I would also like to acknowledge my 'first' advisor, Dr. Jennifer Nyborg. Though our scientific interests were not always shared, she continued to offer support and counsel on all things science and not. Her dedication to research and teaching, her "new model' way of thinking, and her humor in the face of challenges will continue to influence my future.

I have been fortunate to work with a great number of very talented young scientists during my graduate career. I hope I have absorbed some traits that have allowed all of them to excel, and wish them great success in their scientific endeavors.

Finally, I would like to express my gratitude to my friends and my family, who have supported me in spite of the cost in shared time and experiences. My mother Pat and my father Don have encouraged and supported me, and have always set a good example upon which to model my work ethic and to develop my personal and professional relationships. I hope that for them I have 'initialed my work with excellence'.

Table of Contents

Chapter 1

Chromatin Assembly background

1.1 Chromatin:

The integrity of the genome is of utmost importance to every organism. It is from this template that all of the structures and functions of the organism arise. It is of particular importance to the eukaryotes, as their physiologic complexity has mandated a large and complex genome. The eukaryotic genetic material is nearly two meters in length and must be significantly compacted in order to be accommodated within the nucleus, a structure of only a few micrometers in diameter. The compaction, protection and accessibility of the genetic material are governed by its incorporation into a nucleoprotein complex known as chromatin (for review see Wolffe, A. *Chromatin: structure and function*, 3rd edition, 1998). It is through the regulation imposed by chromatin that the level of complexity inherent to all eukaryotes is realized. Conversely, the manner in which the genetic material is packaged mandates further complexity by the organism in order to organize and access the genome. A better understanding of the structure and manner in which chromatin is assembled and maintained is necessary so that we can, in turn, better understand the impact of chromatin on the eukaryotic lifecycle.

There is tremendous complexity with regard to the incorporation of the genetic material into chromatin. While the initial model for the modular nature of chromatin structure was proposed almost 30 years ago (Kornberg and Thomas, 1974), only recently has the first level of its complexity been revealed in detail (Luger *et al*, 1997a). Subsequent to this revelation we have begun to pursue the higher-order complexities of chromatin. The fundamental unit of chromatin, the nucleosome, is an assembly of equal masses of deoxy-ribonucleic acid (DNA) and histone proteins (Finch *et al.*, 1977; Richmond *et al.*, 1984). It is upon these fundamental subunits that chromatin and chromosomes are built. These subunits are strung together like beads on a string, with variable lengths of 'linker' DNA between each nucleosome. Linker histones (e.g. H1 and H5), which are structurally dissimilar to the core histones, bind to the intervening linker DNA and make contacts with the nucleosomes. These interactions facilitate higher order chromatin folding and compaction (For review see van Holde, K.E., in *Chromatin,* 1989).

Many models have been proposed and defended regarding how the nucleosomes are arranged beyond the individual subunits (for review see Hansen, 2002; Widom, 1989; Woodcock and Dimitrov, 2001). It is clear that higher order chromatin structure involves inter-nucleosomal contacts, likely mediated by protein-protein contacts between adjacent (and possibly distant) nucleosomes (Carruthers *et al.*, 2000; Dorigo *et al.*, 2003; Krajewski and Ausio, 1996; Luger and Richmond, 1998b).

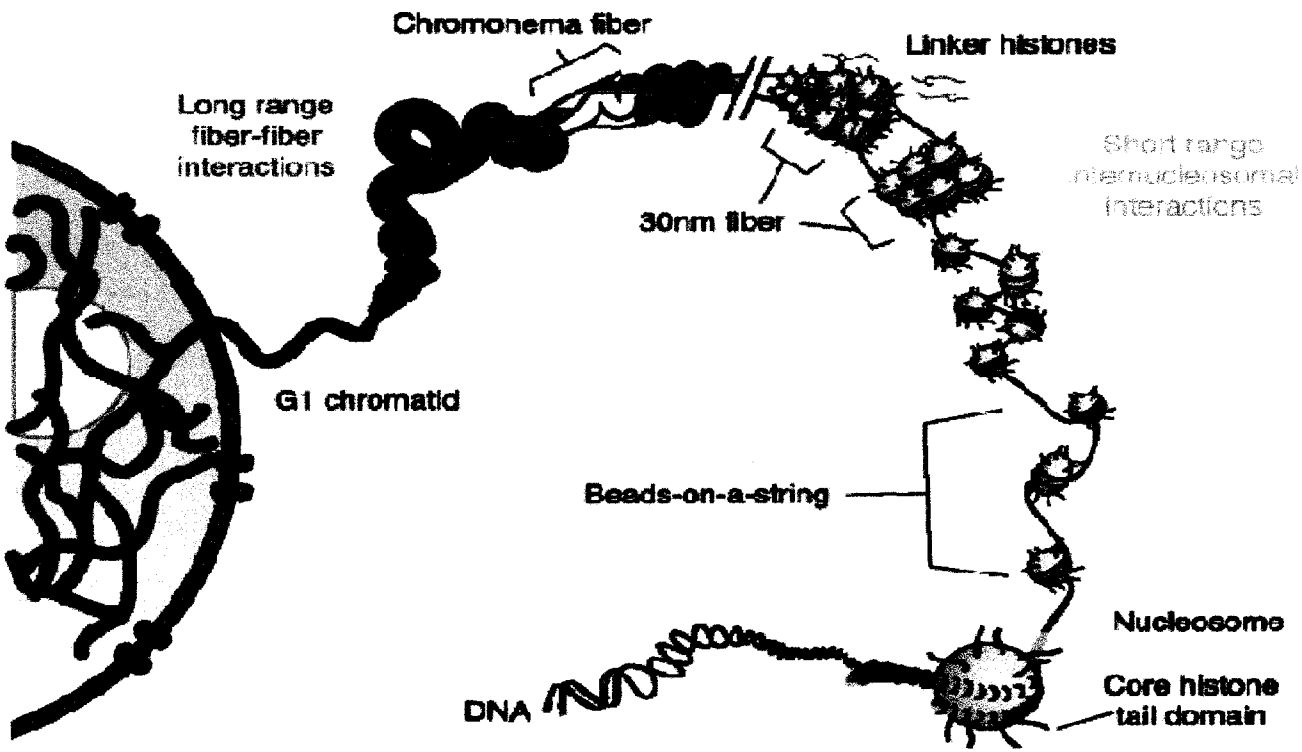

Figure 1.1: The levels of organization of interphase eukaryotic chromatin. The DNA genetic material is wrapped around an octamer of core histones to form the nucleosome. Many nucleosomes and their intervening 'linker' DNA resemble beads on a string. The incorporation of linker histones and inter-nucleosomal contacts mediated by histone tails leads to the 30 nm fiber. Inter-fiber contacts, mediated by the histone tails and accessory proteins, lead to chromonema fibers. Figure reproduced from Horn and Peterson, *Science*, 2002.

Above this level, compaction likely involves components of the nuclear matrix, nuclear membrane and aspects of nuclear compartmentalization (Stein *et al.*, 1999). Further analysis herein will be limited to the architecture and dynamics of the fundamental subunit, the nucleosome. A model of the levels of compaction of eukaryotic chromatin is shown in Figure 1.1.

1.2 The nucleosome and its components:

At the first level of complexity, approximately 146 base pairs (bp) of DNA are wrapped in 1.65 super-helical turns around a core of eight proteins, the core histone octamer (Richmond *et al.*, 1984; Arents *et al.*, 1991; Luger *et al.*, 1997a; White *et al.*, 2001), to form the 'core particle'. This disk-shaped assembly is approximately 42 nm in diameter and 30 nm in width. Though little sequence similarity exists between the four core histone proteins (Sullivan *et al.*, 2002), an extremely high level of structural homology has led the histone protein components to be recognized as some of the most structurally invariant known (DeLange, 1979). Further, primary sequence alignments indicate a common ancestral origin for the archaeal and eukaryotic histones (Grayling *et al.*, 1996).

The histone octamer is composed of two each of the four core histones, H2A, H2B, H3 and H4 (Arents *et al.*, 1991). These small, highly basic proteins are themselves pre-associated into complexes. H2A and H2B form the (H2A-H2B) dimer (Kelley, 1973), while H3 and H4 form a dimer of dimers to yield the $(H3\text{-}H4)_2$ tetramer (Kornberg and Thomas, 1974; Roark *et al.*, 1974). The association of two (H3-H4) dimers is through the formation of a four-helix

bundle composed of the C-terminal helix-strand-helix motifs of two H3 molecules (Arents *et al.*, 1991; Luger *et al.*, 1997a). Thus, the histone octamer is composed of one $(H3\text{-}H4)_2$ tetramer and two (H2A-H2B) dimers. These associations are dependent on the secondary structure of the histones. Each histone molecule is modular in nature, composed of a short (30-50 amino acid) amino-terminal (NH_3-terminal, or simply N-terminal) region (the histone 'tail'), and a highly conserved, α-helical region which forms the canonical 'histone fold' motif (Baxevanis *et al.*, 1995). This motif is composed of two short and one long α-helix, with a loop structure between adjacent helices. The similarity of the histone fold motifs is underscored by rms deviations of only ~1.5 to 2.5 Å among the four polypeptides (Arents and Moudrianakis, 1995). Histone pairs (either H2A and H2B or H3 and H4) associate through intermolecular interactions governed by the long helix, thus forming what is known as the histone 'handshake' conformation, with the two histone components associating in a head to tail fashion. Figure 1.2A illustrates the structural nature of the (H2A-H2B) and (H3-H4) dimers.

Importantly, these histone pairs might be deemed 'obligate' dimers, as the individual histone proteins lack native structure and are thus largely insoluble prior to association (Luger *et al.*, 1997b, Dyer *et al,* 2003, in press). Only upon the formation of a complex with their partner histone do they achieve their native conformation.

Figure 1.2A: Ribbon diagrams of the H2A (yellow) and H2B (red) dimer, and the H3 (blue) and H4 (green) dimer. H2A and H2B associate though intermolecular contacts along the long α-2 helices, as do H3 and H4. The H2B α-C helix and the H3 α-N helix are shown in tan. One half of the (H3-H4)2 tetramer is shown for clarity, and to highlight the remarkable similarity between the two dimers. Figure provided by U.M. Muthurajan.

The overall topologies of the (H2A-H2B) dimer and one-half of the $(H3\text{-}H4)_2$ tetramer are themselves nearly super-imposable, with only slight deviations seen in the loops and helices involved in the H3-H3 interaction (see Figure 1.2B).

The structures of the octamer and nucleosome yield important insight into a likely order of histone incorporation (Arents *et al.*, 1991; Luger *et al.*, 1997a; Richmond *et al.*, 1984; White *et al.*, 2001). The $(H3\text{-}H4)_2$ tetramer occupies the center of the disk-shaped complex, and organizes the central 60 bp of DNA. Basic amino acid side-chains (arginine and lysine) make favorable electrostatic contacts with the negatively charged phosphate backbone through the minor groove of the DNA double helix. Contacts between the surface of the DNA and the histones are regular, occurring every 10 bp as the inner surface of the minor groove reveals itself to the histones (Luger *et al.*, 1997a). Additional hydrogen bonding with the DNA phosphates and non-polar contacts with the deoxyribose groups are also present (for an overview of DNA-histone contacts see Luger and Richmond, 1998a; Richmond and Davey, 2003). The two (H2A-H2B) dimers make contacts with opposite faces of the central tetramer, and organize 30 bp of DNA on either side of the tetramer. Again, electrostatic attractions between basic side chains and the phosphate backbone are important (for an overview of the histone protein components within the nucleosome see Luger and Richmond, 1998b).

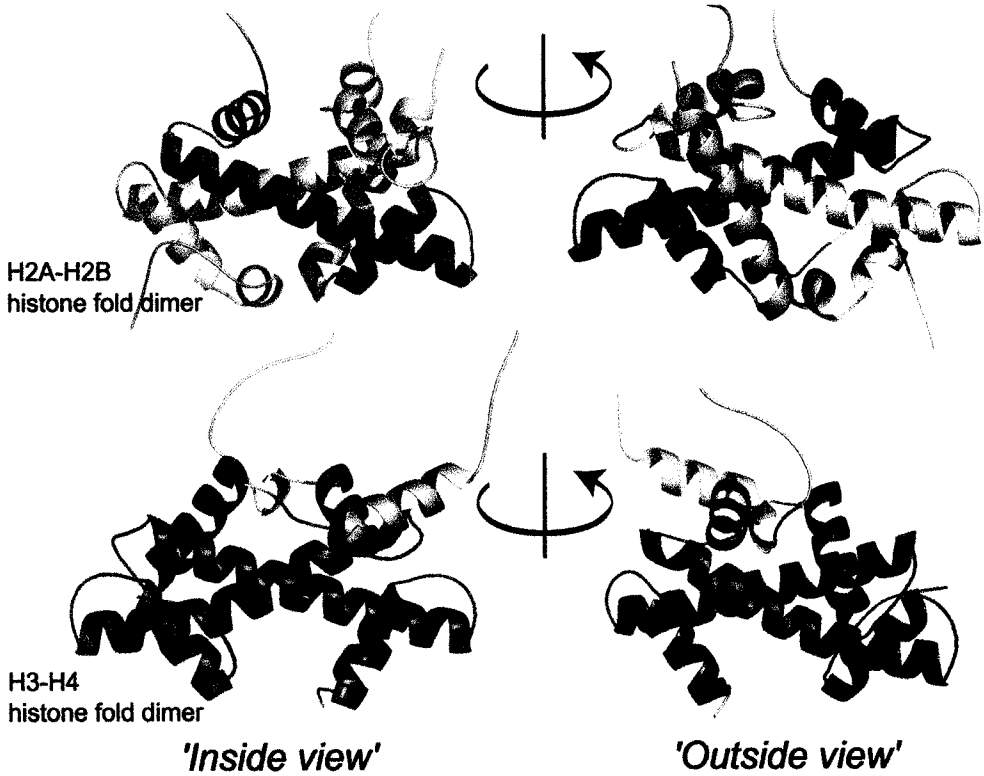

Figure 1.2B: The histone pairs are remarkably conserved and each expose 2 nearly identical faces. Ribbon diagrams of the H2A (yellow) and H2B (red) dimer, and the H3 (blue) and H4 (green) dimer. H2A and H2B associate though intermolecular contacts along the long α-2 helices, as do H3 and H4. The H2B α-C helix and the H3 α-N helix are shown in tan. One half of the (H3-H4)2 tetramer is shown for clarity, and to highlight the remarkable similarity between the two histone dimers. Figure provided by U.M. Muthurajan.

Thus, the central placement of the tetramer mandates its deposition prior to that of the two dimers. Consistent with this, in living cells the $(H3\text{-}H4)_2$ / DNA tetrasome is very stable: following DNA replication about 80% of the incorporated tetramer remains bound permanently (Kimura and Cook, 2001). This is in contrast to (H2A-H2B), where 3% exchanges rapidly (minutes), while 40% exchanges more slowly, (1-4 hours). The mechanism by which this exchange might occur will be addressed below.

The bending of the DNA into a super-helix imparts substantial strain onto the double helix, and the dimensions of both the major and minor grooves are significantly distorted (Luger *et al.*, 1997a). The entropic penalty for this strained conformation is compensated for by the enthalpic contributions of the electrostatic attractions and satisfied hydrogen bond potentials (see Luger and Richmond, 1998a; Muthurajan *et al.*, 2003; Richmond and Davey, 2003). Figure 1.2C illustrates the symmetry and complexity of the nucleosome core particle.

While the α-helical portions of the histones are engaged in both histone-histone interactions and histone-DNA interactions, the unstructured N-terminal histone tails (~28 % of the mass of the histones) protrude through the minor grooves of the nucleosome (Luger *et al.*, 1997a; Luger and Richmond, 1998b). The eight histone N-terminal tails were too disordered to be detected in the electron density maps of the nucleosome crystals (Luger *et al.*, 1997a), as well as those from the histone octamer (Arents *et al.*, 1991).

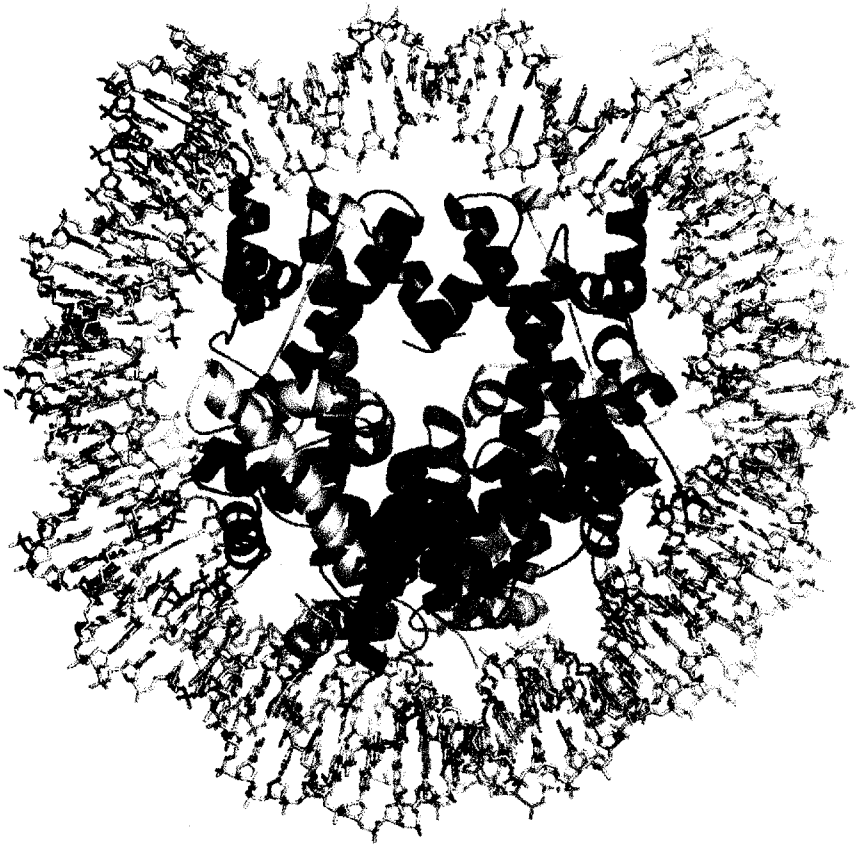

Figure 1.2C: The structure of the nucleosome core particle. Viewed from one face of the disc-shaped core particle, one can easily see the exposed face of the nearest (H2A-H2B) dimer (yellow and red), the exposed faces of the two (H3-H4) dimers (blue and green) on this side of the disc (two similar faces are exposed on the opposite side), the close proximity of the two α-3 helices leading to dimerization of the two (H3-H4) dimers, and the projection of the N-terminal tails outward away from the nucleosome core. Figure provided by U.M. Mutharajan.

Additionally, they were shown by NMR spectroscopy to be unstructured in solution (Smith and Rill, 1989). Further, work from the Moudriankis laboratory (Karantza *et al.*, 1996) showed that removal of the N-terminal tails does not affect the stability of the histone octamer. Thus it appears unlikely that the N-terminal tails contribute to the stability of the octamer or the nucleosome (Luger *et al.*, 1997b). However, it is generally accepted that the tails do play some role in higher chromatin folding and stability (Carruthers *et al.*, 2000; Dorigo *et al.*, 2003; Krajewski and Ausio, 1996). For review see Horn and Peterson, 2002.

Interestingly, an extensively hydrogen-bonded inter-nucleosomal crystal contact was observed between amino acids 16-24 of histone H4 and an acidic region formed by H2A and H2B on the surface of the octamer (Luger *et al.*, 1997a). Further, the basic regions of the N-terminal tails have been shown to bind weakly to the DNA on the outside of the nucleosome (Lee and Hayes, 1997). This contact, unlike the crystal contact, is weak and highly mobile, and thus likely contributes little to nucleosome stability. It is clear, nonetheless, that the most significant role for the N-terminal histone tails is in the regulation of compaction of the next level of chromatin compaction, the inter-nucleosomal contacts that regulate the accessibility of the underlying DNA.

1.3 The N-terminal histone tails:

The importance of the N-terminal tails is likely manifested at the next level (s) of chromatin organization. While deletion of the N-terminal tail of any

single core histone has no affect on viability or growth, deletion of H2A and H2B, or H3 and H4 is lethal (reviewed in Annunziato and Hansen, 2000). Removal of the H3 and H4 N-terminal tails by proteolysis led to alterations in the conformation of the next higher-order structure of chromatin, the 30 nm fiber (Krajewski and Ausio, 1996). As described above, the crystal structure of the nucleosome core particle revealed a contact between an H4 tail from one nucleosome and an (H2A-H2B) dimer on the face of an adjacent nucleosome (Luger *et al.*, 1997a). Whether such contacts are valid *in vivo* is unknown. However, taken together these data allude to the importance of the histone tails towards nucleosome connectivities. The advent of recombinant histones with deleted N-terminal tails ('tailless' histones, Bohm and Crane-Robinson, 1984), select and wholesale point mutations, as well as 'tail swapping' experiments (see for example, Ling *et al.*, 1996; Recht and Osley, 1999; Schuster *et al.*, 1986), and the ability to reconstitute octamers, nucleosomes and nucleosomal arrays with partially and fully tailless histones (An *et al.*, 2002; Georges *et al.*, 2002) has facilitated the exploration of the function of the tails. Currently, the role of the N-terminal tails in regulating chromatin higher-order folding and chromatin accessibility is a very exciting and fast-growing field for both structural and molecular biologists.

Undeniably, the N-terminal histone tails are the business end of chromatin accessibility and regulation. While most of the histone-fold-containing portions of the histone octamer are contained within the boundaries of the mono-nucleosome, and perhaps more so in nucleosome arrays, the N-terminal tails

seemed to be available and poised to carry out the accessibility and, therefore, the regulation and expression of the genetic material. Two non-mutually exclusive hypotheses exist for the role of these tails in controlling the accessibility of the underlying DNA. The N-terminal tails are thought to regulate changes in the structure or composition of the nucleosome or chromatin fiber, and/or to modulate the interaction between the nucleosomal histones and regulatory factors (for review see Grunstein, 1997; Hartzog and Winston, 1997; Wolffe, 1998). A substantial body of evidence is being compiled for both hypotheses, thus it is likely that both play a role in nucleosome dynamics.

The N-terminal histone tails are the substrates for a vast array of amino acid-modifying enzymes, and these modifications are vital to the regulation of chromatin structure and its' accessibility. Common modifications of the nucleosomal histones include acetylation, phosphorylation, ubiquitinylation, glycosylation and methylation. Numerous recent reviews on the topic are available (Cheung *et al.*, 2000; Davie, 1998; Iizuka and Smith, 2003; Lorch *et al.*, 1999). A continuing stream of research articles have sought to deduce the elusive 'histone code' (Jenuwein and Allis, 2001; Strahl and Allis, 2000), that is, the particular set of modifications (stimulus) that will enact a specific response (an increase or decrease in accessibility) from the underlying DNA. However, though numerous examples of such a stimulus-response effect have been uncovered for specific genes (see for example, Bauer *et al.*, 2002; Lachner *et al.*, 2001; Litt *et al.*, 2001a; Rundlett *et al.*, 1998), the universality

of the 'code' between different genetic loci has not been established. It may be that, while histone modifications occur to regulate the output from each specific genetic template, each gene will respond differently to the cumulative effect of the modifications present therein. The number of different types of modifications that occur, in addition to the large number of available, readily modifiable amino acids present in each nucleosome, leads to a level of complexity which reflects the complexity of the eukaryotic genome itself. Thus the failure to establish an absolute 'code' for these modifications may simply reflect a level of complexity which will require significant computational power to correlate. Such an analysis will require many more specific examples of the stimulus-response type.

However, a significant body of evidence exists such that for at least one such modification, lysine acetylation, a simple conclusion can be drawn regarding its effect. (see for example, Ausio and van Holde, 1986; Grunstein, 1997; Kuo *et al.*, 1998; Litt *et al.*, 2001b; Oliva *et al.*, 1990). The basic side chain of lysine within a nucleosome will exhibit attractive electrostatic interactions with the surrounding DNA. Acetylation of the side chain ε-amino group will neutralize the positive charge present, thus partially ameliorating the attractive interaction with the DNA. Research has shown that hyper-acetylation of $(H3\text{-}H4)_2$ leads to a tetramer which prefers a more relaxed DNA, and thus may adopt a more open structure upon inclusion in the nucleosome (Morales and Richard-Foy, 2000). Further, a study on the isolated, acetylated histone tail of H4 has detected increases in the helical

content relative to the unmodified tail (Wang *et al.*, 2000). This same report determined that the α-helical content was increased for acetylated histones within the octamer and the nucleosome core particle as well, consistent with early studies (Prevelige and Fasman, 1987). Thus, at least for this particular modification, there appears to be a plurality to the effect. Lysine acetylation may simultaneously limit electrostatic interactions with the DNA and facilitate a conformational change in the histones and/or nucleosome, which alters DNA accessibility. Readers interested in the role of acetylation in chromatin dynamics are directed to a number of excellent reviews (Kingston and Narlikar, 1999; Kouzarides, 2000; Roth *et al.*, 2001)

The N-terminal histone tails also serve as protein-protein docking sites for a number of regulatory proteins. The karyopherin family of proteins utilize a putative nuclear localization sequence on the N-terminal tails of H2A and H2B to shuttle these histones through the nuclear pore complex into the nucleoplasm (Mosammaparast *et al.*, 2001). Similar sequence can be found in the tails of H3 and H4 (Baake *et al.*, 2001), though the chaperone for transport has not yet been identified. The N-terminal tails of H3 and H4 are required docking sites for the yeast proteins SIR3 and SIR4 (Hecht *et al.*, 1995). This association leads to the formation of a heterochromatic, or repressed, transcriptional state, through decreases in DNA accessibility due to reorganization of the canonical chromatin fiber into specialized higher-order structures (Georgel *et al.*, 2001). Thus, though likely not intimately involved in the structure or stability within the nucleosome itself, the N-terminal tails are

available to accessory proteins for transport of the histones and for contributing to the establishment of specific chromatin structural states.

1.4 Replication-independent and -dependent chromatin assembly:

Profound changes in chromatin structure and organization must take place during each S-phase of the cell cycle. During this period, the anti-parallel double helix must unwind to allow passage of the DNA replication machinery (interested readers should consult one of the many available textbooks, for example, Lewin, B., *GENES IV*, 1997). The passage of the DNA polymerase is concomitant with the removal of the histone octamer from the DNA strands, thus the chromatin must be re-assembled following replication. The vast majority of the bulk chromatin doubles as the DNA is replicated, in a process known as replication-dependent chromatin assembly (Verreault, 2000). However, due to the loss of histone sub-complexes during DNA transcription and DNA repair pathways, nucleosomes must be re-assembled during the resting portions of the cell-cycle as well. This process, replication-independent chromatin assembly, is thought to be important for the deposition of histone variants, a subset of isoforms of the core histones thought to establish specific chromatin domains. For example, two isoforms of histone H3 (H3.3 and Cid) have been shown to be targeted to active genes and centromeric regions, respectively. Only a small fraction of the bulk-assembled chromatin contains these variants, thus their deposition occurs throughout the cell cycle, independent of DNA replication (for review see Ahmad and Henikoff, 2002).

Following passage of the DNA replication machinery, the re-assembly of bulk chromatin is achieved through two distinct mechanisms (for review see Krude and Keller, 2001; Tyler, 2002). Histones can be recycled by direct transfer from the parental strand to the new daughter strands. However, this can only provide for the assembly of one-half of the replicated DNA into chromatin. Additionally, *de novo* chromatin assembly is required to complete the restoration of the chromatin state. This activity requires a set of chromatin assembly factors to chaperone the histone components to the DNA and deposit them in an ordered and regulated fashion.

Interestingly, for many decades chromatin assembly for biophysical and biochemical studies was performed by the method of 'salt deposition' (Richmond *et al.*, 1988; Stein, 1989; Thomas and Butler, 1977). Here, the histones and DNA are mixed at high ionic strength in order to neutralize the large number of charged groups on the DNA (negative) and histone side chains (positive). The salt is then slowly dialyzed away, during which time the tetramer and the dimers are deposited in a uniform manner upon the DNA (either a linear fragment of greater than 146 bp, or a circular (supercoiled or relaxed) plasmid). However, the past 25 years have led to the cloning and characterization of a number of chromatin assembly factors, allowing for a more physiological assembly of histones onto a variety of DNA templates (for review see Krude and Keller, 2001; Philpott *et al.*, 2000; Tyler, 2002; Verreault, 2000). The elucidation of these factors has facilitated our

understanding of the steps required for replication-coupled and *de novo* chromatin assembly.

As described above, the central placement of the $(H3\text{-}H4)_2$ tetramer within the nucleosome mandates its deposition prior to the two (H2A-H2B) dimers. The H3 and H4 N-terminal tails acquire a set of replication–coupled lysine acetylations, at positions 14 on H3, 5 and 12 on H4 (Kaufman *et al.*, 1995; Verreault *et al.*, 1996). At least one of these acetylations (H4 lysine 12) is due to the activity of the major cytoplasmic yeast histone acetyltransferase, HAT1 (Parthun *et al.*, 1996). Having been marked by these modifications as replication-specific histones, $(H3\text{-}H4)_2$ is rapidly deposited behind the DNA replication fork. Subsequently, a histone dimer is deposited on either side of the tetramer/DNA assembly. See Figure 1.3 for a schematic of replication-dependent chromatin assembly.

Interestingly, many assembly factors are capable of the *in vitro* assembly of nucleosomes onto double-stranded DNA in the absence of DNA synthesis. *In vitro* chromatin assembly allows for rapid formation of 'chromatinized' DNA templates, a valuable tool for studying DNA templates in a more physiological context. This has allowed researchers to gain greater insight into the mechanisms involved in the activation of transcription by cellular and viral activators, the reorganization of chromatin due to the activity of chromatin modifying enzymes, and the mechanism of action of ATP-dependent chromatin remodeling complexes (Cheung *et al.*, 2000; Davie, 1998; Iizuka and Smith, 2003; Lorch *et al.*, 1999; Urnov and Wolffe, 2001).

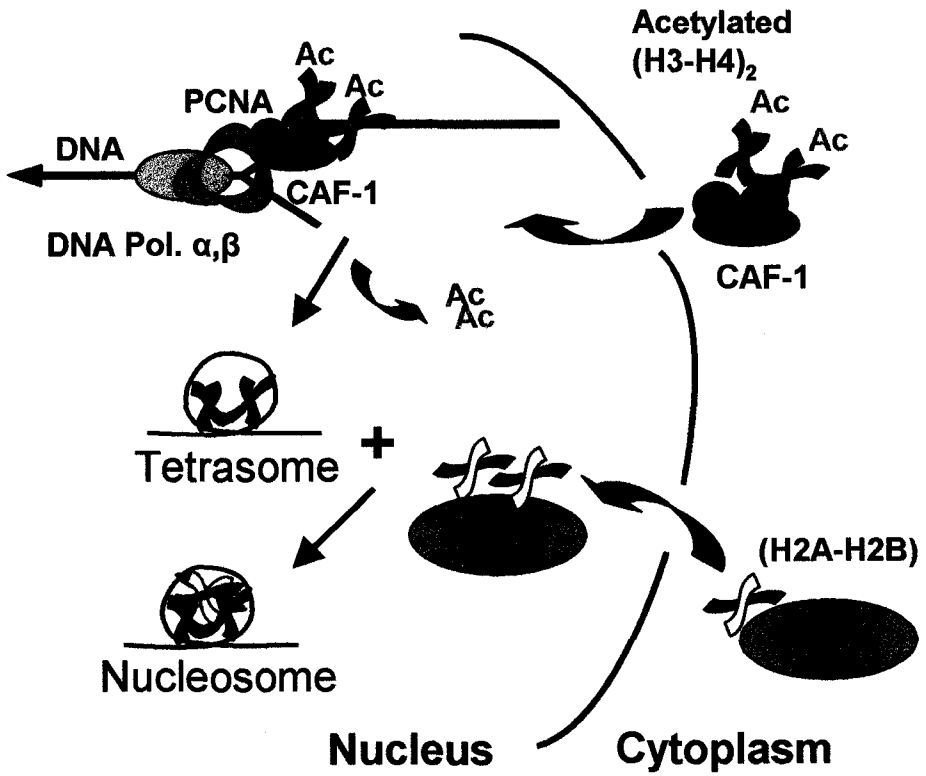

Figure 1.3: Mechanism of DNA-replication dependent chromatin assembly. Following passage of the DNA polymerase, the CAF-1/**Ac**etylated (H3-H4)2 complex is associated with PCNA. The formation of the tetrasome requires the loss of the replication-specific acetylations. The NAP1/(H2A-H2B) complex enters the nucleus and completes the assembly by depositing a dimer on either side of the central tetramer.

Further, this has also allowed for the elucidation of the functional properties of the protein factors involved in chromatin assembly and thus a better understanding of the process *in vivo*.

1.5 Chromatin assembly factors:

The *in vivo* chromatin assembly factor responsible for $(H3\text{-}H4)_2$ deposition, CAF-1, has been shown to trigger nucleosome assembly onto replicating DNA (Smith and Stillman, 1989). CAF-1 is composed of three different subunits (p150, p60, p48), each of which can bind the $(H3\text{-}H4)_2$ tetramer. Interestingly, despite the uniform lysine acetylations on the H3 and H4 tails, these regions are not required for CAF-1 binding (Shibahara *et al.*, 2000). CAF-1 forms a tripartite complex with $(H3\text{-}H4)_2$ and PCNA, a component of the DNA replication machinery which forms a clamp around the DNA (Moggs *et al.*, 2000; Shibahara and Stillman, 1999). Thus, CAF-1 is targeted directly to the site of DNA replication through this interaction. A conserved structural motif within CAF-1 (the WD repeat) has been shown to be required for the interaction with a nuclear histone deacetylase, HDAC-2 (Ahmad *et al.*, 1999). The rapid loss of the replication-specific acetylation following $(H3\text{-}H4)_2$ deposition is consistent with this observation (Tyler, 2002). Yeast cells devoid of CAF-1 are viable, and produce orderly chromatin in their nuclei, though some genetic and functional defects are seen (Kaufman *et al.*, 1997).
An additional factor, RCAF (replication coupled assembly factor) acts synergistically with CAF-1 (Tyler *et al.*, 1999). This factor consists of acetylated histones H3 and H4 (lysines 5 and 12 on H4, lysine 14 on H3) and

the yeast anti-silencing function 1 protein, ASF-1. The cooperative function of these two factors has been investigated by mutation of p150 and ASF-1, which indicated separate but coordinated functions (Tyler *et al.*, 1999).

The above observation indicates that CAF-1 is not the only factor that can deposit histones onto replicating DNA. However, the importance of CAF-1 activity is underscored by a recent investigation. Using a dominant negative form of CAF-1 (an N-terminal deletion of p150 which sequesters limiting p60 from functional complexes), a link between CAF-1 mediated chromatin assembly at the replication fork and DNA damage-induced S-phase arrest was revealed (Ye *et al.*, 2003). The authors conclude that in the absence of rapid histone deposition and nucleosome formation at the replication fork the newly replicated DNA is particularly sensitive to DNA damage.

It is important to note here that replication-coupled chromatin assembly involves targeting of CAF1 to the DNA replication machinery through a specific interaction with PCNA. While it appears likely that an interaction with CAF1 (or a similar factor) is required for replication-independent histone deposition, the mechanism for targeting has not yet been elucidated. However, it is thought that the 'open' conformation of actively transcribed genes leads to preferential inclusion of H3.3, or that there is a replication specific chromatin assembly factor which is capable of discriminating between the very similar H3 and H3.3 isoforms. Alternatively, the 'active' or 'repressed' nature of specific chromatin regions is highly heritable, thus direct targeting of specific histone isoforms may be a result of nuclear

compartmentalization of these chromatin regions. Sequestration of replication-dependent isoforms from these regions would halt their incorporation, thus maintaining the accessibility state of these specific domains (for a discussion of these possibilities, see Ahmad and Henikoff, 2002).

1.6 The histone chaperones:

Following $(H3\text{-}H4)_2$ deposition and de-acetylation, the subsequent deposition of (H2A-H2B) requires an additional chaperone, likely fulfilled by the nucleosome assembly protein (NAP).

The NAP family of histone chaperones is one of the members of a group of protein factors which function in the localization of histones to the nucleus and the deposition of histones onto DNA (Akey and Luger, 2003; Philpott *et al.*, 2000). The three families are composed of nucleoplasmin and the nucleoplasmin-like factors (NLP's), N1 and N2, and the NAP family. Perhaps the best studied of this group is the *Xenopus* factor nucleoplasmin and its homologs. First identified as a nucleosome assembly factor 25 years ago (Laskey *et al.*, 1978), nucleoplasmin (Np) has been described as the archetypal molecular chaperone (Dingwall and Laskey, 1990). Together with the H3 and H4 storage proteins N1 and N2 (Kleinschmidt *et al.*, 1986), these most abundant proteins in the *Xenopus* oocyte nuclei (Mills *et al.*, 1980) are able to store the large amounts of histones present in the frog embryo. Similarly, Np and N1/N2 function together to assemble nucleosomes, both in the absence or presence of DNA replication, onto double stranded DNA

(Dilworth *et al.*, 1987; Kleinschmidt *et al.*, 1990). However, Np and N1 can function autonomously to mediate nucleosome assembly (Cotten and Chalkley, 1987; Laskey *et al.*, 1978; Zucker and Worcel, 1990). Np is a highly acidic protein (pI = 5) of 200 amino acids, where ~ 30% are aspartic and glutamic acid (Dingwall *et al.*, 1987; Earnshaw *et al.*, 1980). The Np monomer self-assembles into a pentamer (Earnshaw *et al.*, 1980), yet crystallizes as a decamer (Dutta *et al.*, 2001). Oligomerization appears to be important for the histone binding and assembly functions (Akey and Luger, 2003; Dutta *et al.*, 2001). Though deemed an (H2A-H2B)-specific chaperone, Np also binds $(H3\text{-}H4)_2$ in apparently equal stoichiometric amounts, and appears to be able to form a pseudo-octamer on the pentamer's distal surface (Dutta *et al.*, 2001). Only the N-terminal acidic tract is required for chromatin assembly, while the two C-terminal and largest of the acidic tracts are dispensable for histone binding, though they are thought to contribute to the stability of Np-histone complexes *in vivo* (Dutta *et al.*, 2001).

The structure-function relationships for Np appear to be similar to those of the Drosophila Np-like protein, dNLP (Ito *et al.*, 1996b). The primary structure of this 152 amino acid polypeptide is 31 % identical to Np, and like Np, has a C-terminal acidic stretch thought to be important for histone binding. Interestingly, despite its high similarity to Np, dNLP requires an additional factor, CAF-1 (see above), to assemble histones into chromatin (Ito *et al.*, 1996a). Like Np, dNLP can bind all four core histones. A recent X-ray crystallographic structure determination of dNLP (Namboodiri *et al.*, 2003)

shows that dNLP is also pentameric, and shows only subtle differences in overall topology compared to Np. The thermostability of the Np/dNLP family is of particular interest, in that the histone binding may require some favorable flexibility or 'conformational plasticity' (Akey and Luger, 2003).

1.7 The nucleosome assembly protein (NAP):

Nearly twenty years ago, a factor capable of the *in vitro* assembly of nucleosomes was reported in human Hela cells (Ishimi *et al.*, 1983). This factor, NAP1, has since been cloned from yeast (Ishimi and Kikuchi, 1991), human (Ishimi *et al.*, 1984; Simon *et al.*, 1994), *Drosophila* (Ito *et al.*, 1996a) soybeans (Yoon *et al.*, 1995), *Paramecium* (Nishiyama *et al.*, 2001), and many other eukaryotes, both plant and animal. The presence of various isoforms of NAP1 in humans (NAP2, Hu *et al.*, 1996; Rodriguez *et al.*, 1997), which appear to function similarly, indicates the presence of several proteins with overlapping functions. Like the $(H3\text{-}H4)_2$ chaperone CAF-1, no gross abnormalities are seen upon *nap*1 gene disruption in yeast. Though *nap*1 knockouts are viable, cell cycle delays, cell morphological changes, and a failure to switch from polar to isotropic bud growth phenotype have been noted (Stanford University *S. cerevisiae* database). However, a targeted knockout of the *Drosophila* Nap1 gene caused embryonic lethality and poorly viable adult escapees, whose offspring were non-viable (Lankenau *et al.*, 2003). Thus, the necessity for this factor may vary depending on the presence or absence of homologs or redundancies in the components of the assembly pathway in different species.

Investigations into NAP1 function have mainly utilized the human, *Drosophila*, and yeast factors. Though some inter-species differences in function likely exist, because of their high level of sequence homology these will be considered as functionally homologous herein, unless specified otherwise.

1.8 NAP1 structural features:

The NAP1 protein is extremely well conserved throughout eukaryotes. Considering the coordinates of the yeast homolog, the conservation is remarkable throughout most of the protein, with the exception of the N-terminus, extending to amino acid 70, which is more divergent between species. Interestingly, the N-terminus has been shown to be dispensable for *in vitro* chromatin assembly by yeast NAP1 (yNAP1) (Fujii-Nakata *et al.*, 1992). Secondary structure predictions suggest nearly equivalent amounts of both α-helical and β-sheet regions interspersed throughout the polypeptide. The most conserved region of the protein, amino acids 310-319 (in the yeast homolog), contains four phenylalanine residues and four polar or charged side chains sandwiched between two proline residues at positions 308 and 318. This region is predicted to be a β-sheet or an unstructured domain. However, the high level of conservation, the flanking prolines, the hydrophobic nature of the phenylalanines, and the hydrophilic nature of the other side chains leads one to speculate as to an exposed domain with a significant structural/functional role.

Particularly notable is the presence of 4 highly acidic regions dispersed throughout the primary sequence. Remarkably, 20-25 % (depending on the species) of the amino acids are aspartic and glutamic acids. Though likely to be important in the binding of the basic histone proteins, a direct role for these specific regions has yet to be established. Interestingly, in the yeast homolog the most prominent of the acidic regions, located near the N-terminus (amino acids 366-403, where 28 of 38 consecutive residues are acidic) is dispensable for chromatin assembly (Fujii-Nakata *et al.*, 1992). Overall, the clear similarity in the organization of the acidic regions and the two conserved regions implies an important structural/functional role for the C-terminal region. See Figures 1.4A and B for alignments of NAP1 from a variety of eukaryotes.

1.9 NAP sub-cellular localization:

The first of the NAP1 proteins to be detected (human AP-1) was determined to be largely localized to the nucleus of Hela cells (Ishimi *et al.*, 1985). A subsequent study in yeast determined localization to be primarily cytoplasmic, though high background cytoplasm staining made interpretation difficult (Kellogg and Murray, 1995a). A very thorough analysis in *Drosophila* revealed strong nuclear staining during early development, and more diverse localization later in development. Within the embryo, dNAP1 is strongly correlated to the cytoplasm during G2 and late S phases, but is largely nuclear during S phase, consistent with its role in chromatin assembly (Ito *et al.*, 1996a).

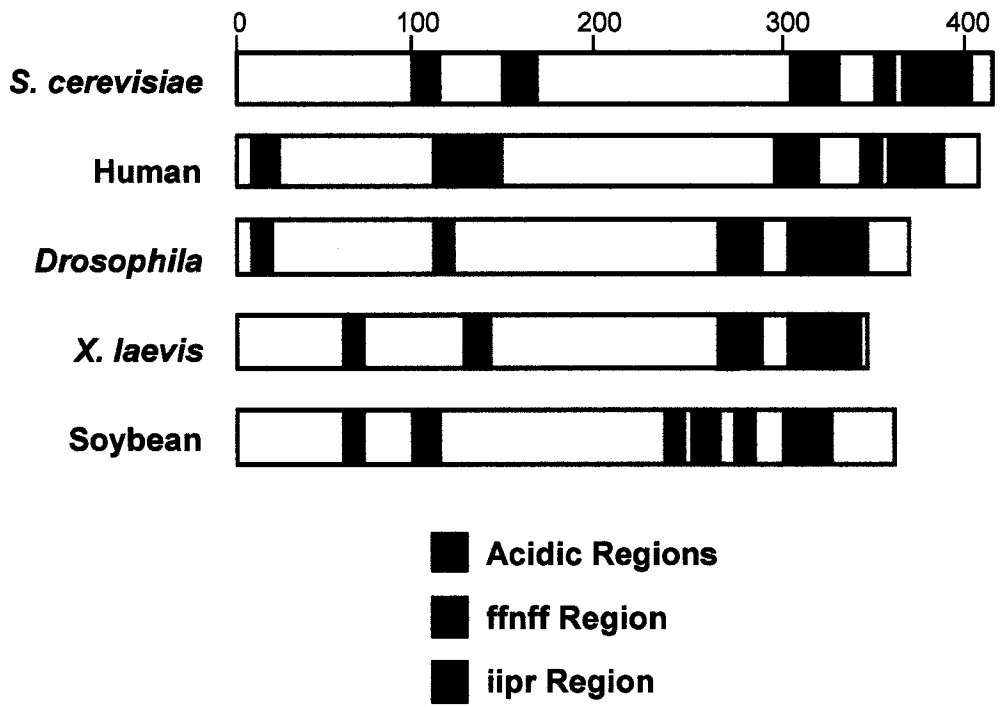

Figure 1.4A: NAP1 structural features. The presence of four extended acidic domains (red) and the similar locations of the highly conserved regions (blue and green) highlight the overall similarities between these (and most other) species. Though some differences in overall length exist, the fundamental homologies prevail.

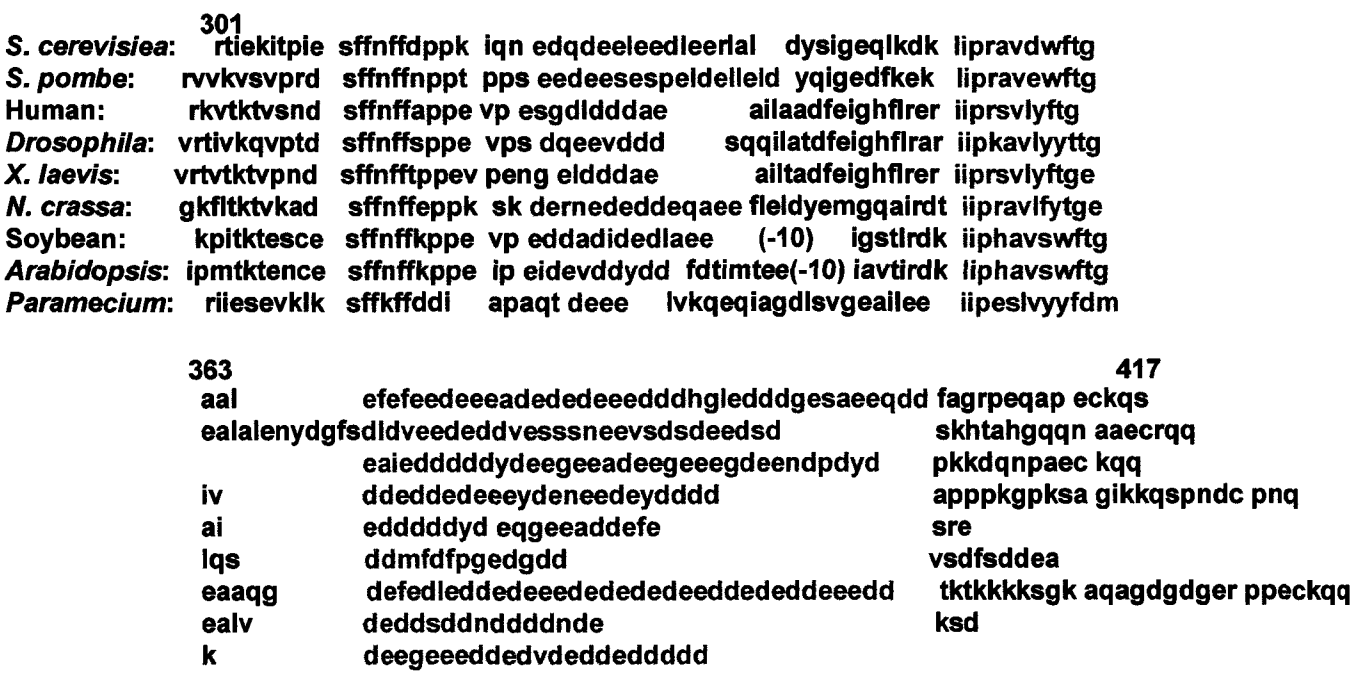

Figure 1.4B: Alignment of the C-terminal domains of 9 NAP1 homologs. The remarkable similarity in the length and content of the acidic regions and the two most highly conserved regions leads to very similar functional properties. Elucidation of the structural/oligomerization properties of the yeast homolog (*S. cerevisiae*) infers that it will likely apply to the other homologs as well.

Red = Acidic Regions
Blue/Green = Highly conserved Regions

There appear to be regions upstream of the yeast gene encoding NAP1 that may confer constitutive expression (Ishimi and Kikuchi, 1991). In Hela cells, NAP1 was later determined to be nuclear during S-phase, and cytoplasmic during G1 (Asahara *et al.*, 2002). Interestingly, a recent investigation into the sub-cellular localization of NAP in rice and tobacco failed to indicate any change from the largely cytoplasmic localization of NAP1 isoforms upon the initiation of an artificial block at early S phase (Dong *et al.*, 2003).

Consistent with its role as a histone chaperone and its cytoplasmic and nuclear localization, NAP1 plays a prominent role in the nuclear localization of histones. H2A and H2B have been found in cytoplasmic complexes with NAP1, whereas H3 and H4 have not (Chang *et al.*, 1997). NAP1 appears to mediate an interaction between the nuclear localization signals on H2A and H2B (Baake *et al.*, 2001) and the primary karylophilin/importin required for nuclear import of the two histones (Mosammaparast *et al.*, 2002; Mosammaparast *et al.*, 2001). Thus, the lack of discrete sub-cellular localization of NAP1 may be due to the shuttling of histone proteins from the site of protein synthesis (cytoplasmic ribosomes) to the site of nucleosome assembly (nucleus).

1.10 NAP1 and cell cycle regulation:

Propagation of eukaryotic cells involves replication of the genetic material and packaging of the newly synthesized DNA into chromatin. These events precede chromosome condensation and segregation prior to cytokinesis, or

cell division (interested readers are encouraged to read one of many excellent textbooks which include chapters on the eukaryotic cell cycle, including Alberts, B. et al., *Molecular Biology of the Cell*, chapters 17 and 18, and references therein). Thus, the prominent role that NAP plays in chromatin assembly is intimately tied to the cell cycle, and, specifically, to the DNA synthesis phase (S-phase). The phenotypes of NAP knockout strains substantiate the correlation between NAP1 and the cell cycle (see above). Further, direct interactions and functional interplay between cell cycle regulatory factors and NAP1 have been demonstrated.

Highly regulated pairs of proteins, the cyclins and cyclin-dependent kinases, govern progress through the cell cycle (for reviews see King, *et al.*, 1994, and Murray and Hunt, *The Cell Cycle: An Introduction*. Oxford Univ. Press, 1993). A direct interaction between NAP1 and the yeast cyclin Clb2 has been demonstrated. A mitotic protein kinase, Gin4, also associates with NAP1, and this interaction is necessary for the Gin4-dependent switch from polar to isotropic bud growth in budding yeast (Altman and Kellogg, 1997). A similar interaction with another B-type cyclin has been described (Kellogg *et al.*, 1995). A subsequent investigation from the same laboratory showed that NAP1 is also associated with a factor, Sda1, which is required for the transition from G1 (the resting phase of the cell cycle) to S (Zimmerman and Kellogg, 2001). Together, these data expand the role of NAP1 beyond chromatin assembly and nucleosome dynamics. Perhaps only when sufficient NAP1 is present in the nucleus to ensure rapid packaging of the newly

replicated DNA are the events leading to DNA replication and cell division initiated.

1.11 NAP1 modification and cell cycle:

Further connections between NAP1 and the cell cycle exist. A post-translational modification of the acidic C-terminus, polyglutamylation, occurs on both NAP1 and NAP2 within Hela cells (Regnard *et al.*, 2000). This modification will increase the total amount of negative charge present. Glutamylation is more commonly seen on tubulin, the protein component of microtubules, and an important component of the cytoskeleton (for review see Liang and MacRae, 1997). NAP1 has been proposed to play a role in destabilizing microtubules at the onset of mitosis (Kellogg and Murray, 1995b). Whether NAP1 polyglutamylation is relevant to this is unknown, though tubulin polyglutamylation is closely regulated with the cell cycle (Regnard *et al.*, 2000). Along these same lines, NAP1 and NAP2 have been shown to be phosphorylated by casein kinase II (CKII) at the G0/G1 boundary (Rodriguez *et al.*, 2000)). Phosphorylated human NAP2 remains cytoplasmic and in complex with histones, while dephosphorylation leads to a rapid transport of NAP2-histone complexes to the nucleus. As NAP1 and NAP2 contain numerous CKII sites throughout the protein, it is difficult to relate the phosphorylation directly to function. However, the CKII sites flank both the nuclear localization signal and the central acidic region on NAP2. It is possible, therefore, to speculate that a protein that relies on acidic sidechains

to bind histones might exhibit enhanced histone binding when phosphorylated at sites nearby, which would significantly increase the local acidic character.

1.12 NAP1 and nucleosome dynamics:

The measured exchange rates for the histone components of the nucleosome described above (Kimura and Cook, 2001) indicate that dimers appear to be very labile within the context of chromatin. Hydrodynamic and electrophoretic studies of the $(H3\text{-}H4)_2$ tetramer bound to DNA have found that this 'tetrasome' is particularly accessible to a site-specific DNA binding factor, due to higher surface charge densities and conformational flexibility, compared to the intact nucleosome (Tse *et al.*, 1998). Thus, removal of one or more of the histone dimers yields a nucleoprotein complex which is uniquely accessible to those factors which regulate the expression of the genes enclosed within chromatin. yNAP1 facilitates the binding of GAL4 to nucleosomes containing GAL4 binding sites, and this requires disruption of the histone octamer (Walter *et al.*, 1995). Thus, yNAP1 appears capable of extracting one or more of the histone dimers, leading to more accessible nucleosomal DNA. More recently, it was shown that in the presence of the transcriptional coactivator and histone acetyltransferase p300 (Bannister and Kouzarides, 1996; Ogryzko *et al.*, 1996. For a review of p300 see Goodman and Smolik, 2000), (H2A-H2B) was transferred to dNAP1 (Ito *et al.*, 2000)). Thus, acetylation of the histone tails by p300 led to disruption of the nucleosomal array, and release of (H2A-H2B), which was sequestered by dNAP1. Consistent with this, a tri-partite complex of p300, (H2A-H2B), and

NAP1 has been isolated from HELA cells and investigated *in vitro* (Asahara *et al.*, 2002). Further, (H2A-H2B) deposition and exchange are targeted to acetylated chromatin *in vivo* (Perry *et al.*, 1993). Thus, NAP1 functions with the components of activated transcription to facilitate the binding of transcriptional activators and to generate a more accessible substrate for transcription. Interestingly, transcription by RNA polymerase II has also been shown to involve the loss of the (H2A-H2B) dimer (Kireeva *et al.*, 2002). Thus, disruption and loss of the dimer is possibly a general mechanism for increased access to the DNA.

Disruption of the octamer within a nucleosomal array requires acetylation of the histones (Ito *et al.*, 2000). Only then does NAP1 accept the histone components released from the nucleosomes. Within a mono-nucleosome, however, where inter-nucleosomal contacts involving the N-terminal tails are limited, yNAP1 readily removes (H2A-H2B) (Park, Y.J., unpublished results). Further, experiments using fluorescently labeled 'free' (H2A-H2B) and $(H3\text{-}H4)_2$ and unlabeled mono-nucleosomes demonstrate that only (H2A-H2B) is removed upon mixing of the components. More interestingly, the unlabeled, incorporated (H2A-H2B) can be rapidly replaced by a labeled dimer. Thus, (H2A-H2B) is more readily exchanged within a nucleosome in the presence of yNAP1. Though a less 'physiological' milieu, this observation reinforces the dynamic nature of the nucleosome, particularly through(H2A-H2B), and extends the possible role of NAP1 in chromatin dynamics.

1.13 Histone binding activity of NAP1:

Functionally, NAP1 is one of the best studied of the histone chaperone family members. Though foremost is its role in histone binding and chromatin assembly, NAP has numerous other activities which involve cell cycle control, facilitation of transcription factor binding to chromatin, and the coactivator dependent disruption of nucleosomes to facilitate transcription. The histone binding function of NAP1, though poorly addressed in the literature, is of utmost importance in order to understand these additional NAP1 functions. In 1987, analysis of the human NAP1 homolog, AP-1 (for assembly protein-1), revealed greater binding to (H2A-H2B) than $(H3\text{-}H4)_2$ (Ishimi *et al.*, 1987). However, this analysis utilized human FM3A cell derived, purified histones. Such preparations contain numerous histone isoforms and a variety of post-translational modifications which may affect yNAP1 binding preferences. Further, a modified enzyme-linked immunosorbent assay (ELISA) was utilized. This assay relies on the use of an anti-AP-1 antibody to determine the amount of AP-1 that is bound to histone-coated polystyrene plates. This is a very indirect method, relying on the antibody to recognize an epitope that may be partially or fully masked within the AP-1 / histone complexes. Thus, these results may not be qualitatively or quantitatively correct.

Upon the cloning of the yeast (*S. cerevisiae*) homolog, it was revealed by ELISA that yNAP1 could form a complex with both of the histone sub-complexes (Ishimi and Kikuchi, 1991). Similarly, *Drosophila* NAP1 (dNAP1) formed a complex with all four core histones, and immunoprecipitation

revealed preferential binding of H2A and H2B (Ito *et al.*, 1996a). Again, this methodology relies on the use of antibodies, this time directed towards the four core histones. The conservation of the amino acid content and secondary structure of the histones has led to problems with cross-reactivity of antibodies directed at the histones. A re-examination of yeast NAP1, again using native core histones (from chicken erythrocytes), utilized a Far-Western blot to determine yNAP1 binding preferences (McQuibban *et al.*, 1998). In this assay histones were separated by SDS-PAGE and 'renatured' following transfer to PVDF membrane. A mono-fluoresceinated yNAP1 was allowed to bind to the histones on the membrane, and the amount of yNAP1 bound was quantitated by use of a fluorescence imager. This methodology revealed that H2B had the greatest, and H4 the lowest, affinity for yNAP1. However, it has been demonstrated that the isolated histones are unstructured and insoluble (Luger *et al.*, 1999). Further, a comparison of the primary sequences of histones from yeast and *Xenopus* reveals that H2B, shown to have the highest affinity for yNAP1 (McQuibban *et al.*, 1998), is more enriched with lysine side chains than the other histones (6-8 more on average). Additionally, histone H4 is ~103 amino acids in length, whereas the others are 131-136 amino acids long. Thus, rather than measuring the affinities towards individual histone structures, this methodology may reveal only electrostatic attractions between small, unstructured basic polypeptides and the acidic yNAP1 molecule. Thus, due to the lack of quantitation and structurally valid

methodologies, the histone binding mode and preferences of yNAP1 remain unresolved.

NAP1 and Np are distinct among the histone chaperones and assembly factors. NAP1 can assemble nucleosomes *de novo*, in the absence of accessory factors (Fujii-Nakata *et al.*, 1992; Ishimi and Kikuchi, 1991; Ito *et al.*, 1996b; Pilon *et al.*, 1997; Terrell *et al.*, 2002). Similar to results achieved with *Xenopus* Np and *Drosophila* NLP (see above), the most prominent acidic region on yNAP1 (at the C-terminus) is dispensable for nucleosome assembly (Fujii-Nakata *et al.*, 1992). It is hypothesized that, at least for Np, the largest acidic tracts, though dispensable for histone binding and nucleosome assembly, function as storage 'reservoirs' for the vast pools of histones present in the *Xenopus* oocytes (Dutta *et al.*, 2001). However, the function of this C-terminal region of NAP1 with regards to histone binding and nucleosome assembly remains unresolved.

1.14 NAP1 and the histone N-terminal tails:

The Lewis laboratory (McQuibban *et al.*, 1998) generated tailless chicken histones by limited trypsin proteolysis. This leads to selective removal of the N-terminal histone tails (Simon and Felsenfeld, 1979). Non-denaturing electrophoresis failed to reveal yNAP1/ tailless-histone complexes, thus it was concluded that the N-terminal tails were required for yNAP1 binding. This conclusion is supported by work from the La Thangue laboratory, in which a direct interaction between *in vitro*-translated NAP2 (Hu *et al.*, 1996; Rodriguez *et al.*, 1997) and isolated N-terminal tail peptides of *Drosophila* histones H2A

and H3 was demonstrated (Shikama *et al.*, 2000). Additionally, it was shown that dNAP1 interfered with the ability of p300 to acetylate the N-terminal tails of free core histones (Asahara *et al.*, 2002). This result suggests that yNAP1 sterically hinders the access of p300 to the N-terminal tails. Further, the McQuibban paper reported that yNAP1 failed to assemble these 'tailless' histones into chromatin. These results are all consistent with a model in which yNAP1 requires the N-terminal tails for histone binding and deposition. Interestingly, the McQuibban report showed that yNAP1 did not bind to poly- or mononucleosomes, even though the N-terminal tails are exposed and available for such an interaction (Arents *et al.*, 1991; Luger *et al.*, 1997a; Richmond *et al.*, 1984). In contrast, dNAP1 has recently been shown by two groups to be capable of assembling recombinant tailless histones into transcriptionally repressed nucleosomal arrays (An *et al.*, 2002; Georges *et al.*, 2002).

Considering these contradictory data, it is possible that the proteolytic treatment of the histones in the McQuibban study also removed additional N-terminal residues, which abrogated yNAP1 binding to the conserved histone-fold motif. It also is likely that the poor resolution of the native gel system used in the McQuibban analysis failed to accurately resolve yNAP1-histone complexes. The recent availability of recombinant tailless histones allows for binding assays with a more stable, uniform substrate. These tailless histones, and an improved, high-resolution native gel system, are utilized in

experiments described herein to accurately and quantitatively assess the binding of yNAP1 to the histone folds and N-terminal tails (Chapter 2).

1.15 NAP1 oligomerization:

A great deal is known regarding the oligomeric state of *Xenopus* Np and *Drosophila* NLP. Early work on Np utilized protein sucrose gradients and gel filtration chromatography to determine that it behaves as though it is larger than the 29 kDa species seen upon SDS PAGE (Laskey *et al.*, 1978). Protein cross-linking and SDS PAGE revealed that Np was a pentamer (Earnshaw *et al.*, 1980). X-ray crystallography of Np confirmed the pentameric nature, and observed that two pentamers formed a decamer within the crystal lattice (Dutta *et al.*, 2001). A subsequent X-ray analysis of dNLP again revealed a pentameric structure, and only slight deviations from the overall conformation of Np (Namboodiri *et al.*, 2003). It is thus considered likely that oligomerization of histone chaperones and assembly factors is a common feature, and may confer a functional advantage (Akey and Luger, 2003).

Early studies on dNAP1 utilized glycerol gradients to determine the properties of dNAP1 / histone complexes (Ito *et al.*, 1996a). This investigation showed that dNAP1 eluted with a molecular weight of ~120 kDa, consistent with a complex containing either 2 or 3 dNAP1 molecules. However, gel filtration chromatography yielded an apparent molecular weight of ~600 kDa, thus the oligomerization state remained unresolved. Using GST pull-downs and deletions of the human NAP2 protein, it was shown that oligomerization-specific interactions were mediated by both the N-terminal 123 amino acids

and C-terminal residues 230-386 (Asahara *et al.*, 2002). These investigators failed to pursue their observations and determine the stoichiometry of the complexes. Interestingly, no cross-linked yNAP1 species were observed using disuccinimidyl suberate (McQuibban *et al.*, 1998). These authors concluded, in contrast to previous observations, that yNAP1 was monomeric at micromolar concentrations. The biochemical, functional and oligomeric properties of the histone chaperones is shown in Figure 1.5.

In Chapter 2 we note that native electrophoresis of yNAP1 derived from a concentrated protein sample revealed two species. Both of these species appear functional, as the addition of (H2A-H2B) slowed the migration of both species. The presence of the slower migrating yNAP1 band could be minimized by dilution and extensive dialysis, suggesting a concentration dependent association. We expanded on this observation and used a variety of biochemical and biophysical methods to determine the oligomerization state of yNAP1, and the mechanism through which it is regulated (Chapter 3).

Chaperone	Subunit MW	pI	Activities	Oligomerization
NAP1	**49 kDa**	**4.2**	Binds $(H3\text{-}H4)_2$ and (H2A-H2B) Autonomous Assembly	Dimers and larger oligomers
Np (Nucleoplasmin)	**22 kDa**	**4.7**	Binds $(H3\text{-}H4)_2$ and (H2A-H2B) Autonomous Assembly	Pentamer/Decamer*
dNLP (Np-like protein)	**17 kDa**	**4.5**	Binds $(H3\text{-}H4)_2$ and (H2A-H2B) Autonomous Assembly	Pentamer
N1/N2	**65 kDa**	**4.4**	Binds $(H3\text{-}H4)_2$ and (H2A-H2B) Autonomous Assembly	ND

Figure 1.5: General properties of the histone chaperones. Shown are the approximate molecular weights of the subunits, their chromatin assembly activity, calculated isoelectric point (pI), and oligomerization state. ND = Not Determined. *crystallographic oligomer.

1.16 Statement of hypotheses and general dissertation layout:

I have addressed two general questions regarding yNAP1 in my dissertation research. First, I have examined the histone binding activity of yNAP1. I have employed several biochemical approaches to determine the preference of yNAP1 for either the (H2A-H2B) dimer or the $(H2\text{-}H4)_2$ tetramer. I have extended this to include an investigation of the mechanism underlying this preference, which involves contributions towards yNAP1 binding by the N-terminal tails of H3 and H4. Finally, the role of the acidic C-terminus of yNAP1 was investigated. The results of these studies are presented in Chapter 2, and a manuscript describing these studies has been submitted to The Journal of Biological Chemistry (McBryant, S.J., Abernathy, S.M., Laybourn, P.J., Nyborg, J.K., and Karolin Luger. *Preferential binding of the histone $(H3\text{-}H4)_2$ tetramer by the nucleosome assembly protein 1 is mediated by the basic amino terminal tails*).

Second, I have examined the self-association properties of yNAP1 by biochemical and hydrodynamic/thermodynamic analyses. This study revealed a mode of self-association which likely contributes to the functional properties of yNAP1. The results of this study are presented in Chapter 3, and a manuscript describing these studies is in preparation for submission to the journal Biochemistry (McBryant, SJ and Olve Peersen. *The yeast nucleosome assembly protein is an obligate homodimer, which self-associates into higher-order species*).

Chapters 4 and 5 will include additional experiments involving yNAP1 structure and function which will not be published, yet are still significant to the thoroughness of this dissertation. Chapter 6 will briefly summarize the significance of the work presented in Chapters 2-5, and will discuss interesting potential future studies on yNAP1 structure and function. A brief discussion on the expression, purification and physical properties of yNAP1 will conclude Chapter 6.

Chapter 2

Preferential Binding of the Histone $(H3\text{-}H4)_2$ Tetramer by the Nucleosome Assembly Protein 1 is Mediated by the Basic Amino Terminal Histone Tails

This chapter is being prepared for submission to The Journal of Biological Chemistry. The text of this manuscript is presented exactly as it was prepared for submission, at the time of the preparation of this dissertation. All figures that are anticipated to be included in that submission are included herein. Additional experiments performed during this investigation that were not submitted for publication, yet are relevant to the investigation, will be included in Chapters 4 and 5. The author list for this submission is as follows: McBryant, S.J., Abernathy, S.M., Laybourn, P.J., and K. Luger. All experiments were performed by S.M., with the exception of the chromatin assembly assay, which was performed by S.A.

2.1 ABSTRACT:

The yeast nucleosome assembly protein 1 (yNAP1) participates in many diverse activities, such as the assembly of newly synthesized DNA into chromatin, and the rearrangement of nucleosomes during transcriptional activation. yNAP1 does not require ATP hydrolysis to perform these functions. Using recombinant histone complexes, we show that yNAP1 has a preference for binding the $(H3\text{-}H4)_2$ tetramer over the (H2A-H2B) dimer. We find that the loss of the histone tails abrogates this preference, and demonstrate a direct interaction between yNAP1 and the tails of H3 and H4. The central core of yNAP1 binds stoichiometrically to one histone-fold domain. Finally, we provide evidence that the highly acidic carboxyl terminal region of yNAP1, while dispensable for nucleosome assembly *in vitro*, contributes to binding via structure-independent electrostatic interactions. Our results are consistent with recent mechanistic investigations of NAP1, and expand our understanding of the histone-chaperone family of assembly factors.

2.2 INTRODUCTION:

The organization of DNA with an equal mass of proteins to form highly organized chromatin is a hallmark of all eukaryotes. It is at this level that the majority of the processes involving the DNA substrate (such as replication, transcription, repair, and recombination) are enacted. The fundamental repeating unit of chromatin is the nucleosome, which consists of 146 base pairs of DNA wrapped in 1.65 supercoiled turns around a core of eight histone proteins, the histone octamer (Luger *et al.*, 1997a). The histone octamer is composed of two

copies each of the four histone proteins; H2A, H2B, H3, and H4. At physiological salt concentrations histones exist either as (H2A-H2B) dimers (Kelley, 1973) and $(H3\text{-}H4)_2$ tetramers (Kornberg and Thomas, 1974; Roark *et al.*, 1974), which can be described as a dimer of two histone fold dimers. Histones dimerize via the structurally conserved histone fold motif that is common to all four histones (Arents and Moudrianakis, 1995; Luger and Richmond, 1998a). A single tetramer binds the central 60 bp of DNA within a nucleosome, while two (H2A-H2B) dimers organize 30 bp of DNA each on either side of the tetramer, with each dimer making contacts with opposing faces of the central tetramer.

DNA binding is mainly afforded by the structured regions of the histones (histone fold and extensions (Luger and Richmond, 1998a)). The N-terminal basic tails of each histone protein are largely unstructured in solution as determined by NMR spectroscopy [Smith, 1989 #22], and are too disordered to be observed in electron density maps from crystals of the histone octamer and the nucleosome (Arents *et al.*, 1991; Davey *et al.*, 2002; Luger *et al.*, 1997a; Richmond *et al.*, 1984). The tails do not appear to contribute to the stability of the nucleosome (Ausio *et al.*, 1989; Luger *et al.*, 1997b; Widlund *et al.*, 2000; Zheng and Hayes, 2003), though they appear to be important for the folding of chromatin fibers *in vitro* (Carruthers and Hansen, 2000; Dorigo *et al.*, 2003). The regulation of their involvement in transcription via combinatorial post-translational modification of selected amino acid residues is currently a topic of intense research (Iizuka and Smith, 2003; Jenuwein and Allis, 2001; Strahl and Allis, 2000).

The transport of histones into the nucleus, and the ordered deposition of histone sub-complexes onto DNA are carried out by highly regulated assembly proteins (Ito *et al.*, 1997; Philpott *et al.*, 2000; Verreault, 2000). *In vivo*, these events often involve the synchronous activity of ATP-driven and ATP-independent assembly factors to deposit histones onto the DNA and organize regularly spaced nucleosomal arrays (Krude and Keller, 2001; Philpott *et al.*, 2000; Tyler, 2002). The $(H3\text{-}H4)_2$ tetramer acquires a unique set of lysine acetylations on H3 and H4 (Chang *et al.*, 1997; Sobel *et al.*, 1995), which allow binding and deposition by the chromatin assembly factor CAF-1 (Verreault *et al.*, 1996). The replication-coupled assembly factor (RCAF) also catalyzes this activity (Tyler *et al.*, 1999).

Deposition of the (H2A-H2B) dimer is facilitated by an ATP-independent nucleosome assembly protein (NAP1) (Akey and Luger, 2003; Philpott *et al.*, 2000; Tyler, 2002). NAP1, which can be classified as a bona fide 'histone chaperone', was initially purified from Hela cells (Ishimi *et al.*, 1984), and has since been isolated from a diverse set of organisms, such as soybeans, yeast, *Paramecium, Drosophila* and *Xenopus* (Ishimi and Kikuchi, 1991; Ito *et al.*, 1996; Nishiyama *et al.*, 2001; Yoon *et al.*, 1995). The H2A and / or H2B N-terminal tails are necessary for chromatin assembly in vivo (Thiriet and Hayes, 2001). NAP1 has been isolated from human cells in complex with histone H2A (Chang *et al.*, 1997), and has thus been considered an (H2A-H2B) histone chaperone. However, AP-1 (the human homolog) and yeast NAP1 (yNAP1) also bind the $(H3\text{-}H4)_2$ tetramer *in vitro* (Ishimi *et al.*, 1987; McQuibban *et al.*, 1998).

NAP1 is involved not only in the assembly of nucleosomes onto DNA (Nakagawa *et al.*, 2001; Thiriet and Hayes, 2001), but also in the remodeling of nucleosomes during transcriptional activation (Ito *et al.*, 2000; Kireeva *et al.*, 2002; Walter *et al.*, 1995), and in the recruitment of coactivators and the activation of transcription by facilitating DNA binding by transcription factors (Asahara *et al.*, 2002; Shikama *et al.*, 2000). NAP1 has been shown to be phosphorylated by cellular kinases in a cell-cycle dependent manner (Rodriguez *et al.*, 2000), and to be associated with components of the cell-cycle regulatory machinery (Altman and Kellogg, 1997; Zimmerman and Kellogg, 2001). Thus, NAP1 likely plays a role in the onset and regulation of mitotic events.

An overabundance of acidic amino acids is a characteristic of histone chaperones (Akey and Luger, 2003). yNAP1 has four highly acidic regions distributed throughout its entire length. The most prominent acidic domain is located near the C-terminus (aa 366-403), where 28 out of 38 amino acids are either aspartic or glutamic acid residues. Surprisingly, this region, as well as a portion of the N-terminus, is dispensable for the chromatin assembly by yNAP1 (Fujii-Nakata *et al.*, 1992). The basic histone N-terminal tails are considered likely targets for NAP1 binding, possibly through an interaction with one or more of the acidic domains within the NAP1 protein. Consistent with this idea, a previous study reported that yNAP1 interacts exclusively with the N-terminal tails of the histone octamer, and that the tails are required for yNAP1-mediated chromatin assembly (McQuibban *et al.*, 1998). However, this same study showed that yNAP1 fails to bind mono- or poly-nucleosomes, despite the fact that these

disordered regions are accessible for such interactions (Luger and Richmond, 1998b). More recently, it was shown that *in vitro* chromatin assembly using the structurally and functionally homologous *Drosophila* NAP1 (dNAP1, (Ito *et al.*, 1996)) occurs in the absence of the histone tails (An *et al.*, 2002; Georges *et al.*, 2002). Thus, the exact role of the N-terminal histone tails in chromatin assembly by NAP1 remains to be elucidated.

Here we investigate the preference and relative affinity of yNAP1 for recombinant histones, and dissect the contribution of histone fold and histone tails to this interaction. In contrast to previous findings (Ishimi *et al.*, 1987; McQuibban *et al.*, 1998)), we show that yNAP1 has a preference for the $(H3\text{-}H4)_2$ tetramer over the (H2A-H2B) dimer. This preference is dependent on the N-terminal tails of H3 and/or H4. We find that yNAP1 binds directly to the tails of both H3 and H4, but we do not observe yNAP1 binding to the N-terminal tails of H2A or H2B, despite similarities in residue content. In the absence of the N-terminal tails, yNAP1 binds the two core histone sub-complexes with equal affinity. yNAP1 binds histones with a 1:1 stoichiometry of yNAP1 for each histone molecule. Finally, we extend the observations of Fujii-Nakata (Fujii-Nakata *et al.*, 1992) and examine a series of yNAP1-derived polypeptides by the use of circular dicroism (CD), topological assembly assays and direct binding assays. The chromatin assembly activity of NAP1 resides solely in the central core of the protein, which also is responsible for histone-fold-specific binding. The acidic C-terminus of yNAP1, while dispensable for chromatin assembly, contributes to binding via structure-independent, electostaic interactions.

2.3 EXPERIMENTAL PROCEDURES:

Expression and purification of recombinant proteins. Full-length yNAP1 was expressed and purified from the pTN2 expression vector as described (Fujii-Nakata *et al.*, 1992), with the following changes. The dialyzed fraction from the 35-65% ammonium sulfate cut was centrifuged, and the supernatant applied to a 10 ml Q-Sepharose FF anion-exchange column (Amersham/Pharmacia). The column was then washed and eluted with a linear NaCl gradient in buffer A (20 mM Tris pH 7.6 [4°C], 0.5 mM EDTA, 10% glycerol, 1mM DTT, 0.1 mM PMSF). Fractions were assayed for yNAP1 by SDS-PAGE, and peak fractions were pooled. The peak was diluted with buffer A to a final NaCl concentration of 150mM, and applied to a 1 ml Mono-Q (Amersham/Pharmacia) anion-exchange column. yNAP1 was eluted with 500 mM NaCl. Peak fractions were assayed by SDS-PAGE, dialyzed into buffer A with 150 mM NaCl, and stored in small aliquots at –80°C. All amino acid coordinates are reported using the sequence specified by accession number J05759.

GST-yNAP1 deletion mutants were generated by PCR amplification from the pTN2 plasmid, with PCR primers encoding BamH1 and Sma-1 restriction sites. His_{-6} tagged proteins were generated by PCR amplification of the pTN2 plasmid with primers encoding Nde1 and BamH1 restriction sites. Restriction enzyme digested and purified PCR products were ligated into similarly digested pGEX4T2

(Amersham/Pharmacia) for GST-fusions or pET15b (Novagen) for His_6-fusions. These constructs were transformed into DH5*α* cells, and screened by restriction digestion and by sequencing to confirm the identity of the clones. GST-fusions were purified by standard methods, dialyzed into buffer A (100 mM NaCl) and stored in aliquots at –80°C. His_6 fusions were expressed and purified over Ni^{2+}NTA resin and further purified by Mono-Q chromatography. Peak fractions were dialyzed against buffer A (150 mM NaCl) and stored in aliquots at –80°C. Insoluble His_6 74-293 and 74-353 were extracted from inclusion bodies by solubilization of lysed, centrifuged cell pellets in 8M urea. The solution was centrifuged, and the supernatant applied to Ni^{2+}NTA as described above. Full-length yNAP1, when subject to a similar denaturation/renaturation, recovers full chromatin assembly activity (Fujii-Nakata *et al.*, 1992), as does His_6-74-365.

GST-fusion proteins for the S. *cerevisiae* N-terminal tails (Hecht *et al.*, 1995) were expressed and purified by standard methods (see above). These expression plasmids encoded H2A (aa1-35), H2B (aa 1-35), H3 (aa 1-46), and H4 (aa 1-34). Recombinant yeast and *Xenopus laevis* histones were purified as described (Luger *et al.*, 1999b; White *et al.*, 2001; Dyer *et al.*, 2003 in press). Native yeast and *Drosophila* core histones were purified as described (Pazin *et al.*, 1994; Pilon *et al.*, 1997a). The amino acid coordinates of the N-terminally deleted histone cores have been previously described (Bohm and Crane-Robinson, 1984). Histones were stored in 1M NaCl, 50% glycerol at –20°C. Native *Drosophila* histone H1 was purified as previously described (Croston *et al.*, 1991).

GST pull-down assays. Coomassie stained GST pull-down assays were performed by incubating 100 pmoles of GST or GST-fusion proteins with 20 µl glutathione agarose (Sigma) in 200 µl TPD-25 (20 mM Hepes pH 7.9, 0.5 mM EDTA, 10% glycerol, 0.05% NP-40, 5 µM Zinc sulfate, 2.5 mM $MgCl_2$, 25 mM KCl, 1 mM DTT) for 2-3 hours at 4°C. After extensive washing, secondary (target) proteins were added (the amounts are indicated in the figure legends), and incubated for 16 hours at 4°C. Bound proteins were washed extensively with TPD-250 (250 mM KCl) and briefly with 1X PBS prior to loading on SDS-PAGE. Proteins were visualized by staining with Coomassie Brilliant Blue. For GST pull-down assays using detection by western blot (anti-His_6 [H-15], Santa Cruz Biotechnology), 10 pmoles of GST or GST-fusion was bound to 10 µl of glutathione agarose, and 20-50 pmoles of target protein was added prior to 16 hour incubation in TPD (25 mM KCl). Following washing as described above, proteins were separated by 12% SDS-PAGE, transferred to nitrocellulose and detected by ECL (Amersham Biosciences).

Gel Filtration Chromatography. Fractionation was performed on a FPLC Purifier® (Amersham/Pharmacia) using a Superdex S-200 prep-grade 13/30 column. Samples were prepared and run in buffer A (150 mM NaCl) at 0.5 ml/min. Fractions were precipitated by TCA prior to SDS-PAGE. Elution volumes were measured by peak integration using Unicorn (Amersham/Pharmacia); and Kav's were calculated by Vr-Vo/Vc-Vo, where Vr is retention volume, Vo is void volume for the column (8.16 mL) and Vc is the column volume (24 ml). Kav was plotted against the molecular weights (log) for standards (Gel Filtration

Calibration Kit, Amersham/Pharmacia) run in buffer A (150 mM NaCl). Best-fit exponential for the plot was determined in Cricket Graph III and the MWapp was determined by substitution of Kav into the equation for the line.

Electrophoretic mobility shift assays. EMSA's were performed by incubating yNAP1 at 10 μM in a 20 μl reaction with the indicated concentrations of histones at 4°C for 16 hours to establish equilibrium. All proteins were previously dialyzed into EMSA buffer (20 mM Tris pH 7.6 [4°C], 100 mM NaCl, 1 mM EDTA, 1 mM DTT). One-half of the binding reactions were transferred to a chilled tube containing 5 μl 20% sucrose, and the samples were loaded onto a 5% acrylamide, 0.2X TBE gel (8 x 10 cm, 1.5 mM thick), electrophoresed for 60 min at 150 V, and stained with Coomassie. Molar ratios of histones to yNAP1 (where bound yNAP1=100%) were determined following digitization of the Coomassie stained gels and quantitation using ImageQuant (Molecular Dynamics). The stoichiometry of yNAP1/histone primary complex was determined by extrapolation of a linear fit of the plot of unbound yNAP1 (abscissa) versus molar ratio of histone to yNAP1. The intersection on the ordinate (histone: yNAP1 ratio) represents the molar ratio at which all yNAP1 is in complex. Though all data points are shown, only the lower ratio, most linear portion of the data was utilized in the fit. Digitization noise led to the poor fit of data points as the percent of free yNAP1 approached zero.

Proteolytic Cleavage. Trypsin digestion of yNAP1 was performed at an enzyme concentration of 1μg/mg yNAP1 protein (1:1000 w/w), at a yNAP1 concentration of 1mg/ml, and at 22°C for the indicated time. The digestion

products were resolved by 18% SDS-PAGE and Coomassie staining. For N-terminal sequencing, proteins were transferred to PVDF membrane (Bio-Rad) prior to sequencing (Applied Biosystems, Procise 491 protein sequencer, Perkin Elmer Cetus). Maldi-TOF mass spectrometry was performed on a Voyager DE Pro (Perseptive Biosystems).

Chromatin assembly. *In vitro* assembly reactions were performed at yNAP1 to core histone mass ratios of 4:1, as described (Ito *et al.*, 2000), and assembled DNA was separated on 1.2% agarose gels and stained with SYBR-Gold (Molecular Probes). Core histones were prepared as described (Luger *et al.*, 1999a). The use of mass ratios caused a progressive increase in the moles of yNAP1 utilized as construct molecular weight decreased (76 pmoles yNAP1, 88 pmoles 74-417, 102 pmoles 74-365, 108 pmoles 74-353, 136 pmoles 74-293). Thus, the relative assembly activity of smaller constructs is over-estimated in this assay.

Circular dichroism: CD spectra were collected on a Jasco 720 spectrometer at 5° C. 20 spectra were obtained and averaged for each polypeptide in 20 mM NaH_2PO_4 pH 7.0, 50 mM NaCl. The molar ellipticity [Θ] was obtained by normalization of the measured ellipticity (in mdeg) Θ, using $[\Theta] = \Theta * 100 / (n * l * c)$, where n is the number of residues, c is the total concentration in mM and l is the cell pathlength in cm. Percent helix is estimated as described previously (Chen *et al.*, 1972).

2.4 RESULTS:

2.4A yNAP1 preferentially binds the $(H3/H4)_2$ tetramer over the (H2A/H2B) dimer. Recombinant histones of both yeast and *Xenopus* origin were refolded at 2 M NaCl into (H2A-H2B) dimers, $(H3\text{-}H4)_2$ tetramers, and octamers [consisting of two (H2A-H2B) dimers and one $(H3\text{-}H4)_2$ tetramer]. The formation of correct histone complexes was verified by gel filtration (Dyer, et al., 2003 in press), and the purified histone complexes were assayed for yNAP1 binding using a GST pull-down assay (Figure 2.1A). While yNAP1 showed robust and nearly equivalent binding to (H2A-H2B) dimers and $(H3\text{-}H4)_2$ tetramers in separate reactions, a clear preference for the tetramer was observed when dimers and tetramers were allowed to compete directly (Figure 2.1A, lanes 7, 8). Note that the histone octamer dissociates into (H2A-H2B) dimer and $(H3\text{-}H4)_2$ tetramer under physiological conditions.

Since identical results were obtained with recombinant histone complexes from *Xenopus laevis* (Figure 2.1A) and yeast (data not shown), we utilized *Xenopus laevis* recombinant histones in subsequent experiments.

To investigate whether assembly-specific posttranslational modifications alter the relative affinity of yNAP-1 for different histone pairs, we directly compared yNAP1 binding to recombinant and native *Drosophila* core histone octamers in the GST pull-down assay (Figure 2.1B). A clear preference for the $(H3\text{-}H4)_2$ tetramer over the (H2A-H2B) dimer was observed for both preparations. In case these replication-dependent *Drosophila* core histone modifications differ from

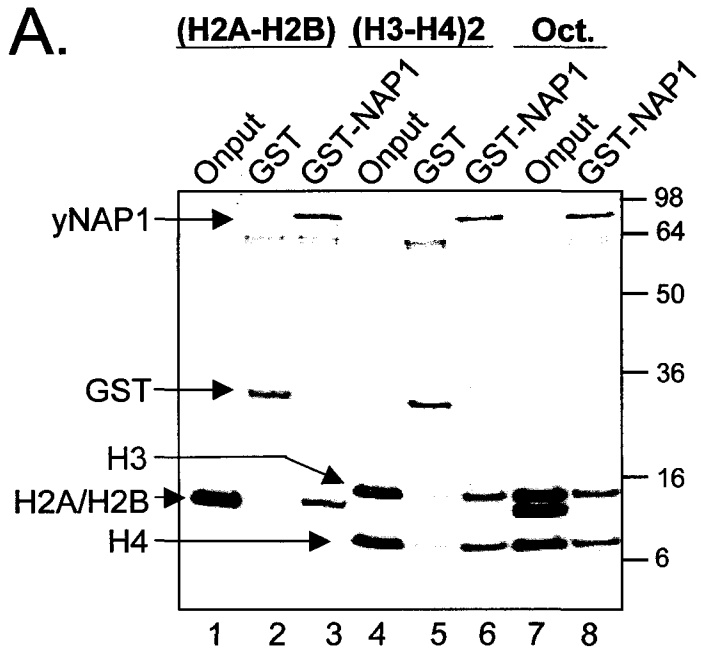

Figure 2.1A: yNAP1 preferentially binds the histone tetramer. yNAP1 GST pull-down assays on (H2A-H2B) dimers, (H3-H4)2 tetramers, and 'octamer' (= two dimers and one tetramer under the conditions used). Purified recombinant *Xenopus laevis* histone dimers (90 pM), tetramers (47 pM), or octamers (50 pM), were incubated with 100 pM GST alone, or GST-yNAP1 fusion protein bound to glutathione agarose beads. Bound proteins were separated by 18% SDS-PAGE and visualized by Coomassie staining. Forty percent of each onput is shown (lanes 1, 4, and 7). Non-specific protein-protein interactions were monitored using GST alone (lanes 2, 5). The position of bound histones, GST, yNAP1 and protein standards (kDa) are indicated.

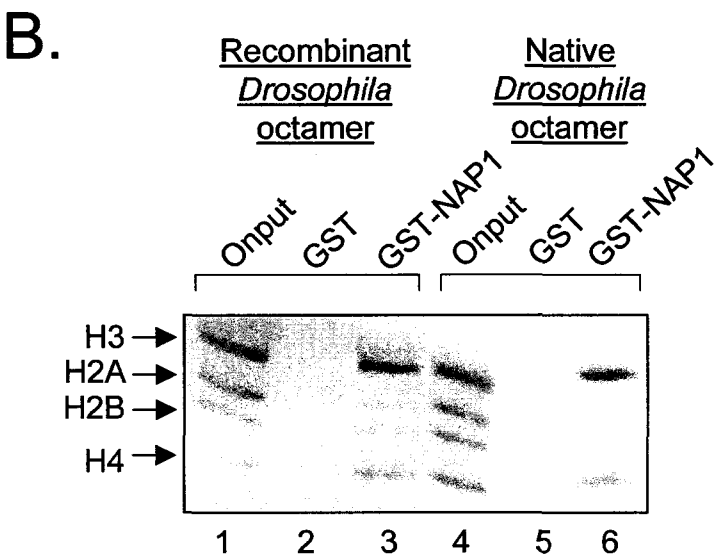

Figure 2.1B: yNAP1 preferentially binds the histone tetramer (species differences). Comparison of recombinant and native *Drosophila* core histone octamer binding to yNAP1. Purified recombinant or native histone *Drosophila* octamers (50 pM) were incubated with 100 pM GST alone, or GST-yNAP1, as indicated. Bound proteins were identified as described above. Thirty-six percent of each onput is shown (lanes 1, 4). The four core histones are indicated.

those found in yeast, we performed an identical experiment with native and recombinant *S. cerevisiae* octamers, with identical results (data not shown).

We used analytical gel filtration chromatography (GFC) to compare the types of complexes formed by yNAP1 with the histone pairs. Consistent with previous observations for *Drosophila* NAP1 (dNAP1) (Ito *et al.*, 1996), yNAP1 (49.15 kDa) eluted with an anomalously high apparent molecular weight (MWapp) of 220 kDa (Figure 2.1C). Subsequent hydrodynamic measurements have identified this species as yNAP1 dimers, and a small fraction of larger oligomers (S. McBryant and O. Peersen, manuscript in preparation). Only a modest change in the elution position was observed when yNAP1 and equimolar histone dimer were pre-incubated. The observed MWapp of 251 kDa is consistent with a single yNAP1 dimer in complex with a single (H2A-H2B) dimer (MWapp 28.6 kDa by gel filtration, data not shown). SDS-PAGE evaluation of peak fractions indicated yNAP1:dimer mass ratios of approximately 4:1, assuming equivalent Coomassie staining (Figure 2.1D).

C.

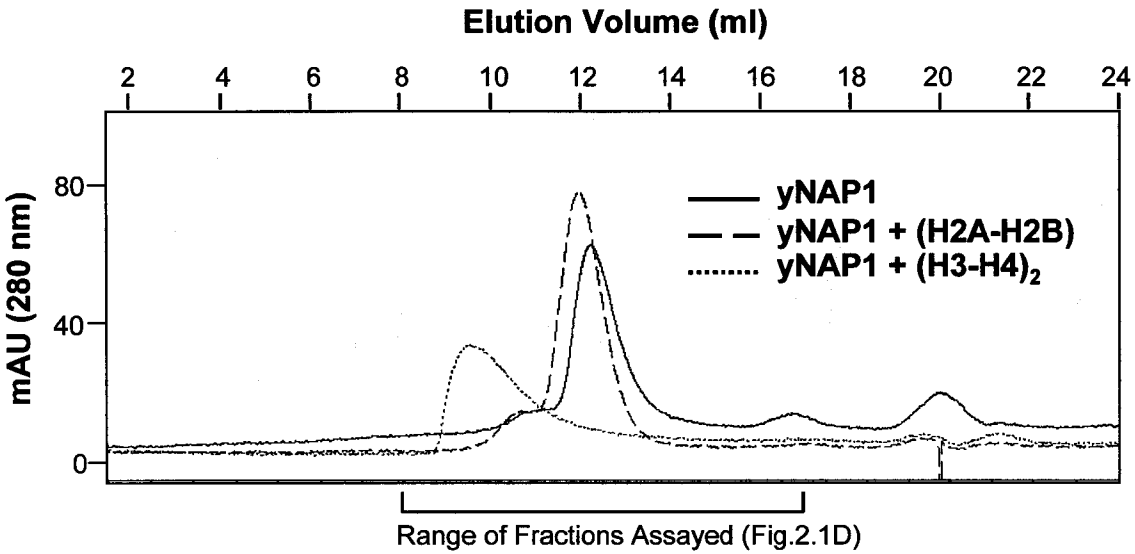

Figure 2.1C: yNAP1 preferentially binds the histone tetramer (GF-chromatogram). Gel filtration chromatography of yNAP1/histone complexes. Gel filtration was performed on 15 μM yNAP1 alone, or mixed with equimolar amounts of histone dimer, tetramer, or octamer, as indicated. A chromatographic absorbance trace at 280 nm is shown. The elution volume is indicated at the top, and the fractions assayed in 1.1D are indicated at the bottom. The yNAP1-octamer mix trace nearly overlapped with that observed with the yNAP1-tetramer mix, and is thus omitted for clarity. The void volume for the column is 8.16 ml.

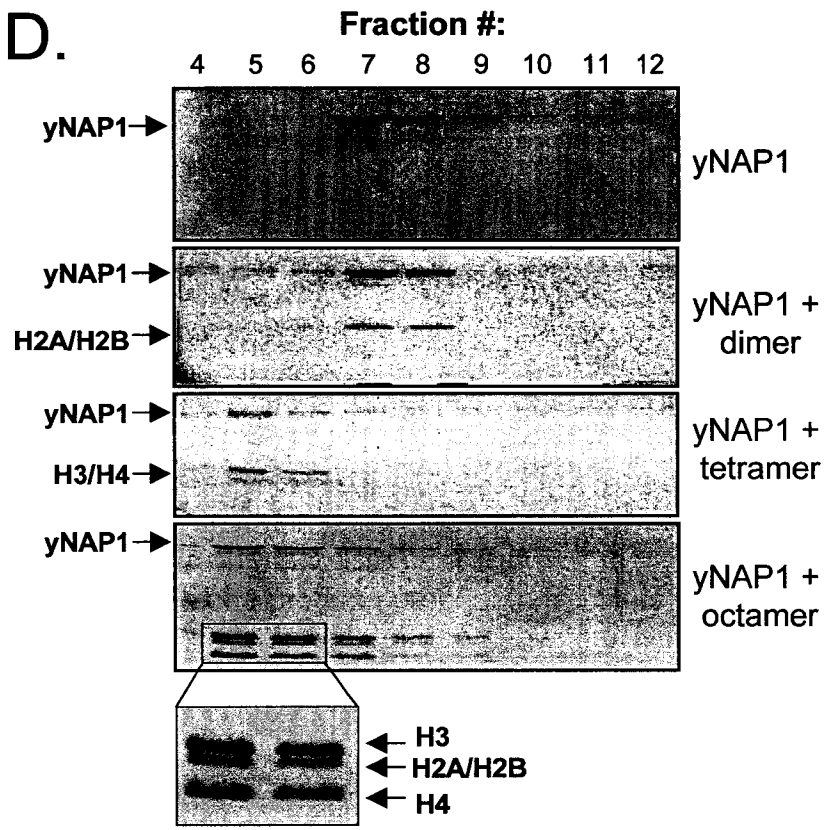

Figure 2.1D: yNAP1 preferentially binds the histone tetramer (GF-fractions). SDS-PAGE analysis of the yNAP1-histone chromatographic fractions. Precipitated proteins from the indicated column fractions (top) were analyzed by 18% SDS-PAGE followed by Coomassie staining. For reference, column fraction 4 correlated with the elution volume of 8-9 ml. Column fraction 12 correlated with the elution volume of 16-17 ml. The positions of the relevant proteins are indicated to the left. Inset, a region of the SDS gel showing the histone proteins present in fractions 5 and 6 was enlarged to show the relative amounts of dimer and tetramer that elute with yNAP1 following gel filtration of the yNAP1-octamer mixture.

This mass ratio is also consistent with a complex containing one ~100 kDa yNAP1 dimer and one ~28 kDa (H2A-H2B) dimer. In contrast, the yNAP1/tetramer complex eluted near the void volume for this column (>1 MDa). The observed elution volume for the yNAP1/tetramer complex suggested a substantial change in either the shape or size of yNAP1. SDS-PAGE evaluation of peak fractions indicated a mass ratio that is not consistent with a large excess of $(H3\text{-}H4)_2$ (Figure 2.1D). Gel filtration of yNAP1 with the recombinant histone octamer also resulted in a significant change in the elution profile when compared to yNAP1 alone, again eluting near the void volume (data not shown). When fractions were evaluated by SDS-PAGE, preferential binding of $(H3\text{-}H4)_2$ to yNAP1 was again observed (Figure 2.1D, inset).

2.4B yNAP1 forms distinct complexes with (H2A-H2B) and $(H3\text{-}H4)_2$.

We next determined the stoichiometry of the yNAP1 histone complexes. An electrophoretic mobility shift assay (EMSA) was developed to directly visualize and quantitate yNAP1 / histone complexes (Figure 2.2). Increasing concentrations of histone pairs, in the presence of a constant amount of yNAP1, resulted in distinct bands. As the ratio of $(H3\text{-}H4)_2$ tetramer to yNAP1 approached ~0.25:1.0 (Figure 2.2A, lane 10, Figure 2.2C, lane 4) all of yNAP1 was incorporated into the primary complex. In contrast, a yNAP1 to (H2A-H2B) dimer ratio of 0.5:1 was required for a complete supershift of yNAP1 (Figure 2.2B, lane 6, Fig 2.2D, lane 3).

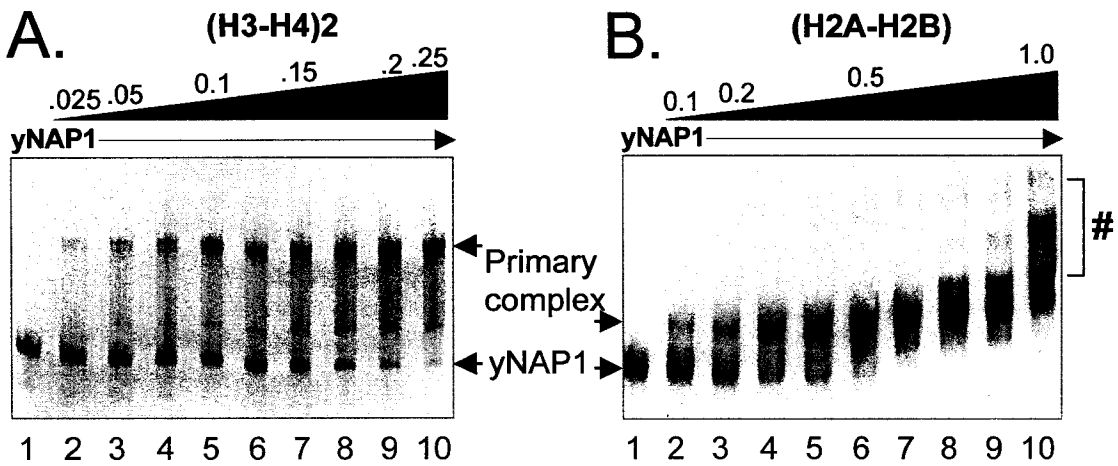

Figure 2.2A, B. Visualization of yNAP1-histone complexes (EMSA). yNAP1 binding to increasing concentrations of the histone pairs by native gel electrophoresis. (A) Increasing concentrations of the histone (H3-H4)2 tetramer (0.025 to 0.25 molar equivalents) were incubated with a constant amount of yNAP1 (10 μM). Protein-protein complexes were analyzed by EMSA and visualized by Coomassie staining. The double banding is a gel artifact of this particular experiment, which otherwise best typifies the binding pattern. (B) Increasing concentrations of the histone (H2A-H2B) dimer (0.1 to 1.0 molar equivalents) were incubated with a constant amount of yNAP1 (10 μM). Analysis and visualization was as described above. # indicates larger complexes formed as histone:yNAP1 ratios increase.

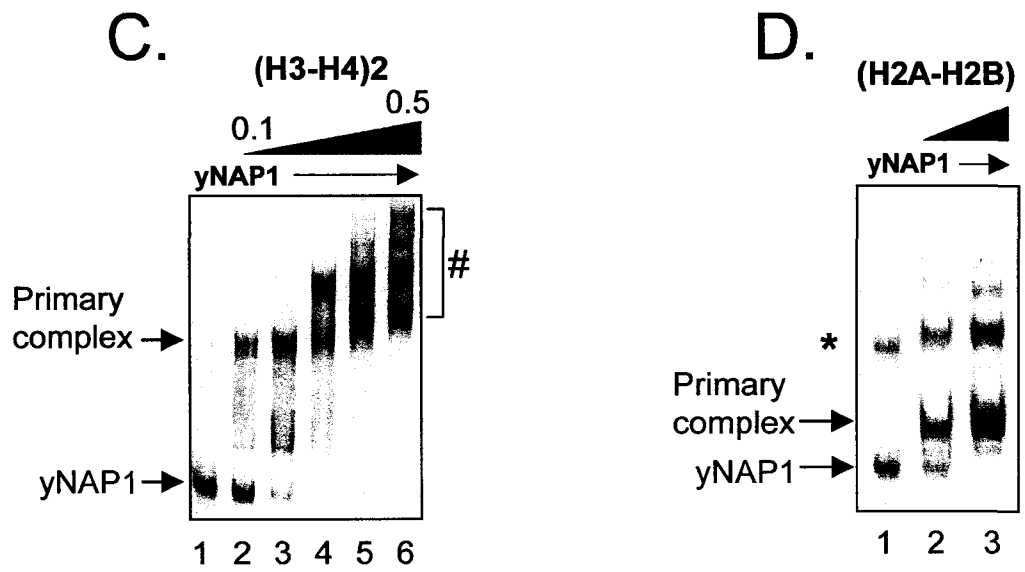

Figure 2.2C, D: Visualization of higher-order yNAP1-histone complexes (EMSA). (C) To visualize higher-order complexes, increasing ratios of the histone (H3-H4)2 tetramer (0.1 to 0.5 molar equivalents) were incubated with a constant amount of yNAP1. Analysis and visualization was as described for panel A. # indicates larger complexes formed as histone:yNAP1 ratios increase. (D) 150 μM yNAP1 was diluted to 10 μM and incubated in the absence and presence of the histone (H2A-H2B) dimer (0.25 and 0.5 molar equivalents. Analysis and visualization was as described for panel A. * indicates the additional band of yNAP1 not seen at lower concentrations,

The higher (slower migrating) yNAP1 band observed in figure 2.2D (lane 1, asterisked) is routinely observed when using a highly concentrated solution of yNAP1 (150 μM), and persists in the presence of reducing agent. It possibly represents a higher association state also observed by other methods (S. M. and Peersen, manuscript in preparation). Although we were able to eliminate this in subsequent experiments by dilution and extensive dialysis at concentrations less than 20 μM, it is noteworthy that this oligomer is competent for histone binding as a slight decrease in mobility is seen in the presence of (H2A-H2B) (Figure 2.2D, lane 2). At increased histone ratios, higher-ordered complexes between yNAP1 and the (H2A-H2B) dimer (or the $(H3\text{-}H4)_2$ tetramer) are formed. These formed as histones were titrated above the 0.25:1 ratio of tetramer to yNAP1, and 0.5:1 dimer to yNAP1 (denoted by #: Figure 2.2B, lanes 8-10, Figure 2.2C, lanes 4-6).

Quantitation of yNAP1 binding to the histone dimer and tetramer was performed by plotting the concentration of free yNAP1 (digitized pixels) versus the molar ratio of histone to yNAP1. We performed a linear extrapolation of the data to the x-intercept, which indicates the molar ratio of histone to yNAP1 where 100% of yNAP1 is in complex (Fig 2.2E, 2.2F). The value obtained for (H2A-H2B) (0.56, +/- 0.09, N=4), indicates that yNAP1 binds ~0.5 molar equivalents of the dimer. Similarly, the value for $(H3\text{-}H4)_2$ (0.29, +/- 0.04, N=3) indicates that yNAP1 binds ~0.25 molar equivalents the tetramer. Thus, two yNAP1 molecules bind a histone dimer, while four yNAP1 molecules bind a histone tetramer. This data supports the hypothesis that one yNAP1 molecule binds to each histone present in the respective histone complexes.

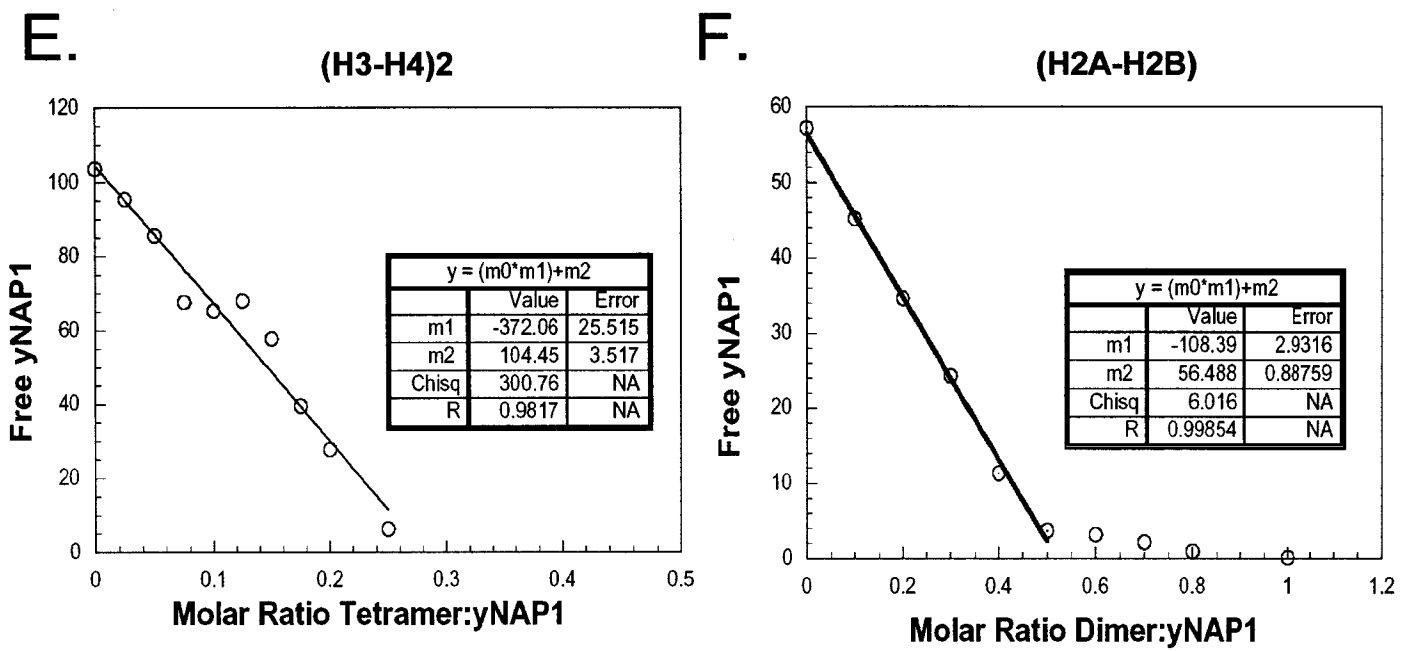

Figure 2.2E, F: Quantitation of yNAP1-histone complexes by EMSA. (E) Representative plot of histone tetramer titration onto constant yNAP1 used for stoichiometric quantitation. The abscissa shows the amount of free yNAP1 (as digitized pixels), while the ordinate shows molar ratios. Linear curve fit and extrapolation to the X-intercept yields stoichiometry of histone to yNAP1. (F) Representative plot of histone dimer titration onto constant yNAP1 used for stoichiometric quantitation. Axes and analysis are similar to (E).

2.4C The N-terminal histone tails are not required for binding to yNAP1, but provide selectivity for the $(H3\text{-}H4)_2$ tetramer.

Previous approaches using trypsin-treated native histone preparations (McQuibban *et al.*, 1998) revealed little or no binding to tailless octamers. We directly examined the interaction of yNAP1 with tailless core histones using yNAP1 GST pull-down assays. Figure 2.3A shows that yNAP1 binds 'tailless' histone dimers and tetramers with approximately equal apparent affinity (compare lanes 2 and 6). Thus, the preference of yNAP1 for the $(H3/H4)_2$ tetramer might be due to additional interactions between yNAP1 and the N-terminal tails of either histone H3 or H4. To test this hypothesis, GST-fusion proteins with the N-terminal tails of *S. cerevisiae* core histones were tested for their ability to bind yNAP1 in a GST pull-down assay. Figure 2.3B shows that no yNAP1 binding was detected to the N-terminal tail of either histone H2A or H2B (lanes 3-6). In contrast, robust yNAP1 binding to the N-terminal tails of histone H3 (lanes 7, 8), and modest binding to the tail of H4 (lanes 9, 10), was observed.

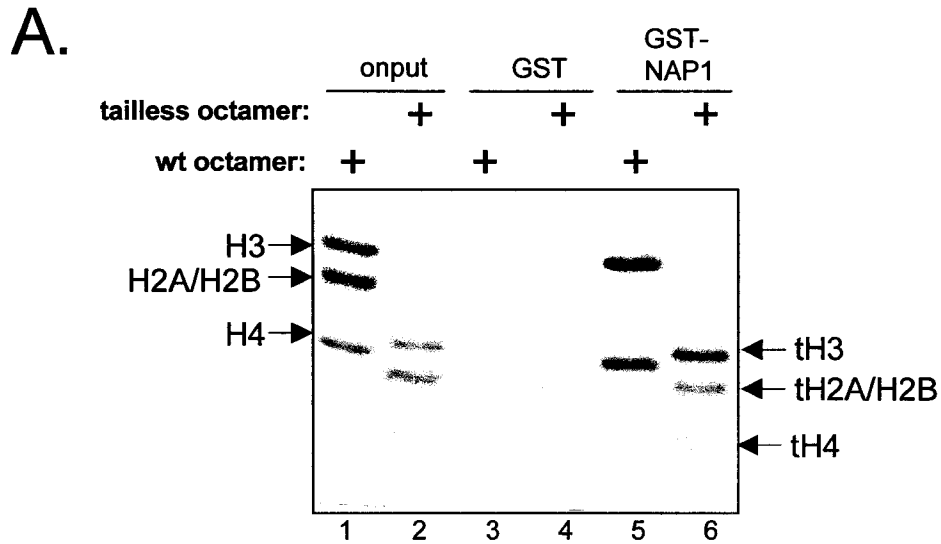

Figure 2.3A: Direct binding of yNAP1 to the tailless octamer. yNAP1 GST pull-down assays on the wild type and tailless histone 'octamer'. Purified full-length histone octamer (wt octamer) and N-terminally deleted octamer (tailless octamer) (50 pM each) were incubated with 100 pM GST alone, or GST-yNAP1 fusion protein bound to glutathione agarose beads. Bound proteins were identified by 18% SDS-PAGE followed by Coomassie staining. Forty percent of each onput is shown. Non-specific protein-protein interactions were monitored using GST alone (lanes 3,4). The positions of the intact and tailless histones are indicated, with a "t" prefix denoting tailless.

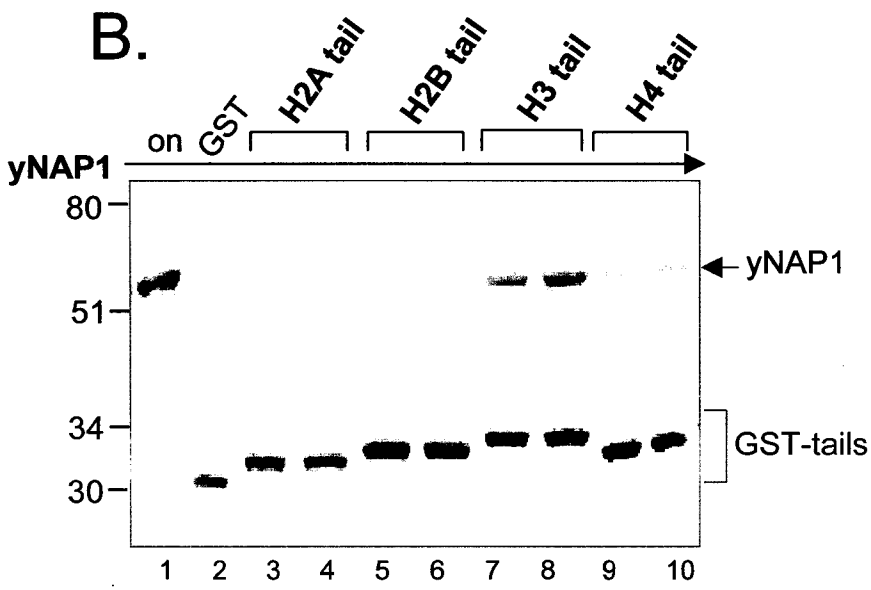

Figure 2.3B: Direct binding of yNAP1 to the H3 and H4 histone tails. Analysis of yNAP1 binding to the histone N-terminal tails by GST pull-down. Two concentrations of yNAP1 (50 and 100 pM; left and right lane within each bracket, respectively) were incubated with GST alone, or GST-histone tail fusion proteins (GST-H2A tail, GST-H2B tail, GST-H3 tail, and GST-H4 tail) (100 pM each) bound to glutathione agarose beads. Bound proteins were separated by 15% SDS-PAGE and visualized by Coomassie staining. Onput (lane 1) contains 20 pM of yNAP1. The GST control was performed in the presence of 100 pM yNAP1 (lane 2). Bound yNAP1, the GST-histone tails and protein standards are indicated.

2.4D Distinct domains of yNAP1 are required for histone binding and chromatin assembly.

An earlier study utilized convenient restriction sites within the coding region to generate deletion mutants of yNAP1 (Fujii-Nakata *et al.*, 1992). To extend this study, we subjected yNAP1 to limited trypsin proteolysis in order to gain insight into its functional domains. This revealed two stable products with apparent molecular weights of 33 and 24 kDa (Figure 2.4A). Subsequent mass spectrometry and N-terminal sequencing of the digestion products revealed that the larger peptide consisted of amino acid residues 74-293 (calculated molecular weight 25,099 kDa), while the smaller peptide comprised residues 302-417 (molecular weight 13,212 kDa) (data not shown). The C-terminal fragment contains a majority of acidic residues, accounting for its anomalously slow migration on SDS PAGE. Attempts to separate and purify the two cleavage products by conventional ion exchange, hydrophobic, and gel filtration chromatography failed (data not shown). Only denaturing, reverse phase HPLC resolved the two peptides. There are additional cleavage sites C-terminal to arginine 301 that were not accessible to trypsin. We therefore concluded that the cleavage site is located in a flexible surface loop of a single-domain protein encompassing amino acids 74 – 417.

Based on these results and on sequence comparisons, we next generated a series of deletion mutants of yNAP1. Figure 2.4B shows these constructs schematically, including relevant features.

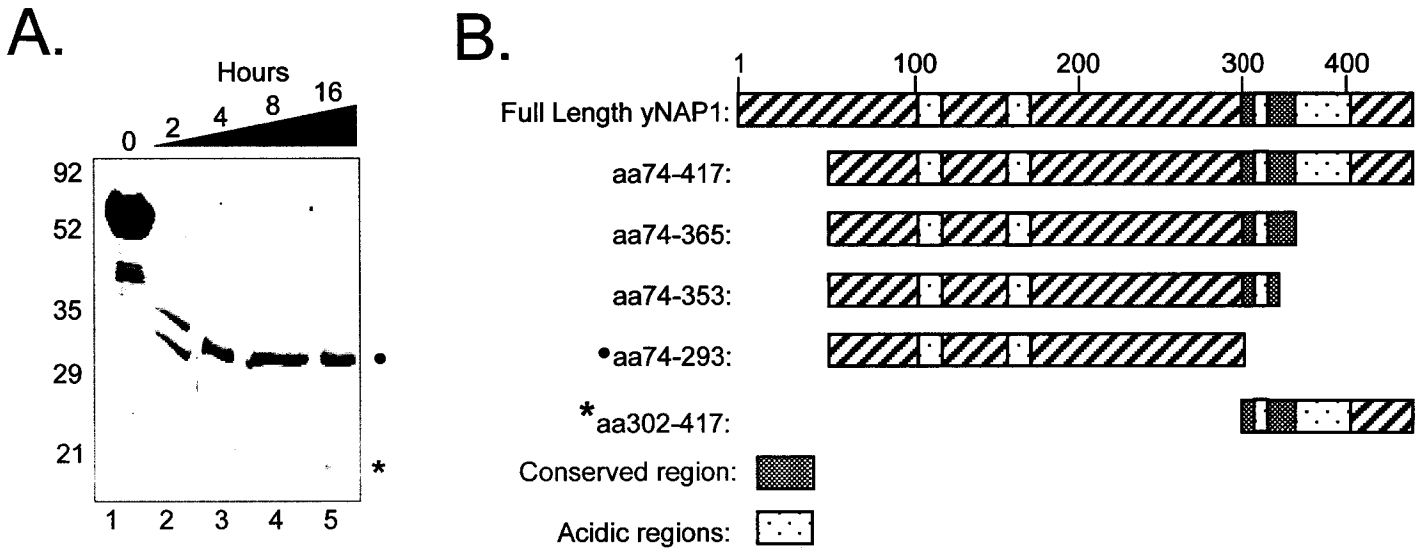

Figure 2.4 A, B: Proteolytic cleavage of yNAP1. (A) Proteolysis of yNAP1 reveals two stable polypeptides. Purified yNAP1 (60 µg) was incubated with trypsin (0.06 µg) for the indicated times. Aliquots from the time course were separated on 15% SDS-PAGE, and visualized by Coomassie staining. Lane 1 shows 10 µg undigested yNAP1. The two yNAP1 proteolytic digestion products are denoted by symbols, and protein standards are indicated. (B) Schematic illustration of yNAP1 truncation mutants constructed based on the proteolysis described in A. The coordinates and significant structural features of yNAP1 are shown.

The secondary structure of all deletion mutants was analyzed by circular dichroism. The CD spectrum of full-length yNAP1 (Figure 2.4C) indicates a ~25 % content in α-helix. We used this as a measure of the structural integrity of the deletion mutants. Due to its presumably unstructured N-terminal region, full-length yNAP1 is less helical (on a per residue basis) than the smaller N- and C-terminally deleted constructs (amino acids 74-417 and 74-365, respectively). However, deletion of 12 more residues from the C-terminus (construct 74-353) generated a CD spectrum displaying significant loss of negative intensity at 222 nm, indicative of substantial loss of α-helical character. Thus, the residues spanning 354-365 contribute substantially to the structural integrity of the protein. This region harbors a stretch of amino acids that is extremely well conserved within the NAP1 family (Pro-Arg-Ala-Val-Asp-Trp-Phe-Thr-Gly, amino acids 354-362). The C-terminal construct (aa 302-417), that was intimately associated with the core region (aa 74-293) following limited proteolysis, appears unstructured when assayed in isolation.

All yNAP1 deletion mutants were tested for their ability to assemble nucleosomes onto plasmid DNA. Topological assays indicated that only amino acids 74-365 are required for robust chromatin assembly (Figure 2.4D). The loss of the largest acidic region of yNAP1 (amino acids 365-417) had little effect on chromatin assembly, consistent with a previous report (Fujii-Nakata *et al.*, 1992). As inferred from the vital role of amino acids 354–365 in maintaining structural integrity, the loss of these amino acids (fragment 74-353) resulted in significant loss of chromatin assembly activity (Figure 2.4D).

C.

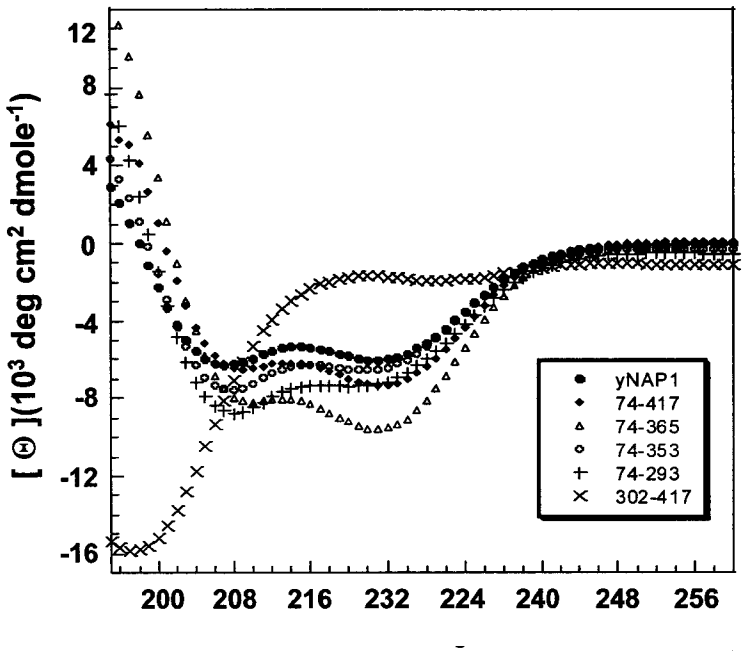

Figure 2.4C: Deletion mutants of yNAP1 reveal distinct domain structure-function relationships (CD). Circular dichroism (CD) analysis of the structural integrity of the truncated yNAP1 proteins. Spectra are buffer corrected, and normalized for concentration and number of residues to allow direct comparison of secondary structure content between proteins.

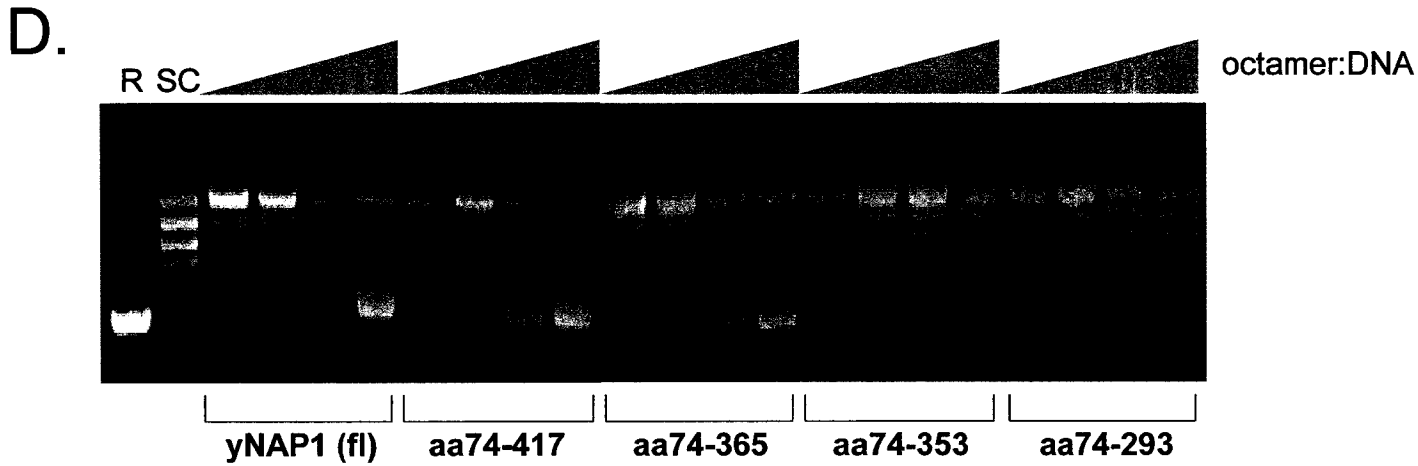

Figure 2.4D. Deletion mutants of yNAP1 reveal distinct domain structure-function relationships (topological). Chromatin assembly properties of the yNAP1 deletion mutants. One-dimensional DNA topological assay comparing chromatin templates assembled with recombinant core histones in the presence of the indicated yNAP1 deletion mutant. The DNA topoisomers were resolved on an agarose gel, and the DNA stained with SYBR-Gold. The supercoiled (SC) and topoisomerase-1 relaxed (R) DNA, and the increasing octamer: DNA ratios (0.14:1, 0.43:1, 0.71:1, 1:1) are indicated. Assembly function of the yNAP1 mutants was assessed by the ability of the proteins to induce supercoils (reflective of nucleosome deposition) into the relaxed, circular DNA plasmid.

Similarly, a construct representing the larger of the trypsin proteolysis fragments (aa 74-293) failed to assemble chromatin. The trace amounts of supercoiled DNA observed for yNAP1 aa 74-293 and aa 74-353 are similar to that observed in the absence of yNAP1 (data not shown). As expected, the construct representing the smaller of the proteolysis fragments (aa 302-417) also failed to assemble chromatin (data not shown). Results from CD and nucleosome assembly assays for each yNAP1 fragment are summarized in Table 2.1.

2.4E The unstructured, acidic C-terminus of yNAP1 binds basic proteins in a non-specific manner.

Irrespective of chromatin assembly activity, all of the constructs tested above retained the ability to bind both types of histone sub-complexes (Figure 2.5A). Interestingly, the most C-terminal construct (yNAP1 aa 302-417), though lacking secondary structure and chromatin assembly activity, bound histone dimers and tetramers as strongly as full-length yNAP1 (Figure 2.5A, compare lanes 3 and 6, and lanes 10 and 13). Figure 2.5B demonstrates that all the deletion constructs tested were also capable of binding both the full-length and tailless histones (Table 2.1). Interestingly, with the exception of GST-302-417 (lanes 11 and 12), all of these constructs showed a clear preference for H3 and H4 if incubated with full-length histones, and this preference disappeared upon incubation with tailless histones. GST-302-417 retained nearly equivalent ratios of dimer and tetramer, independent of the histone tails (Figure 2.5B, compare lanes 11 and 12).

A.

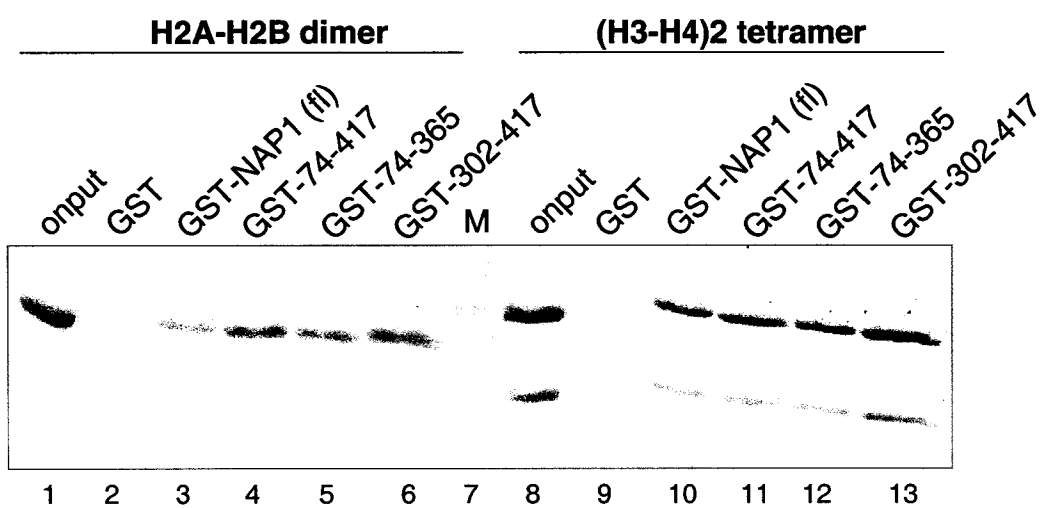

Figure 2.5A: Deletion mutants of yNAP1 binding histone pairs. yNAP1 deletion mutants bind the dimer and tetramer. GST pull-down assay with yNAP1 deletion mutants and the (H2A-H2B) dimers and (H3-H4)2 tetramers. Purified histone dimers (90 pM) (lanes 2-6), or tetramers (47 pM) (lanes 9-13) were incubated with GST alone, or the indicated GST-yNAP1 fusion proteins (GST-NAP [fl], GST-74-417, GST-74-365, GST-302-417) (100 pM each) bound to glutathione agarose beads. Bound proteins were separated by 18% SDS-PAGE and visualized by Coomassie staining. Forty percent of the dimer and tetramer onput is shown in lanes 1 and 8. The 16 kDa molecular weight marker is shown in lane 7. Non-specific protein interactions were monitored using GST alone (lanes 2, 9).

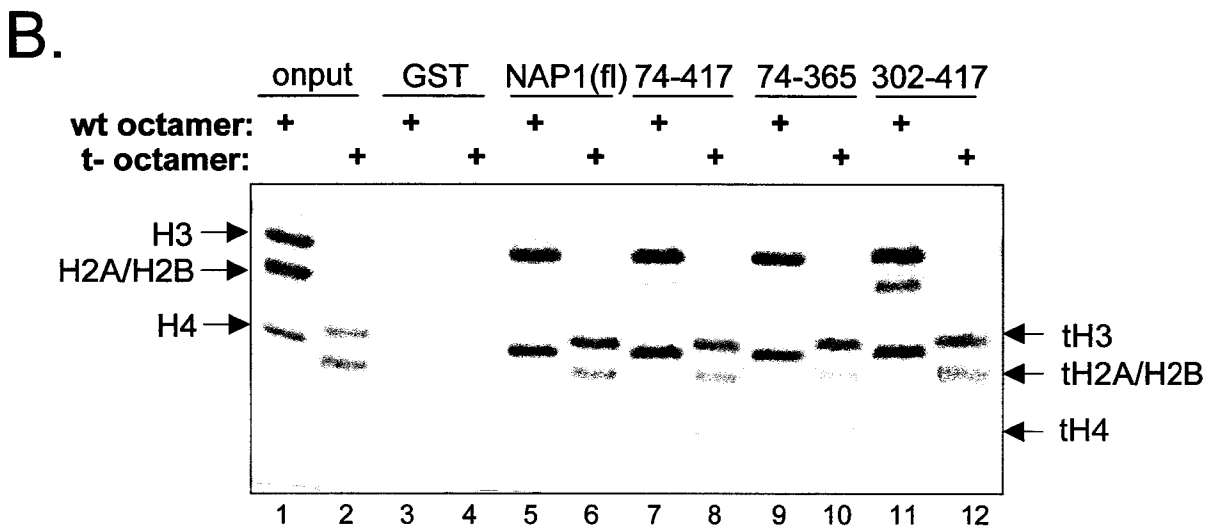

Figure 2.5B: Deletion mutants bind tailless histones with less (H3-H4) preference. yNAP1 deletion mutants bind to the both full-length (wt) and tailless octamer. Purified full-length and N-terminally deleted octamers (50 pM each) were incubated with GST alone, or the indicated GST-yNAP1 fusion proteins (100 pM each), as described in panel A. Forty percent of the wt and tailless octamer onput is shown in lanes 1 and 2. Bound histone proteins are indicated to the right and left of the figure. The tailless histones are denoted with a "t" prefix.

Because of the highly acidic and unstructured nature of this C-terminal yNAP1 construct, it is likely that the binding results from an electrostatic, structure-independent interaction with the basic histone proteins.

We sought to determine which regions of yNAP1 were responsible for preferential binding to the H3 and H4 N-terminal tails, and thus for conferring selectivity for the $(H3\text{-}H4)_2$ tetramer. We tested yNAP1 constructs which either contain or lack the acidic C-terminus for their ability to bind isolated, H3 and H4 N-terminal tails. Figure 2.5C shows that yNAP1 74-417, which functions in chromatin assembly and histone binding assays similar to full-length yNAP1, interacts strongly with both the N-terminal tails of H3 and H4 (Figure 2.5C, lanes 3, 4). This binding is comparable to the binding of full-length yNAP1 (see Figure 2.3B, lanes 7-10). Carboxyl-terminal deletion of amino acids 417-366 (yNAP1 74-365) resulted in significant loss of histone H3 binding, and completely abrogated H4 tail binding (Figure 2.5C, lanes 7, 8).

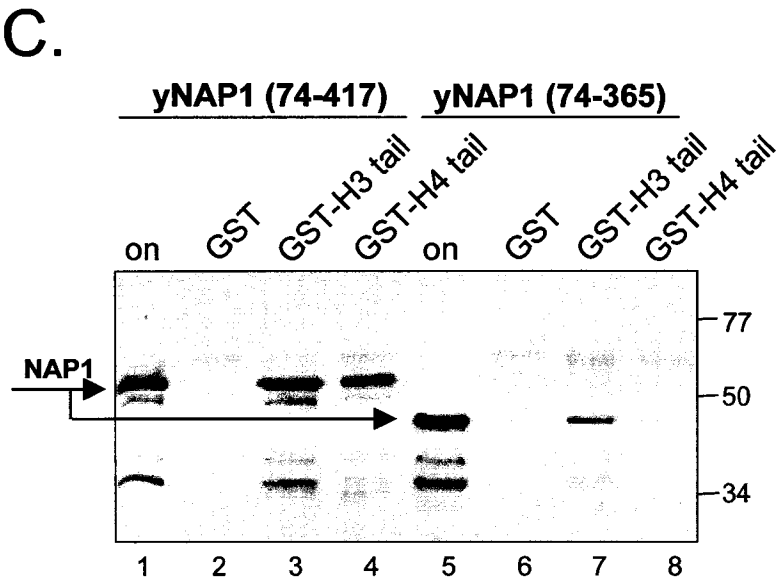

Figure 2.5C: The C-terminal portion of yNAP1 is required to bind the N-terminal histone tails. Deletion of the yNAP1 C-terminus reduces histone tail binding. Purified His6-tagged yNAP1 deletion mutants (aa74-417, lanes 1-4) or aa74-365, lanes 5-8) (20 pM each) were incubated with GST alone, or the indicated GST-H3 or -H4 tail (10 pM each). Bound yNAP1 deletion mutants were separated by 12% SDS-PAGE and probed with an anti-His6 antibody for Western blot analysis. Twenty five percent onput of each yNAP1 mutant is shown in lanes 1 and 5. Note: the smaller polypeptides also recognized by the anti-His6 antibody are minor impurities or C-terminal degradation products of yNAP1.

To investigate whether this interaction was simply based on electrostatic interactions, or whether it was specific for histone tails, we compared the abilities of full-length and truncated yNAP1 to interact with purified native *Drosophila* histone H1 in a GST pull-down assay (Figure 2.5D, Table 2.1). Histone H1 is highly basic, but does not contain the histone fold, and there is no sequence homology between it and the core histones (compare Figures 1.2A and 2.5E). Full-length GST-yNAP1 bound well to H1, although deletion of the C-terminal acidic region (aa 366-417) completely abrogated H1 binding. A fragment containing the acidic region (aa 302-417) bound H1 as well as full-length yNAP1. Thus, it appears that yNAP1 contains two distinct binding domains. The first, which is contained within the central region of the protein (aa74-365), specifically recognizes the histone fold. The second, located at the extreme C-terminus of yNAP1 (aa 365-417), is responsible for nonspecific binding to positively charged proteins. Figure 2.6 shows the histone binding domains schematically.

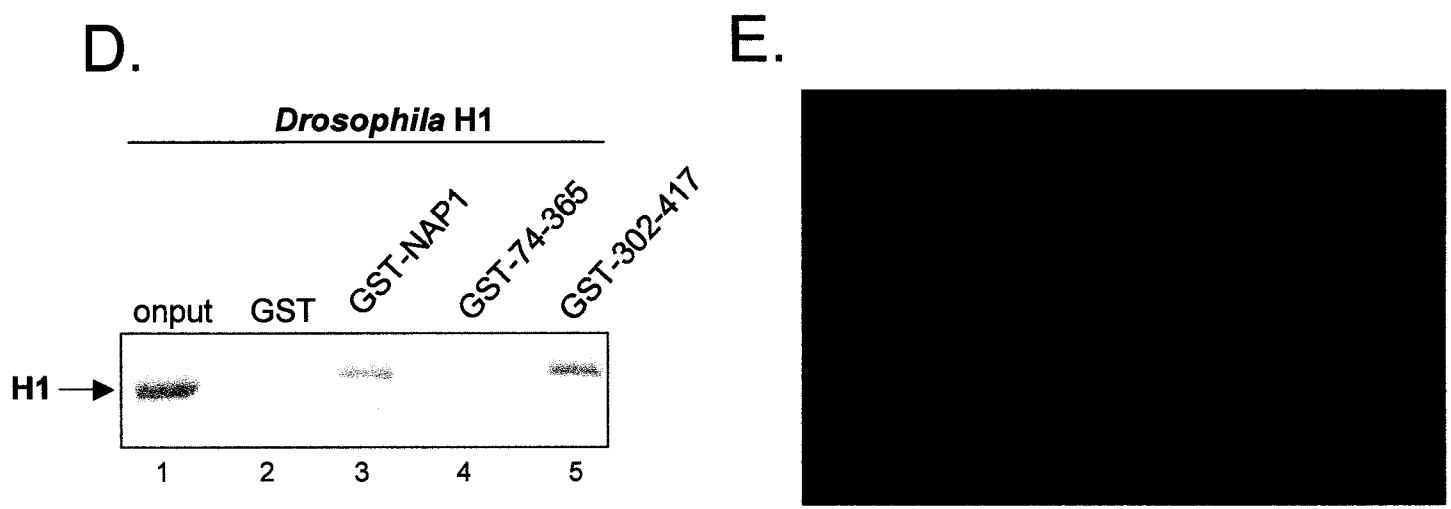

Figure 2.5D and E: The C-terminal portion of yNAP1 has a non-specific binding property. (E) The acidic C-terminus mediates binding to a histone-fold lacking, basic protein. Purified *Drosophila* histone H1 (100 pM) was incubated with GST alone, or the indicated GST-yNAP1 deletion mutant (100 pM). Bound H1 was separated on 15% SDS-PAGE and visualized by Coomassie staining. Twenty five percent H1 onput is shown in lane 1. (F) The NMR structure of histone H1 shows its lack of structural similarity to the core histones. The central 'winged helix' motif (green) is flanked on either side by large, basic, and unstructured N- and C-terminal extensions (blue), which become ordered only upon DNA binding. Figure from Cerf, *et al.*, 1993

Table 2.1: Properties of yNAP1 and Derivatives.

				Histone binding:			
yNAP1 construct:	Assembly	Solubility	$(H3\text{-}H4)_2$ Preference	H2A/H2B	H3/H4	H3/H4 tails	H1
yNAP1	+	+	Yes	+	+	+	+
aa74-417	+	+	Yes	+	+	+	+
aa74-365	+	+	No	+	+	–	–
aa74-353*	–	–	nd	nd	nd	–	nd
aa74-293*	–	–	nd	nd	nd	–	nd
aa302-417	–	+	No	+	+	+	+

* The indicated His_6-tagged yNAP1-truncated proteins were soluble only following urea denaturation/ renaturation. The renatured protein was used in the topological, and tail-binding assays. The GST-tagged proteins were insoluble, and therefore could not be used in the GST pull-down assays (histone binding assays).

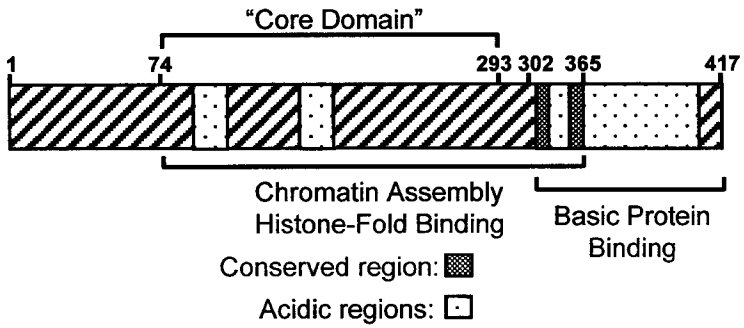

Figure 2.6: Schematic of functional domains on yNAP1. The protease resistant "core domain", minimal chromatin assembly domain, and basic protein binding domain are indicated, as are the conserved and largest acidic regions.

2.5 Discussion:

Here, we demonstrate through direct binding and competition assays that yNAP1 preferentially binds the $(H3\text{-}H4)_2$ tetramer over the (H2A-H2B) dimer. We established the stoichiometry of binding by gel shift assay, and determined that one yNAP-1 dimer binds one histone-fold dimer. The preference for $(H3\text{-}H4)_2$ is conferred by the N-terminal tails of H3 and H4, which interact directly with yNAP1. No binding of yNAP1 to the N-terminal tails of H2A and H2B is observed. We further demonstrate that the acidic C-terminal region of yNAP1 participates in H3 and H4 tail binding, and that this region also binds other basic proteins due to nonspecific charge-charge interactions.

The observation that yNAP1 preferentially binds recombinant $(H3\text{-}H4)_2$ over (H2A-H2B) contradicts previous studies showing preferential binding of 'native' H2A and H2B (Ishimi *et al.*, 1987; McQuibban *et al.*, 1998). We showed that the preference towards the tetramer occurs with both recombinant and native histones, and thus the discrepancies with earlier studies are unlikely to be a consequence of posttranslational modifications that are only found in native histones. Differences in results may stem from differences in the assays used to demonstrate binding, and in the folding and aggregation state of the histones. Here, we studied the binding of refolded and highly defined histone (H2A-H2B) dimers and $(H3\text{-}H4)_2$ tetramers to yNAP1 by gel filtration, native gel electrophoresis and direct binding assays. To our knowledge, these complexes are structurally equivalent to the *in vivo* substrate. In contrast, the two previous studies either used far-western analysis to detect NAP1 binding to individual

denatured core histones that have been separated by SDS-PAGE and blotted to a membrane (McQuibban *et al.*, 1998), or utilized a modified ELISA to determine the binding preference of the human homolog AP-1 (Ishimi *et al.*, 1987). None of these assays would work properly if the histone fold is what is recognized. Thus, the observed difference may well be a result of the integrity of the histone substrate used. In addition, the modified ELISA relied on antibody recognition of fixed / immobilized AP-1 / histone complexes, which may have sterically hindered the AP-1 epitope, particularly with the larger $(H3\text{-}H4)_2$ complex. Perhaps yNAP1 only displays its preference for the $(H3\text{-}H4)_2$ tetramer when presented with homogeneous, folded histone-pairs. Additionally, while the NAP1 homologs share considerable amino acid similarities, some differences, including a long N-terminal acidic region in the case of human AP-1, do exist.

We established a binding stoichiometry of 0.5 molar equivalents of (H2A-H2B) dimer, and 0.25 molar equivalents of $(H3\text{-}H4)_2$ tetramer per mole of yNAP1. Due to the internal symmetry of the histone fold, each (H2A-H2B) dimer exposes two structurally similar histone-fold faces on the surface, whereas the tetramer exposes four histone-fold faces (Akey and Luger, 2003; Arents and Moudrianakis, 1995). We thus conclude that each yNAP1 monomer is capable of binding one histone fold motif. Attempts to determine binding constants were limited by the sensitivity of Coomassie staining, which mandated the use of NAP1 amounts, well above the likely dissociation constant (Kd) for these complexes. Both fluorescent and radio-isotopically labeled yNAP1 showed aberrant native gel mobility and/or hindered/abrogated histone binding capability.

In direct competition assays, yNAP1 shows a marked preference for the tetramer over the dimer, whi9ch is a consequence of the preferential binding of yNAP1 to the N-terminal tails of H2 (and, to an extent, H4) over those of H2A and H2B. Thus, we propose that the histone fold domains as well as the N-terminal tails of the histones contribute to binding, and that the relative affinities of the two histone complexes may be modulated by post-translational modifications of the histone tails. The acidic C-terminus of yNAP1 (aa 365-417) appears to contribute to the overall affinity due to its acidic nature, whereas the domain of yNAP1 that specifically recognizes the structural properties of the histone fold dimer (either H2-H4 or H2A-H2B) resides between yNAP1 amino acids 74-365. The acidic domain also is responsible for the preference in recognizing the H3 N-terminal tail. The protein binding characteristic of yNAP1 domains are summarized in Table 2.1.

An additional observation arises from careful inspection of gel shift experiments where increasing concentrations of histones were added to yNAP1. With concentrated solution of yNAP1 we observe an additional band that is also shifted upon the addition of histones. yNAP1 thus appears to display concentration-dependent oligomerization, consistent with the high MWapp observed by analytical gel filtration, as well as by hydrodynamic measurements of yNAP1 (S. McBryant and O. Peersen, manuscript in preparation). An early study with the *Drosophila* homolog reported that dNAP1 elutes from gel filtration and sediments in a glycerol gradient as a much larger species (600 kDa and 120 kDa, respectively) (Ito *et al.*, 1996). The *Xenopus* histone binding protein

nucleoplasmin exists as a pentamer (Dutta *et al.*, 2001; Earnshaw *et al.*, 1980), as does the *Drosophila* nucleoplasmin like protein dNLP (Namboodiri *et al.*, 2003). Our own experiments using gel filtration also showed a large increase in MWapp upon addition of $(H3\text{-}H4)_2$ tetramer. Ligand- or concentration- induced changes in the oligomerization state, and the expected symmetries resulting from self-association likely play a role in histone-fold recognition, binding and release by yNAP1 *in vivo* (Akey and Luger, 2003).

The acidic C-terminus of yNAP1 has been shown to be dispensable for chromatin assembly (Fujii-Nakata *et al.*, 1992; herein (Figure 2.4D). How might this domain function in nucleosome assembly *in vitro*? We propose that this acidic region acts through an electrostatic mechanism to enhance the histone binding activity of yNAP1. As our chromatin assembly reactions contain significant amounts of yNAP1, and were allowed to proceed for 16 hours, the requirement for this 'ancillary' function of the acidic C-terminus may be negated. It is possible that a thorough comparative, kinetic analysis of yNAP1 and select deletion mutants could test the plausibility of this hypothesis.

What is the implication of our results for nucleosome assembly? The fact that the $(H3\text{-}H4)_2$ tetramer organizes the central turn of the DNA supercoil (Davey *et al.*, 2002; Luger *et al.*, 1997a) requires its deposition onto the DNA prior to the deposition of the two dimers. The $(H3\text{-}H4)_2$ tetramer acquires a unique set of lysine acetylations, and is then deposited onto the DNA by CAF1, RCAF, N1/N2, or other factors (Chang *et al.*, 1997; Sobel *et al.*, 1995; Tyler, 2002). However, we and others have found that yNAP1 assembles nucleosomes onto plasmid

DNA in the absence of other chaperone factors, and that these nucleosomes are closely and regularly spaced (146 bp) (McQuibban *et al.*, 1998; Pilon *et al.*, 1997b; Terrell *et al.*, 2002). Further, it has been shown *in vitro* by an elegant set of experiments (Nakagawa *et al.*, 2001) that the tetramer can be bound by NAP1 and transferred to a supercoiled plasmid to form a looped DNA / $(H3\text{-}H4)_2$ complex, a 'tetrasome'. When a NAP1 / (H2A-H2B) complex is added, a dimer is transferred to this 'tetrasome' in proportion to the amount of tetramer present. No such deposition is observed in the absence of tetramer, indicating that dimer deposition depends on the protein – protein interactions between the DNA-bound $(H3\text{-}H4)_2$ tetramer and (H2A-H2B). We have also observed that (H2A-H2B) dimers can be exchanged from a folded nucleosome in a yNAP1 – dependent manner, but that under the same conditions the exchange of $(H3\text{-}H4)_2$ tetramer is virtually non-existent (Y.J. Park and K.L., unpublished results). Thus, it appears that it is both the difference in affinity between the dimer and tetramer for NAP1, as well as the increased affinity of the (H2A-H2B) dimer for the $(H3\text{-}H4)_2$ tetramer – DNA complex as compared to free DNA, which ensures the ordered deposition of histones *in vitro*.

Our results shed light on the mode of recognition and binding of histone sub-complexes by NAP1. However, many questions remain open. For example, what is the mechanism of yNAP1-dependent deposition onto DNA? How are histone sub-complexes released from the complex with yNAP1 in the presence of DNA? How can yNAP1 bind and remove a histone dimer from intact chromatin? And finally, what is the true function of NAP1 *in vivo*? One attractive hypothesis is that

NAP1 not only participates in the replication-dependent assembly of chromatin, but also plays a role in the exchange of (H2A-H2B) dimers (and possibly, in the incorporation of histone H2A variants) during interphase, for example during transcription, recombination, or repair. Indeed, (H2A-H2B) dimers have been shown to exchange at a more rapid rate than the $(H3\text{-}H4)_2$ tetramer *in vivo* (Kimura and Cook, 2001). yNAP1 has also been shown to be receptive to (H2A-H2B) which has been released from nucleosomes subsequent to remodeling and histone acetylation (Ito *et al.*, 2000). Finally, it was recently proposed that transcription by RNA polymerase II through nucleosomes results in the transient formation of a 'hexasome', a nucleosome from which one (H2A-H2B) dimer has been removed (Baer and Rhodes, 1983; Kireeva *et al.*, 2002). The potential of NAP1 to participate in and facilitate all of these vital processes warrants further investigation.

Acknowledgements.

We would like to thank Raji Edayathumangalam and Srinivas Chakravarthy for their help in the preparation of recombinant histones, and Kasey Konesky for the native histone H1. The GST-tail constructs were a generous gift from Dr. Michael Grunstein. We thank Dr Robert Woody for his expertise in analyzing CD data and his critical analysis of binding data. We also appreciate the contributions of Young-Jun Park towards the progress of this study, as well as for making unpublished data available to us. The intellectual input of Dr. Olve Peersen is also acknowledged. This study was supported by a grant from the

National Institutes of Health/NCI to JKN (CA80002), and by a grant from the NIH/NIGMS (GM067777) to KL.

Chapter 3

The yeast nucleosome assembly protein is an obligate homodimer which self-associates into higher-order oligomers

This chapter is being prepared for submission for publication in the journal Biochemistry. The text of this manuscript is presented exactly as it was prepared for submission, at the time of the preparation of this dissertation. All figures that are included in that submission are included herein. Additional experiments performed during this investigation that were not submitted for publication, yet are relevant to the investigation, will be included in Chapter 4. The author list for this submission is as follows: McBryant, S.J., O.B. Peersen. All experiments were performed by S.M..

3.1 ABSTRACT:

The self-association properties of the yeast nucleosome assembly protein 1 (yNAP1) have been investigated using biochemical and biophysical methods. Non-denaturing electrophoresis and protein cross-linking of yNAP1 indicate the presence of multiple species at physiological ionic strength. A broad elution profile seen upon gel filtration chromatography is converted to a more discrete peak by the use of higher ionic strength, and this conversion is independent of concentration. Sedimentation velocity analytical ultracentrifugation reveals strong concentration dependence at physiologic ionic strength. A range of species of ~ 4.5 to 12 S is seen, though no discrete species are discernable within the sedimentation velocity boundaries. This indicates a rapid association-dissociation equilibrium on the time scale of the experiment. This range of species is rapidly and reversibly converted to a homogeneous 4.7 S species with an increase in ionic strength. Sedimentation equilibrium data collected at multiple loading concentrations, ionic strengths, and rotor speeds were fit to a variety of self-association models. The 4.7 S species captured at high salt is shown to be yNAP1 dimers, and at physiologic ionic strength these self-associate to form tetramers and hexamers. The association constants for the dimer to tetramer and tetramer to hexamer are very similar, and fall within the range of concentrations sampled in these experiments. A plot of the weight average molecular weight obtained from equilibrium analysis versus concentration strongly suggests the hexamer to be the terminal species. Finally, the addition of 1 M guanidine

hydrochloride converts the heterogeneous mixture to the homogeneous 4.7 S species, even at physiological salt concentration. Slightly higher concentrations were sufficient to convert the 4.7 S species to a 2.5 S species, consistent with the modeled S value for a yNAP1 monomer. Sedimentation equilibrium of guanidine denatured samples confirms the identity of the 2.5 S species as yNAP1 monomers. Circular dicroism indicates that the initial transition from a polydisperse to monodisperse population with the addition of guanidine requires only a minimum change in secondary structure. The final conversion to monomer is concomitant with nearly a complete loss of secondary structure. Together, these results indicate that yNAP1 forms dimers that rapidly and reversibly self-associate in solution. The dimeric nature of the fundamental unit may have implications for the histone binding activity and nucleosome assembly function.

3.2 INTRODUCTION:

Incorporation of the genetic material into highly organized chromosomes is a hallmark of eukaryotes. The fundamental unit of chromatin is the nucleosome, a repeated assembly of basic histone proteins and DNA that facilitates the high level of compaction of the eukaryotic genome into the limited confines of the nucleus (Kornberg, 1974). It is at this level that the accessibility and utility of the genome is regulated. This nucleoprotein complex is maintained by a host of accessory proteins and ATP-dependent remodeling factors that facilitate assembly, disassembly and architectural changes which allow for the replication, repair and activated transcription of the genome (Kingston and Narlikar, 1999; Urnov and Wolffe, 2001)

The nucleosome is a large nucleoprotein assembly containing a minimum of 146 bp of DNA and an octamer of histones proteins (Richmond *et al.*, 1984). The histone octamer is composed of a central $(H3\text{-}H4)_2$ tetramer flanked on either side by two (H2A-H2B) dimers (Arents *et al.*, 1991). The positions of these histone complexes within the nucleosome, as determined by X-ray analysis, mandate that the tetramer be deposited on the DNA first, followed by the dimers (Luger *et al.*, 1997), for review see (Akey and Luger, 2003). Consistent with this, kinetic studies have determined that the (H2A-H2B) dimer exchanges rapidly while the tetramer is very stable (Kimura and Cook, 2001). The ordered assembly of the nucleosome is the responsibility of a large and often redundant family of protein factors known as histone chaperones or chromatin assembly factors (for reviews see Krude and Keller,

2001; Tyler, 2002). Generally acidic in nature, these factors serve to deposit the basic histone proteins onto the newly synthesized DNA. Well studied members of this family include the *Xenopus* factor nucleoplasmin (Np) and its *Drosophila* homolog dNLP, and the NAP-type histone chaperone (for reviews see Akey and Luger, 2003; Philpott *et al.*, 2000). Though no obvious sequence homology exists between the nucleoplasmin and NAP-type chaperones, functional similarities have led them to be grouped together within the histone chaperone family.

Np is a small (22 kDa), acidic (pI 4.73) and highly abundant nuclear factor found in *Xenopus* eggs and oocytes (Dingwall, *et al.*, 1987). Np functions autonomously in the assembly of histones onto DNA (Earnshaw *et al.*, 1980) and in concert with the H3 and H4 storage proteins N1/N2 to maintain the repository of excess histones in eggs and oocytes (Kleinschmidt *et al.*, 1990). Chemical cross-linking showed its active form to be a pentamer (Earnshaw, *et al* 1980). A recent crystallographic study confirmed this observation and noted that the symmetry of the pentamer appears to translate functionally into its ability to bind all four core histones simultaneously, possibly generating an intact histone octamer on the periphery of each component of the five-member ring (Dutta, et al., 2001). Similarly, the 17 kDa dNLP homolog was also shown by X-ray crystallography to be pentameric (Namboordiri, et al., 2003). dNLP does not function autonomously (Ito *et al.*, 1996b), and requires the $(H3\text{-}H4)_2$ chaperone dCAF-1 (Kaufman, 1996; Smith and Stillman, 1989).

The ubiquitous nucleosome assembly protein 1 (NAP1) has been well studied with regards to its nucleosome assembly activity (Fujii-Nakata *et al.*, 1992; Ito *et al.*, 1996a; Nakagawa *et al.*, 2001), and its histone binding ability (McQuibban, *et al.* 1998, McBryant *et al.*, 2003, submitted). Much larger than nucleoplasmin, the 48 kDa NAP1 is also highly acidic, with a calculated pI of 4.23 due to 24 % aspartic and glutamic acid content. Though long considered an (H2A-H2B) histone chaperone, recent evidence suggests that the affinity for $(H3\text{-}H4)_2$ is greater (McBryant, *et al.*, 2003, submitted). This result is consistent with a mechanistic investigation of NAP1 assembly function in which NAP1 sequentially deposits $(H3\text{-}H4)_2$ and then (H2A-H2B) onto DNA (Nakagawa *et al.*, 2001). NAP1 is an important tool for researchers studying chromatin transcription *in vitro*, as it functions in the assembly of uniformly spaced nucleosomes onto plasmid DNA (Ito *et al.*, 1996a; McQuibban *et al.*, 1998; Pilon *et al.*, 1997; Terrell *et al.*, 2002). Like Np, NAP1 also functions as a 'histone sink', transiently accepting (H2A-H2B) following disruption of the nucleosome during activated transcription (Ito *et al.*, 2000; Kireeva *et al.*, 2002).

Very little is known about its oligomerization state or how this may relate to its chromatin assembly function. Yeast NAP1 (yNAP1) has been reported to sediment as a higher molecular weight band in sucrose gradients (Fujii-Nakata, *et al*, 1992) and *Drosophila* NAP1 elutes from a gel filtration column with an apparent molecular weight of 600 kDa (Ito, *et al.*, 1996a). It was also reported that, unlike nucleoplasmin, yNAP1 fails to cross-link with

disuccinimidyl suberate, suggesting that yNAP1 exists as a monomer at micromolar concentrations (McQuibbban, *et al.* 1998). However, the true oligomeric state of NAP1 remains undefined.

In this study, protein cross-linking, gel filtration chromatography, analytical ultracentrifugation, and circular dichroism spectroscopy are applied to examine the self association properties of yNAP1. The data show that the fundamental unit is a dimer, and that the dimer self associates in a concentration-dependent fashion into tetramers and ultimately hexamers. A moderate amount of denaturant is required to disrupt the yNAP1 dimer, and this disruption is concomitant with a profound loss of secondary structure. Self-association of dimers into larger oligomers is governed by electrostatic attractions, and thus may be regulated by the presence of the basic histone proteins. The implications of the oligomerization of yNAP1 towards histone binding and nucleosome assembly are discussed.

3.3 Experimental Procedures

Reagents and Buffers. All buffers and solutions were made with reagent grade chemicals and distilled, deionized (Millipore) water. Analytical ultracentrifugation (AUC) buffers contained 20 mM sodium phosphate, pH 7.6, 1 mM dithiothreitol (DTT) (Sigma) and the indicated amount of sodium chloride (NaCl). Buffers were named AUC-150 etc. to indicate the sodium chloride concentration in mM. Chromatography buffers contained 20mM Tris–HCl, pH 7.6 (4 °C), NaCl at the indicated concentration, 10% glycerol, 1 mM

DTT, and 0.1 mM PMSF, except for gel-filtration experiments, where PMSF was omitted. Solutions were sterile filtered prior to use.

Protein Purification and Handling. The N-terminally T-7 epitope tagged yNAP1 (49,142 Da) was expressed in E. coli DE3 and purified essentially as described (Fujii-Nakata, *et al.*, 1984), with the following modifications. The 65% ammonium sulfate precipitant was dialyzed into 0.1 M NaCl, applied to an 8 mL Q-Sepharose Fast Flow anion-exchange column (Amersham Biosciences), and eluted with a 10 column volume linear gradient from 0.1 to1.0 M NaCl. The protein peak was determined by evaluating fractions on SDS PAGE. The ionic strength of pooled peak fractions was determined by conductivity, diluted to 150mM NaCl, and applied to a 1 mL Mono-Q anion-exchange column (Amersham Biosciences). The column was washed with 10 column volume steps at 150, 250 and 330mM NaCl, and yNAP1 was eluted at 500 mM NaCl. Appropriate fractions were analyzed by SDS PAGE and the protein peak was concentrated in Centricon C-30 units (Amicon) and dialyzed to the appropriate ionic strength prior to gel filtration chromatography (where necessary). yNAP1 purifies to > 95% as judged by SDS PAGE. All protein concentrations were determined by spectrometry (Pace *et al.*, 1995) using ε (276 nm) = 36,100 $M^{-1}cm^{-1}$.

Gel Electrophoresis. Proteins were dialyzed into 20 mM Tris pH 7.6 (4° C), 100 mM NaCl, 1 mM EDTA prior to electrophoresis. Native polyacrylamide gel electrophoresis was carried out in 1.5 mm thick, 8x10 cm, 5% acrylamide (60:1 acrylamide:bis-acrylamide) gels. Gels were pre-run in

0.2X TBE for 30 minutes prior to sample loading. Electrophoresis proceeded for 60 minutes at 150 volts at 4 °C. All gels were run in the Mini-Protean II (Biorad) and stained with Coomassie brilliant blue R250.

Chemical Cross-linking. Prior to cross-linking, yNAP1 was dialyzed extensively against 0.1 M sodium borate, pH 9.0, to remove the inhibitory, amino-rich Tris buffer from the reaction. Self-association of yNAP1 was characterized directly by chemical cross-linking using dimethyl suberimidate (Davies and Stark, 1970; Thomas and Kornberg, 1978). Solutions of dimethyl suberimidate (Sigma) were prepared in 0.1 M sodium borate, pH 9.0, at 10 mg/mL, and used at a final concentration of 1.0 mg/mL. Proteins were incubated at 0.25 mg/mL (5 μM) for the indicated times at 20-22 °C, and aliquots removed were quenched by the addition of glycine (500 mM in water) to 50 mM. The samples were dialyzed extensively against 20mM Tris (pH 7.6, 4° C), 100 mM NaCl, 1 mM EDTA and 1 mM DTT, and concentrated in Microcon C-30 micro-concentrators (Amicon). Proteins were separated by non-denaturing PAGE as described above. Native and cross-linked yNAP1 was subject to MALDI-TOF spectrometry on a Voyager DE-Pro mass spectrometer (Perseptive Biosystems) in linear mode.

Gel-Filtration Studies. Gel filtration chromatography was performed on a AKTA FPLC (Amersham Biosciences) using a Superdex S-200 16/60 (120 mL) column (Amersham Biosciences). Following equilibration in either 150 or 500 mM NaCl chromatography buffer, 100-500 μL samples were applied and run at 0.5 mL/min. The retention volumes were calibrated using the Gel

Filtration Calibration standard set (Amersham Biosciences). Kav for the standards and yNAP1 were determined as described in the calibration kit and plotted versus molecular weight on a log scale. The resulting equation for the best-fit line was used to determine the apparent molecular weight based on the Kav for yNAP1.

Analytical Ultracentrifugation Studies. All AUC experiments reported in this paper were conducted in a Beckman XL-I ultracentrifuge using absorbance optics (228 or 280 nm) at 5° C. Velocity measurements utilized a charcoal filled, Epon 2-sector centerpiece and quartz windows, 400 µl sample and 420 µl reference volumes. All samples were centrifuged in a Beckman An60Ti 4-hole rotor. Radial calibration was performed prior to each measurement to compensate for rotor stretching.

Sedimentation velocity measurements were performed at 45,000 RPM, absorbance measurements were acquired continuously in 0.002 cm increments, and the maximum attainable number of scans was collected (60-80). Velocity data were edited and analyzed using the boundary analysis methods of van Holde and Weischet as performed by Ultrascan Version 5.0 software (Demeler *et al.*, 1997). All sedimentation coefficients are reported in units of svedbergs (S), where 1 S = 1 x 10^{-13} s, and corrected to water at 20 °C (20,W). Continuous distributions of mass analysis [c(m)] were derived from continuous distributions of s [c(s)] using the SEDFIT program (Lebowitz *et al.*, 2002), as c(s) distributions are not as sensitive to the fitted parameter f/fo.

Modeling of hydrodynamic parameters was performed within the Ultrascan software.

Equilibrium experiments were performed using a six-sector, charcoal filled Epon centerpiece at three different speeds. 100 µl samples and 110 µl reference volumes were used. To account for different loading concentrations while staying within the dynamic range of the detector, absorbance data were collected at 228, 280 and 289 nm. The state of equilibrium was evaluated by comparing successive scans taken 4 hours apart and comparing each to the previous scan. The time required for equilibrium was predicted closely by the modeling feature in Ultrascan. Data were acquired in 0.001 cm increments, and 20-30 measurements were averaged at each radial position. Equilibrium data were edited and analyzed using a self-association model within Origin software (Microcal and Beckman) to determine the best fit, as shown by the appearance of random residuals. The partial specific volume (v-bar, 0.7174 at 5 °C) was calculated from the primary amino acid sequence (Perkins, 1986), and solvent densities (ρ) were calculated within the Ultrascan software. The apparent isopotential partial specific volume (φ_2'), which compensates for preferential binding of the denaturant to the protein, was calculated for solutions containing guanidine (Durchschlag, H., in *Thermodynamic Data for Biochemistry. and Biotechnology*, 1986, Chapter 3, p. 45). However, the value for solutions of 1-2 M GnHCl did not differ significantly from v-bar (0.76 vs. 0.73 at 22 °C, resp.), and thus had negligible affects on S(20,W) and Mw values.

Circular Dichroism: CD spectra were collected on a Jasco 720 spectropolarimeter at 5 °C. 20 spectra were obtained and averaged for each polypeptide in 20 mM NaH_2PO_4 pH 7.6, 75 mM NaCl. Measurement of yNAP1 extended from 260-190 nm, while those with increasing guanidine hydrochloride (GnHCl) were limited to 260-202 nm due to the high absorbance of GnHCl in the far UV. The molar ellipticity [Θ] was obtained by normalization of the measured ellipticity (Θ, in mdeg), using [Θ] = Θ *100 / (n*l*c), where n is the number of residues (430), c is the total concentration in mM and l is the cell path-length in cm (Adler *et al.*, 1973). The percentage of secondary structure types was determined by an average of the three different analyses contained within the CDPro analytical software (Sreerama and Woody, 2000). Analysis of changes in α-helical content upon addition of denaturant were calculated as described previously (Chen, *et al*, 1972).

3.4 Results:

3.4A Analysis of yNAP1 by Native Gel Electrophoresis and Chemical Cross-Linking. We have earlier noted the presence of two species upon native-gel electrophoresis of yNAP1 (McBryant, et al, 2003 submitted) (Figure 3.1A, lane 1). It appears that the slower migrating of these species is also functional, as its mobility is decreased in the presence of the (H2A-H2B) dimer (Figure 3.1A, lane 2). The decrease in mobility is less than that of the primary (lower) band, consistent with a smaller net increase in molecular weight upon histone binding. The presence or absence of reducing agents

had little or no affect on the species (data not shown), thus we believed it to be a true oligomer rather than a disulfide-linked species. We subjected yNAP1 to chemical cross-linking using dimethyl suberimidate and analyzed the products by gel electrophoresis. Denaturing SDS-PAGE gels revealed a broad, diffuse band centered at 150 kDa (data not shown). This often occurs due to the heterogeneity with which cross-linking reagents ligate their substrates, which upon denaturation causes band broadening. Native gel electrophoresis, however, revealed distinct species consistent with self-association (Figure 3.1B, denoted by *).

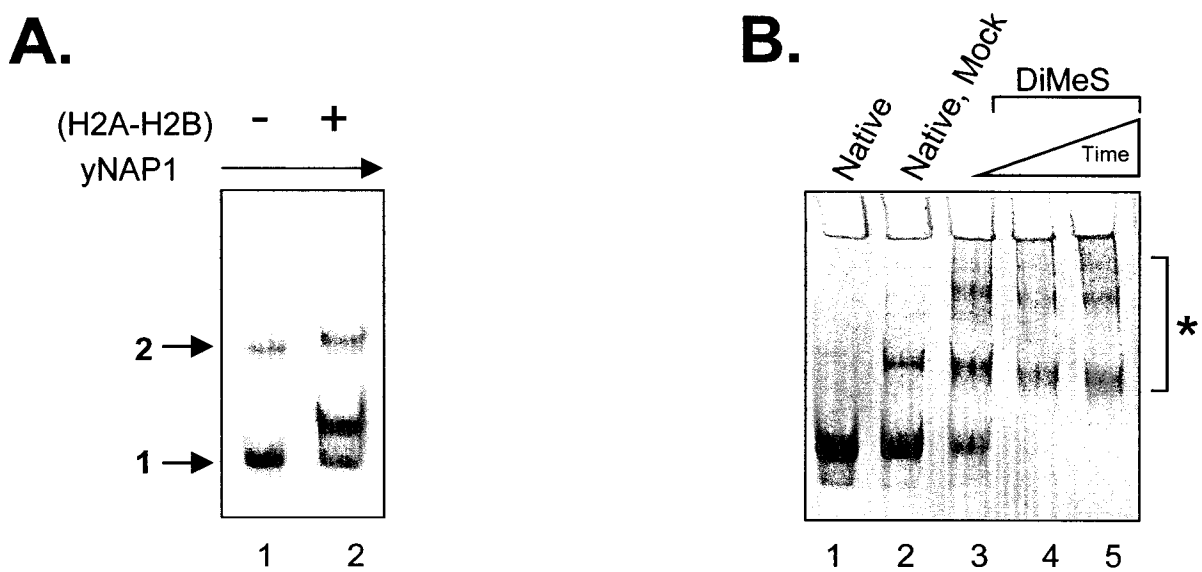

FIGURE 3.1A,B: Analysis of untreated and cross-linked yNAP1 (Native PAGE).
(A) Oligomer of yNAP1 seen by native gel: lane 1, 10μM yNAP1 (5μg); lane 2, 10 μM yNAP1 and 2.5 μM histone (H2A-H2B) dimer. (B) Native PAGE: lane 1, 5 μg native yNAP1; lane 2, 2.5 μg yNAP1 in cross-link buffer; lanes 3-5, 15 μg of yNAP1 cross-linked with Dimethyl Suberimidate (1 mg/mL) for 15, 60 and 120 minutes.
* indicates cross-linked species.

An unambiguous identity for each of the slower migrating species could not be determined from native PAGE. We sought to more carefully define the species revealed by chemical cross-linking by subjecting the products to MALDI-TOF mass spectrometry. Comparison of the mass spectra of untreated and cross-linked yNAP1 (Figure 3.1C, left and right panels, respectively) reveals a significant increase in the amount of 100 kDa material present (peak MW 102,239 Da), as well as a small amounts of larger molecular weight species. MALDI spectrometry sensitivity falls off dramatically at molecular weights exceeding 100 kDa, and it is unlikely that significant populations of larger oligomers would be revealed by this methodology. The change in molecular weight of the monomeric species following cross-linking (51,163 versus 49,063 prior to cross-linking), as well as concomitant increases in the molecular weights of the oligomer is almost certainly due to the presence of multiple molecules of dimethyl suberimidate (MW 273.2). This indicates that ~15 molecules of dimethyl suberimidate were, on average, required to cross-link yNAP1 into a dimeric species. The small peak near 100 kDa in the untreated sample is a result of matrix interactions, not of covalently linked proteins. Thus, chemical cross-linking revealed a significant population of yNAP1 oligomers of 102 kDa.

3.4B Analysis of yNAP1 Heterogeneity by Gel Filtration Chromatography. To obtain further information about the yNAP1 species present in solution, the purified protein was subjected to calibrated gel filtration chromatography (GFC). As shown in Figure 3.2A (upper panel),

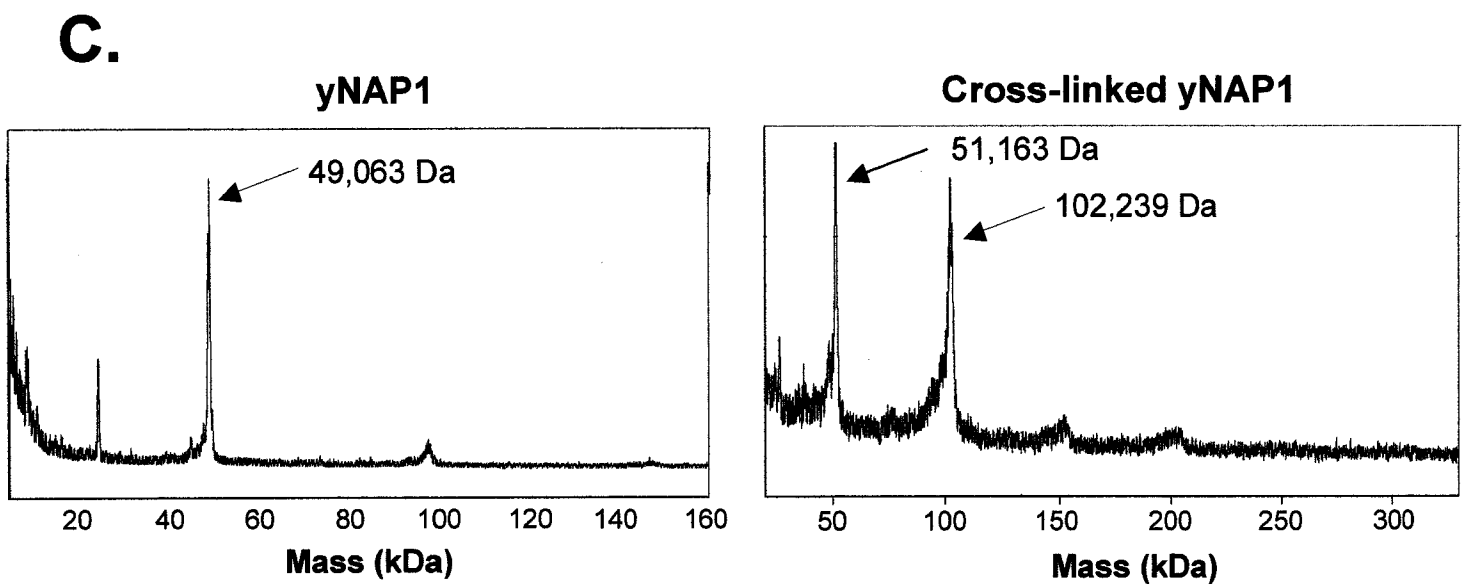

FIGURE 3.1C: Analysis of untreated and cross-linked yNAP1 (MALDI TOF). Samples were treated as described in Experimental Procedures. Charge-corrected masses are indicated.

yNAP1 elutes as a broad peak at +/- physiological ionic strength (150 mM). yNAP1 is a highly heterogeneous and likely multimeric population under these conditions. The apparent molecular weights (MWapp) contained within the limits of this peak span from nearly 1 MDa to approximately 400 kDa. In contrast, separation under higher ionic strength (500 mM) revealed the presence of two discrete peaks, a smaller peak with a MWapp of ~550 kDa, and a dominant peak with a MWapp of ~300 kDa (Figure 3.2B). When a portion of the fraction from the center of this largest peak was re-injected onto the same column at high ionic strength, yNAP1 eluted at nearly the same position (Figure 3.2A, lower panel). This most prominent species is thus stable to changes in loading concentration, and little exchange to other species is observed. The Stokes radius of the most prominent species was determined by a standard curve analysis of the gel filtration standards (Figure 3.2B). The resulting value of 55 Å in 500 mM salt is unusually large for a 49 kDa molecule. Thus, gel filtration revealed a much larger than expected species, as well as a mechanism (ionic strength) with which to control the heterogeneity of yNAP1.

3.4C Hydrodynamic Determination of the Self-Association of yNAP1. A similar trend of polydispersity in low ionic strength and monodispersity in high ionic strength was observed by sedimentation velocity ultracentrifugation analysis. The polydisperse nature of yNAP1 at moderate ionic strength (150 mM) was confirmed by the presence of broad sedimentation boundaries. At 11 μM protein and 150 mM NaCl, van Holde-

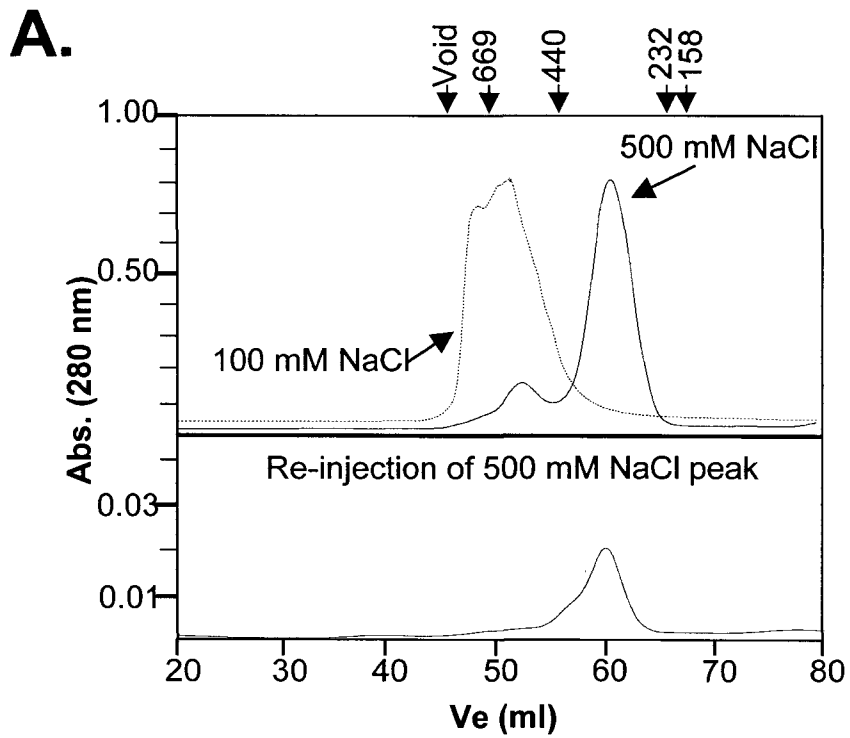

FIGURE 3.2A: Gel filtration chromatography of yNAP1.(A) Absorbance traces at 280 nm. Upper panel: Equivalent amounts of protein were separated in either 100 or 500 mM NaCl. Lower panel: 0.1 ml of the peak fraction from separation in 500 mM NaCl was re-injected in 500 mM NaCl. Note the different scales for the two panels.

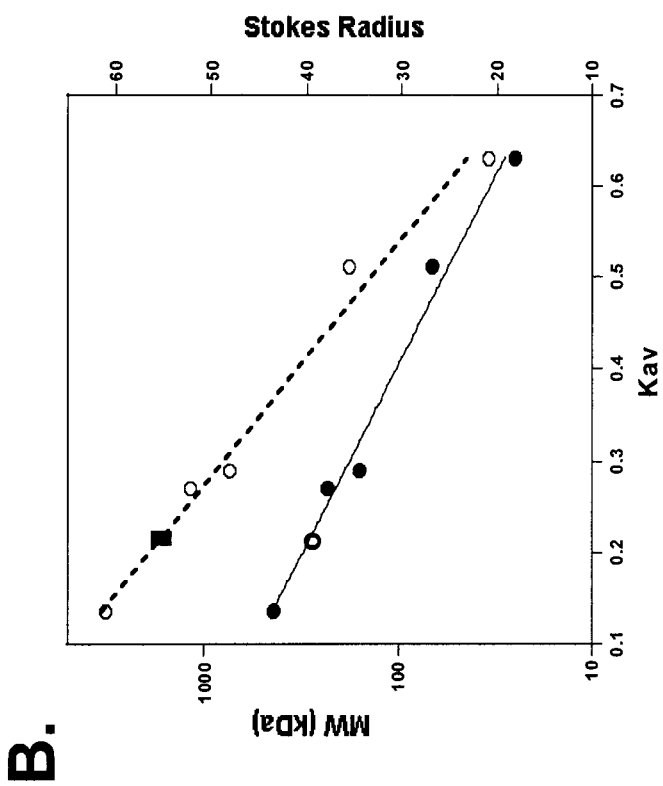

FIGURE 3.2B: Molecular weight and Stokes radius of yNAP1. (B) Plot of molecular weight (log) and Stokes radii versus Kav for gel filtration standards. An exponential fit and apparent molecular weight of yNAP1 (**o**), and a linear fit and apparent Stokes radius of yNAP1 (■) are shown.

Weischet analysis revealed a distribution of sedimentation coefficients from 5-7 S. No discrete species were detectable by visual inspection of the G(s) plots (Figure 3.3A) nor from the boundaries themselves (data not shown). This is consistent with a sample in a rapid associative equilibrium within the time scale of the experiment (~4 hours). However, sedimentation in 500 mM NaCl revealed a single, homogeneous and monodisperse species of ~ 4.5 S (Figure 3.3A). yNAP1 is readily interconverted between these two states. A sample purified by gel filtration chromatography at 500 mM NaCl and dialyzed to 150 mM NaCl was rapidly returned to the monodisperse state by the addition of concentrated NaCl to a final concentration of 500 mM (Figure 3.3A). Second moment analysis of the 500 mM NaCl samples yielded an S value of 4.7 for the monodisperse species. Thus, we had a mechanism for controlling the polydispersity of yNAP1, allowing us to further characterize its oligomerization state in solution.

We more precisely determined the salt concentration required to switch yNAP1 between the poly- and monodisperse states by carrying out sedimentation velocity experiments under salt concentrations ranging from 10-500mM NaCl. van Holde-Weischet analysis revealed a transition from the most polydisperse sample at 75 mM NaCl to the monodisperse, 4.5 S sample at ≥300 mM NaCl (Figure 3.3B). Lower salt concentrations (< 50mM) led to less polydispersity, likely due to charge repulsion between the highly negative-charged yNAP1 molecules. Thus, maximum 'buffering' of the yNAP1 negative charge occurred at 50-75 mM NaCl, facilitating oligomerization.

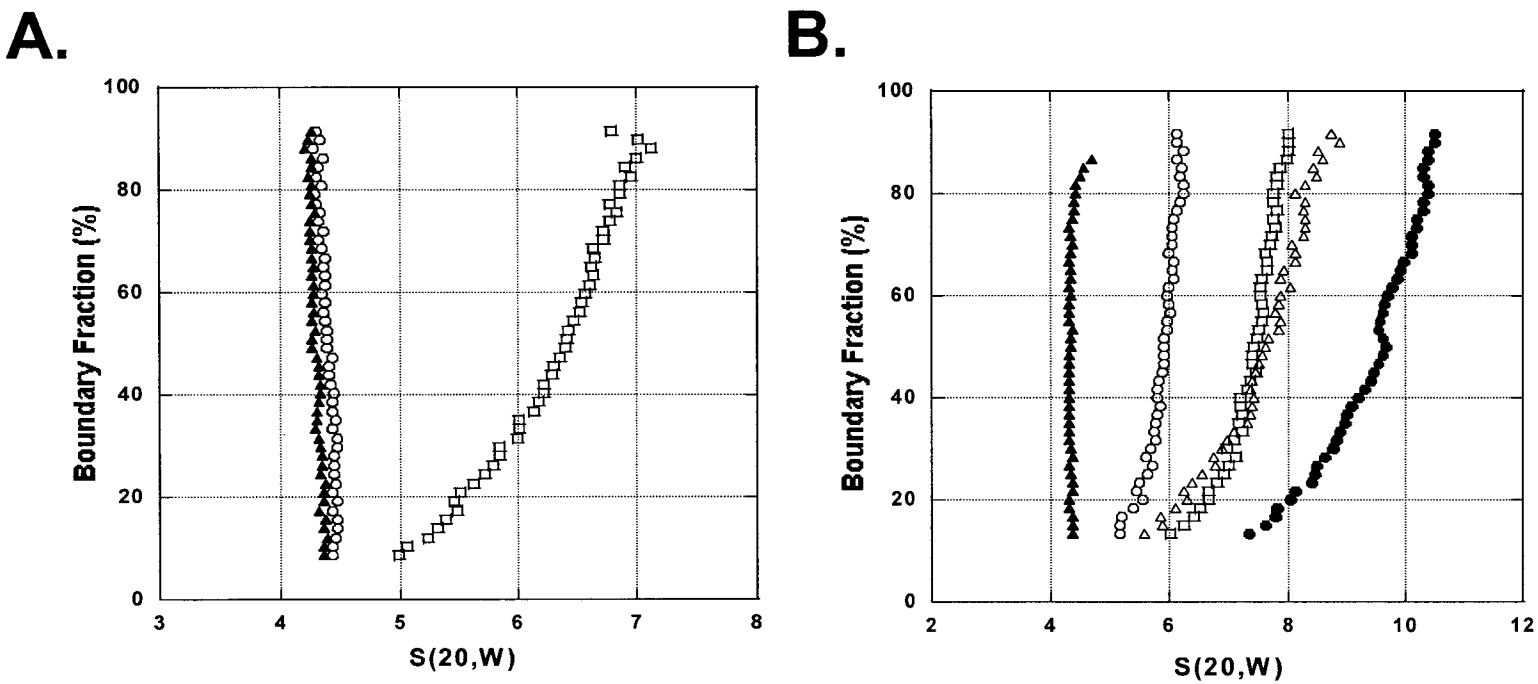

FIGURE 3.3A, B: Sedimentation velocity shows the affects of salt concentration on the polydispersity of yNAP1. (A) G(s) plots of 11 μM yNAP1 at 150 mM NaCl (□), 500 mM NaCl (▲), and a solution dialyzed to 150 mM, then brought to 500 mM immediately prior to sedimentation (o). (B) G(s) plots of 11 μM yNAP1 at 10 (o), 25 (▫), 75 (●), 125 (Δ), and 300 (▲) mM NaCl. Data were analyzed as described in experimental procedures.

C.

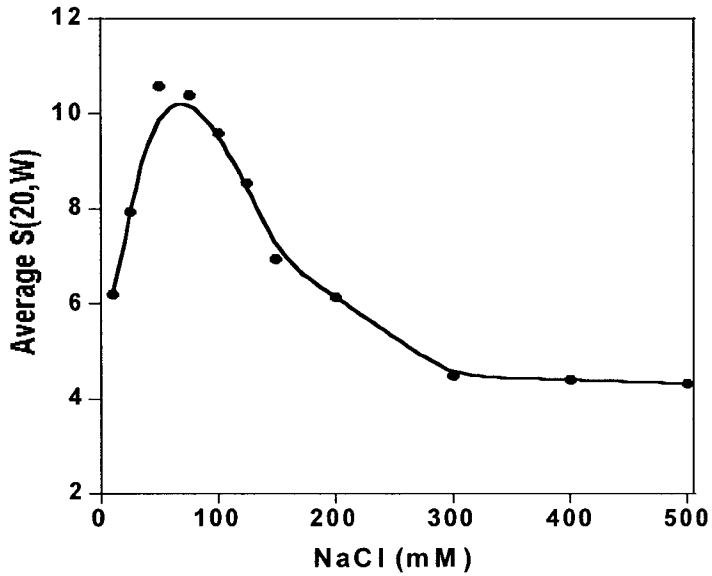

FIGURE 3.3C: Sedimentation velocity shows the affects of salt concentration on the polydispersity of yNAP1. Plot of the average S(20,W) obtained from the upper 10% of the boundaries for 11 μM yNAP1 at a range of NaCl concentrations. A smoothed curve is shown.

Significant polydispersity remained at near physiological ionic strengths. The average S values for the upper 10% of each boundary analysis were calculated and plotted versus NaCl concentration (Figure 3.3C). This illustrates the two transitions that yNAP1 underwent with changing ionic strength and highlights the NaCl concentrations at which yNAP1 is minimally (≥300 mM) and maximally (50-75 mM) polydisperse.

The ability of high salt to overcome the concentration dependent association was confirmed by sedimentation velocity analysis of yNAP1 over a range of protein concentrations, at both 75 mM and 500 mM NaCl. The average value of the range of sedimentation coefficients increased with increasing protein concentration at 75 mM NaCl (Figure 3.3D), while sedimentation at high salt (500 mM) led to overlapping G(s) plots (Figure 3.3E).

To gain insight into the identity of the species seen by G(s) analyses, a continuous distribution of mass [c(M)] modeling analysis was performed on the sedimentation velocity data. c(M) for samples of identical ionic strength (75 mM) over a range of protein concentrations (2, 11 and 25 μM) allow a better understanding of the self-association of yNAP1 (Figure 3.4). A strong trend in the average molecular weight is seen in the continuous distribution analyses. The population shifts from a dominant peak with a maximum at ~100 kDa at 2 μM to a more polydisperse distribution at 25 μM with a dominant peak at ~200 kDa (Figure 3.4, left). An intermediate concentration

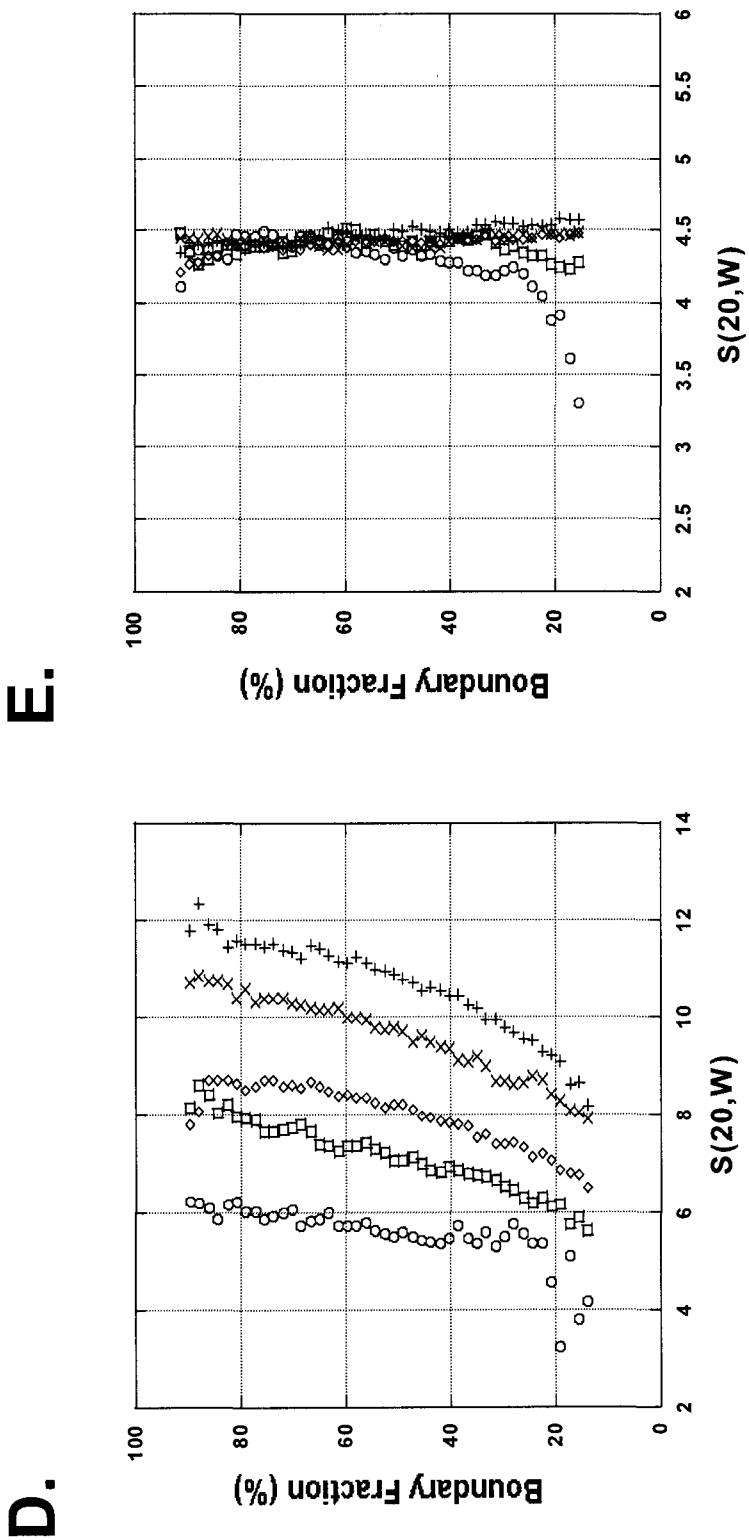

FIGURE 3.3D,E: Loss of yNAP1 concentration dependence at high salt. G(s) plots of yNAP1 (0.5 µM (**o**), 2 µM (□), 5 µM (Δ), 10 µM (x) and 25 µM (+) in 75 mM NaCl (D), or 500 mM NaCl (E). Solutions were sedimented and analyzed as described in experimental procedures.

(11 μM, upper right panel) shows a distribution of molecular weights similar to the 25 μM sample, though with the dominant peak at a slightly lower molecular weight. Thus, yNAP1 displays an increase in the distribution of mass with increasing concentration, consistent with a mass action equilibrium, with larger species being formed at the expense of smaller species.

The concentration dependence can, however, be overcome by high ionic strength. We analyzed the effect of increasing salt on samples of identical yNAP1 protein concentration (11 μM) (Figure 3.4, right panels). The distribution at the most polydisperse salt condition (75 mM NaCl) showed a broad population of species with molecular weights from 100 to 200 kDa. In contrast, at 200 mM NaCl the species present are best described by a dominant fraction of 100 kDa species and a smaller population of species of >150 kDa. Analysis of the 300, 400 and 500 mM NaCl samples revealed a dominant peak at 100 kDa, and little (< 5%) or no larger species (data not shown). The loss in heterogeneity of the mass distributions with increasing salt accurately reflected the loss of heterogeneity in the G(s) analyses. This continuous distribution of mass analysis also gave our first evidence as to the identity of the 4.7 S species, since 100 kDa is very near the molecular weight of a yNAP1 dimer (98,284 Da.).

Calculated molecular weights, partial specific volumes (v-bar), solvent densities (ρ) and the observed S values allow modeling of shape and other hydrodynamic properties of a macromolecule. Table 3.1 lists these

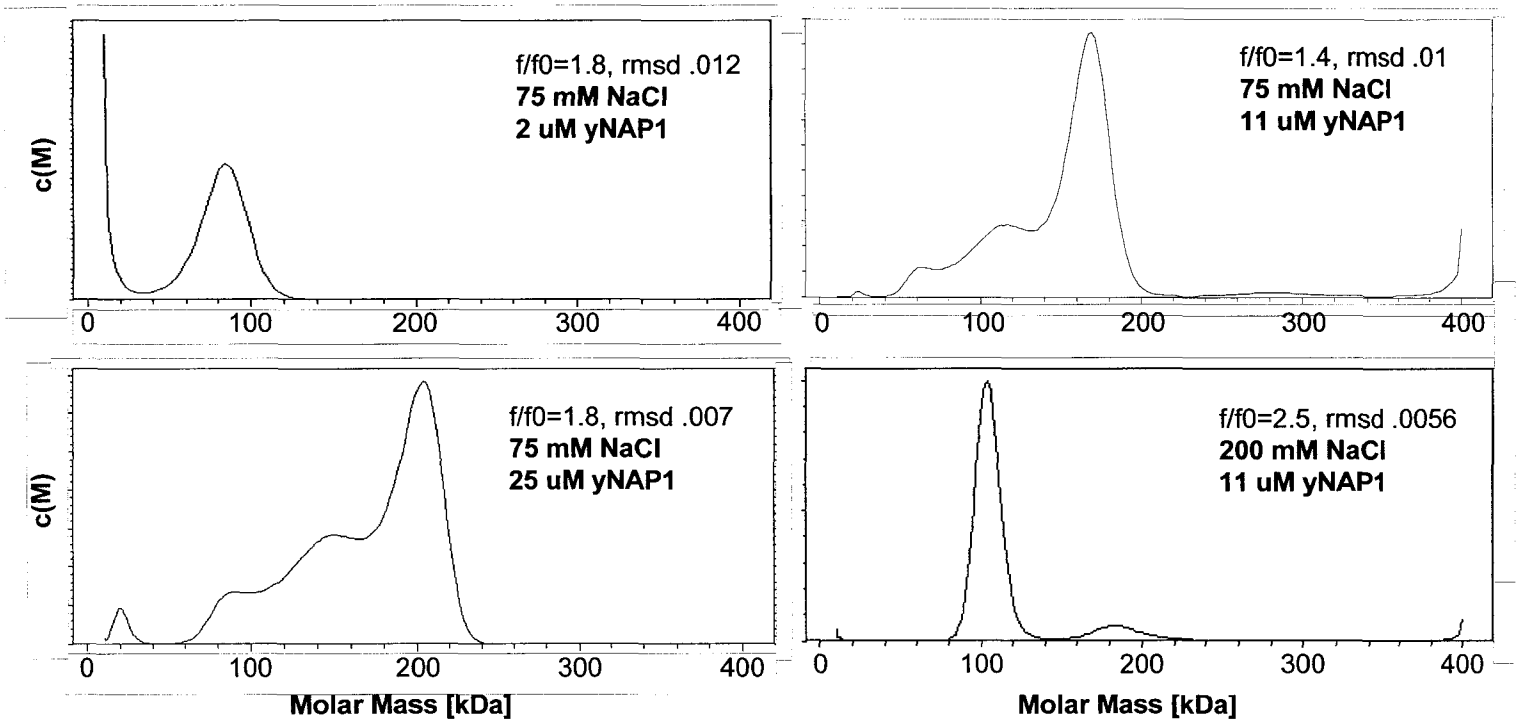

FIGURE 3.4. c(M) modeling analysis of sedimentation velocity data shows yNAP1 concentration dependence at 75 mM NaCl, and the loss of yNAP1 concentration dependence at high salt. Upper left: 2 μM yNAP1 in 75 mM NaCl, lower left: 25 μM yNAP1 in 75 mM NaCl, upper right: 11μM yNAP1 in 75 mM NaCl, lower left: 11 μM yNAP1 in 200 mM NaCl. Data was initially modeled by c(S), followed by c(M) to reveal the molecular weight distributions. The appropriate buffer and partial specific volume constraints were utilized, and the f/fo was fitted by non-linear regression within SEDFIT.

Table 3.1: Modeling S and shape

Species	Modeled: Shape	Modeled: Native S_{calc}	Modeled: Denaturing S_{calc}	S_{obs}
Monomer Axial Ratio	Sphere Ellipsoid 5.5 / 3.2*	3.1 S 1.4-3.1 S 2.4 S	2.7 S 1.2-2.7 S 2.4 S	**2.4 S** Denat.
Dimer Axial Ratio	Sphere Ellipsoid 1.8	4.9 S 2.2-4.9 S 4.7 S	n/a	**4.7 S** Native
Tetramer	Sphere Ellipsoid	8.4 S 3.8-8.4 S	n/a	
Hexamer	Sphere Ellipsoid	10.9 S 5-10.9 S	n/a	

The axial ratio was adjusted for the input molecular weight to yield S_{calc} value(s) most similar to those determined experimentally (S_{obs}) for the monomer and dimer under denaturing * and native conditions, respectively. The S_{calc} values for ellipsoids represent a range of axial ratios of 25:1 to 1:1.

properties for yNAP1. The 4.7 S yNAP1 species models well to prolate and oblate ellipsoids of axial ratio 1.8:1. Most interestingly, however, this fit required an input molecular weight of 98,300 Daltons, that of a yNAP1 dimer. The spherical value of 4.9 S is too high to accurately represent the species seen by sedimentation velocity. Modeling using the monomeric molecular weight (49,150 Da.) failed to yield a sufficiently large S value, regardless of the axial ratio input. Thus, the 4.7 S species is best described as a non-spherical yNAP1 dimer.

Sedimentation equilibrium measurements of yNAP1 were performed at multiple loading concentrations, three different rotor speeds, and two different salt concentrations (Table 3.2). The weight average molecular weight (Mw) of yNAP1 was essentially unaffected by increasing protein concentration or rotor speed when 500 mM NaCl was present. The Mw fluctuated near the value consistent with a yNAP1 dimer (98 kDa). In contrast, yNAP1 in 75 mM NaCl showed a clear increase in Mw as protein concentration was increased, indicative of self-association. The highest Mw observed (280 kDa) was at the highest initial loading concentration (100 μM). This is most consistent with a significant fraction of the population existing as yNAP1 hexamers (295 kDa). The smallest weight average molecular weight observed was 106 kDa (0.5 μM protein, 18,000 RPM), indicating that yNAP1 dimers are likely the smallest component of the solution.

We fit the equilibrium data from equivalent concentrations of yNAP1 (13.8 μM) and matched rotor speeds (16,000 RPM) at both 75 and 500 mM

Table 3.2:
Weight Average Distributions by Equilibrium Analysis

Concentration [μM]	[NaCl]	Molecular Weight (Mw)*
0.5	500 mM	82
1.4		94
5.5		106
13.8		92
0.5	75 mM	115
1.4		141
5.5		204
13.8		248
25		263
50		239
100		257

* The weight average molecular weights (Mw) are the average of the values determined for each speed (14,16,18K RPM).

NaCl to a variety of self-association models (Figure 3.5A). The 500 mM NaCl yNAP1 data were best fit to a monodisperse population of dimers (as judged by the residuals and the square root of the variance (rms)). The higher Mw than expected for a pure population of dimers (98,300 Da.) likely leads to the dispersion of residuals at the highest concentrations, although the value is within the error inherent to equilibrium measurements. The residuals and rms values for fits of this data to the other models (pure monomer, trimer, or tetramer) were very poor (data not shown). Further, no species smaller than 4.5 S were identified in sedimentation velocity boundary analysis for even the lowest protein concentrations assayed at 500 mM NaCl (Figure 3.3E). Thus, the sample is best described as a nearly pure solution of yNAP1 dimers.

The 75 mM NaCl yNAP1 sample is more complex (Figure 3.5B). The fitted molecular weight of 228 kDa is consistent with neither a tetramer (197 kDa) nor a hexamer (295 kDa). While a fit to a pure tetramer population yields reasonably good residuals and rms values, we know from the sedimentation velocity experiments (both G(s) and c(m) analyses) the population is polydisperse, not pure (Figures 3.3A, 3.4). Fitting the data to models encompassing more heterogeneity (dimer-tetramer, tetramer-hexamer, tetramer-octamer, etc.) was informative. The dimer-tetramer model failed to converge, as did all models that encompassed a dimer as the lowest species (data not shown). Additionally, any attempt at fitting these data to models including monomeric species failed to converge. The tetramer-hexamer (4-6), tetramer-octamer (4-8), and tetramer-hexamer-octamer

A.

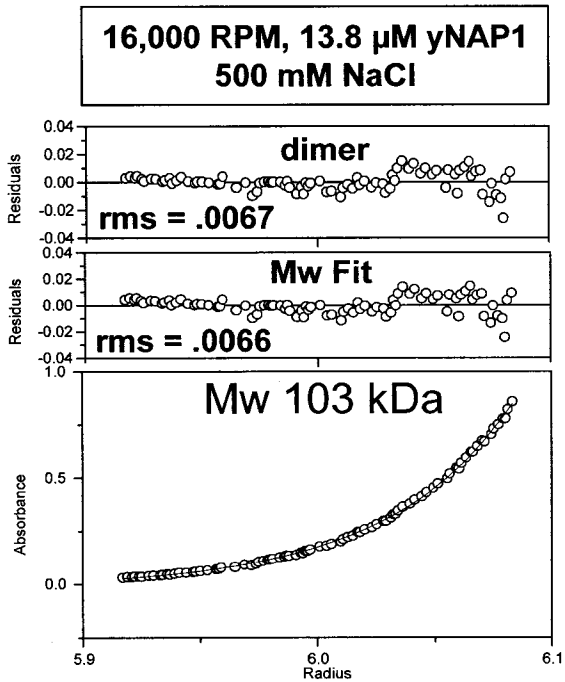

FIGURE 3.5A: Determination of the oligomerization state for yNAP1 at 500mM NaCl. The fitted Mw (103 kDa) and the residuals and root mean square deviations (rms) for the fitted Mw and for a yNAP1 dimer are shown.

B.

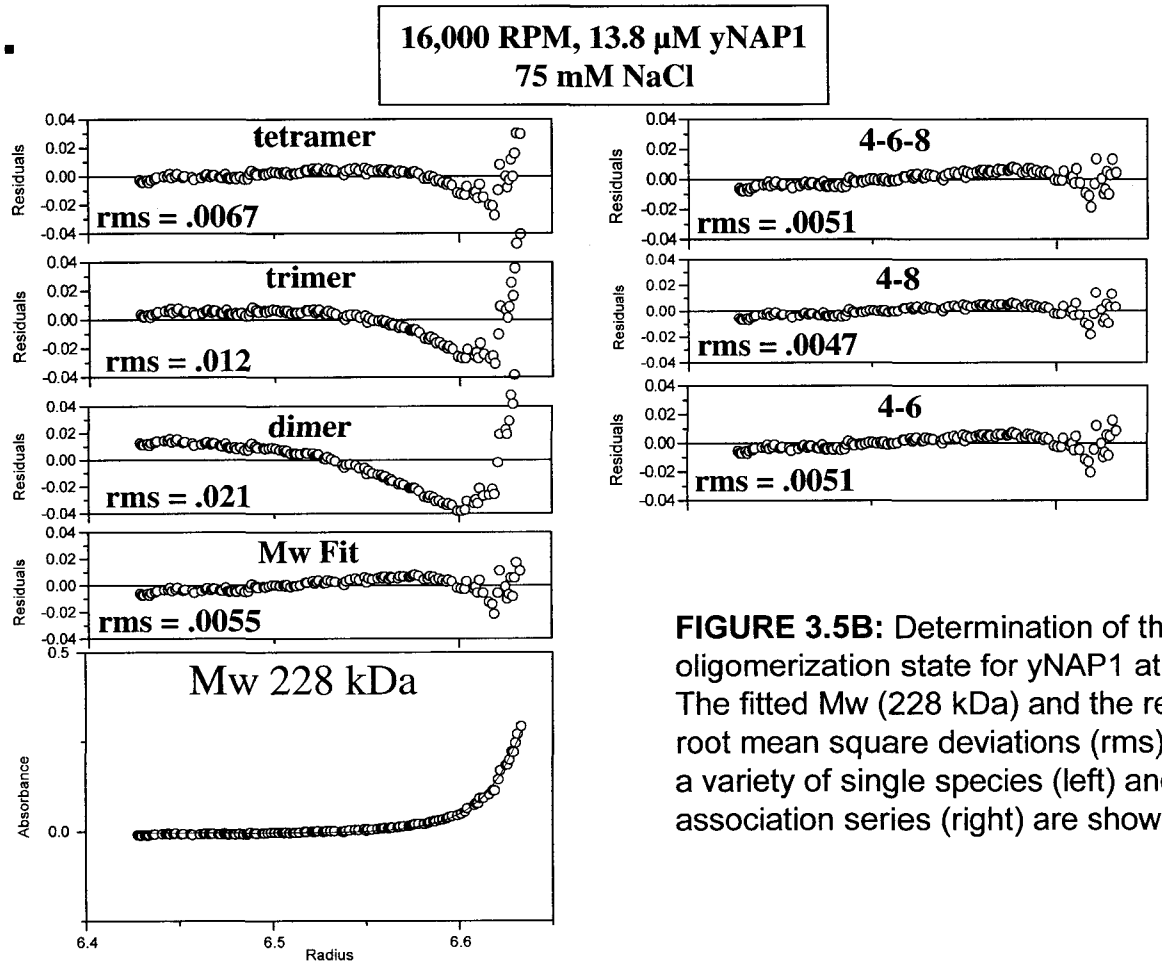

FIGURE 3.5B: Determination of the oligomerization state for yNAP1 at 75mM NaCl. The fitted Mw (228 kDa) and the residuals and root mean square deviations (rms) for the fits to a variety of single species (left) and self-association series (right) are shown.

(4-6-8) models yielded reasonable residuals and similar rms values, though the best fit was to the tetramer-octamer equilibrium (rms = 0.0047). However, analysis of sedimentation velocity boundaries at 75 mM NaCl failed to distinguish discrete species, and the range of S values for a single concentration of protein was limited to a range of ~1.5 S (see Figure 3.3D). Thus, there are likely no more than two discreet species present in the equilibrium. Further, the fundamental subunit is a dimer, thus the oligomers likely multiply by a factor of two as self-association proceeds. Taken together, this indicates that the most likely association scheme is dimer-tetramer-hexamer. The presence of octamers could not be ruled out by this extrapolation. To answer this, we conducted sedimentation equilibrium experiments at high concentrations (25, 50 and 100 μM) and 75 mM NaCl (Table 3.2). The weight average molecular weight from these and other samples was plotted as a function of loading concentration (Figure 3.6). Even at the highest concentration, the weight average molecular weight did not exceed 300 kDa, the molecular weight expected for the yNAP1 hexamer. Further, the plot indicates no significant increase in the distribution of the population above 25 μM protein. Thus, we believe that oligomerization is complete at this concentration, and the ultimate species is hexameric.

3.4D Influence of Denaturant on the Polydispersity of yNAP1. Even at the lowest concentration of yNAP1 used in the ultracentrifugation experiments, 0.5 μM, few species smaller than the 4.7 S dimer had been seen, even at concentrations of reducing agent (1 mM TCEP or DTT)

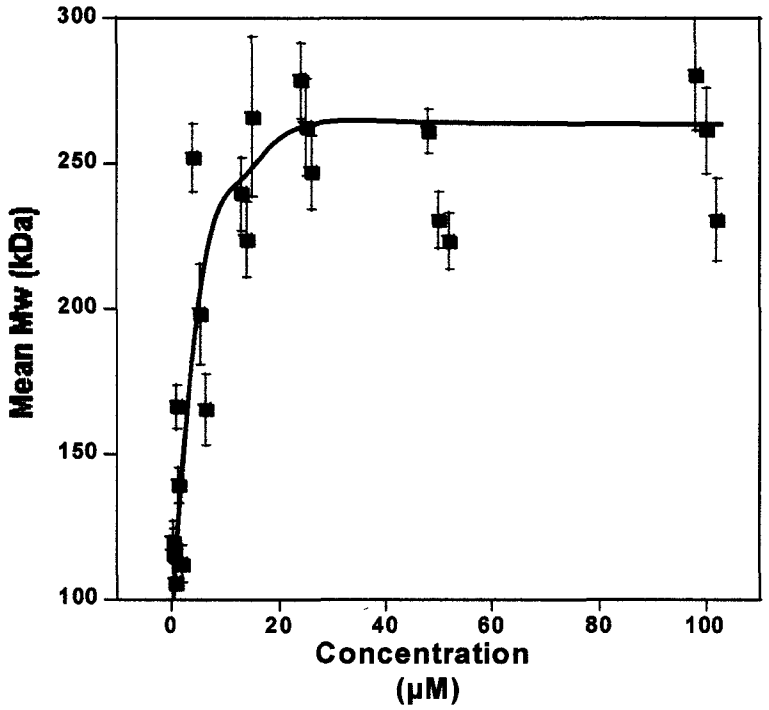

FIGURE 3.6: Determination of the terminal oligomerization state for yNAP1. The mean molecular weight is plotted versus protein concentration. Error bars are derived from the weighted fit within Origin. The data points for each rotor speed are offset slightly along the x-axis for clarity.

sufficient to reduce disulfide bonded dimers. A monomeric (49,150 kDa) yNAP1 species modeled to S = 1.4-3 (Table 3.1), dependent, of course, on the axial ratio. In order to characterize the yNAP1 monomer, samples containing identical protein concentrations but increasing molar concentrations of guanidine hydrochloride (GnHCl), were utilized in sedimentation velocity experiments. van Holde-Weischet analysis of yNAP1 in 1 M GnHCl and 75 mM NaCl (Figure 3.7) led to G(s) plots nearly identical to that of the monodisperse 4.5 S species seen at high ionic strength (compare to Figures 3.3A and E). Thus, yNAP1 heterogeneity can be abrogated by either high salt or a modest amount of denaturant, which is itself ionic. At a slightly higher concentration of denaturant, 1.8 M GnHCl, a sharp transition occurred and the monodisperse 4.5 S species was replaced by a monodisperse 2.4 S species. This species agrees well with that modeled as a 49 kDa monomer, with S = 2.4 at an axial ratio of 3.2 (see Table 3.1). Absolute determination of molecular mass was determined by performing sedimentation equilibrium on samples of constant yNAP1 concentration and increasing denaturant. Table 3.3 shows the results of this analysis. The mean of the weight average molecular weights from 3 different concentrations of protein and 3 different rotor speeds are shown. 1 M GnHCl leads to a species of 89 kDa, very near that expected for a yNAP1 dimer. The Mw of yNAP1 at 1.8 M is nearly identical to the monomeric mass (47.6 vs. 49.1 kDa). An intermediate amount, 1.5 M GnHCl, yields a Mw value intermediate to that of 1M and 1.8 M. Thus, consistent with the modeling and changes in S value

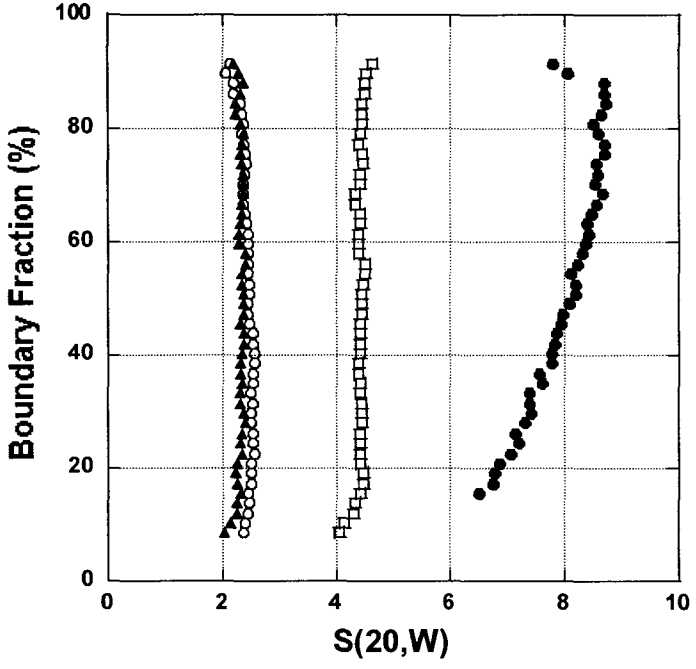

Figure 3.7: Sedimentation velocity shows changes in yNAP1 heterogeneity in the presence of GnHCl. G(s) plots of 5 µM yNAP1 equilibrated at 0.0 M (•), 1.0 M (□), 1.8 M (o) and 2.0 M (▲) GnHCl. Solutions were sedimented and analyzed as described in experimental procedures.

Table 3.3: Equilibrium Sedimentation Analysis of yNAP1 in GnHCl.

Sample Condition	Weight Average Molecular Weight
0.0 M GnHCl	226 (+/- 22) kDa
1.0 M GnHCl	89 (+/- 7) kDa
1.5 M GnHCl	69 (+/- 7) kDa
1.8 M GnHCl	48 (+/- 3) kDa

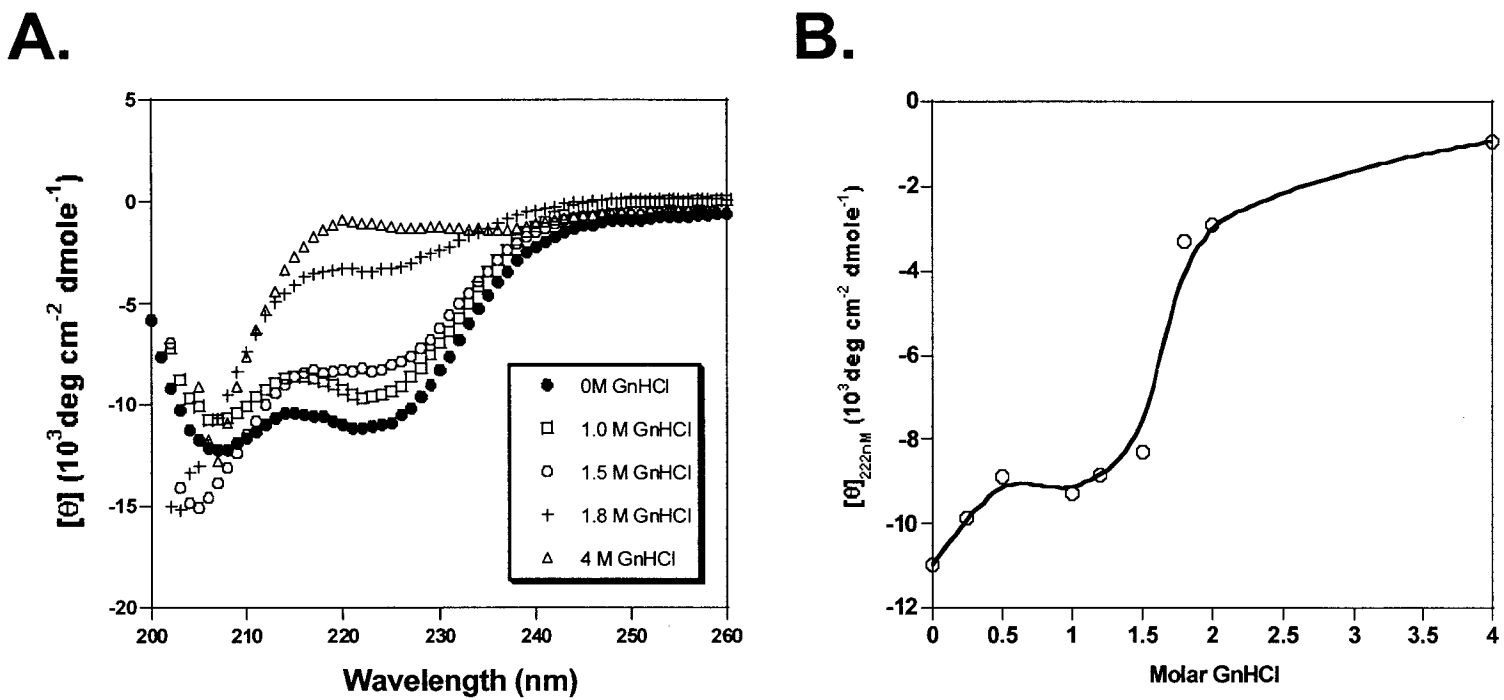

FIGURE 3.8A,B: Measurement of secondary structure changes upon treatment of yNAP1 with GnHCl. (A) 10 µM yNAP1 was equilibrated with 0.0, 1.0, 1.5, 1.8, and 4.0 M GnHCl in 75mM NaCl. CD spectra were then collected at 5° C. CD signal is normalized on a per-residue basis. (B) Plot of changes in CD signal at 222 nm versus molar concentration of GnHCl from data collected for (A) and additional concentrations of GnHCl. $[\Theta]_{222\ nm}$ is the normalized, per residue CD signal at 222 nm. A best fit curve of the data is shown.

and polydispersity seen by sedimentation velocity analysis (Figure 3.7), a moderate amount of denaturant reveals the yNAP1 monomer. Low concentrations of denaturant acted in a similar manner to increasing ionic strength, with regards to loss of yNAP1 polydispersity. Slightly higher concentrations led to a sharp transition to a species consistent with a yNAP1 monomer.

We sought to determine what structural changes, if any, were associated with the loss of heterogeneity and the subsequent conversion to the monomeric species. Circular dichroism (CD) spectroscopy is exquisitely sensitive to changes in secondary structure in polypeptides. We analyzed the CD spectra of yNAP1 with increasing molar concentrations of GnHCl (Figure 3.8A). Based on the spectrum obtained in 75 mM NaCl in the absence of denaturant, yNAP1 is ~34% α-helical, ~33% β-sheet and turn, and ~33% unstructured. While only subtle changes are seen with concentrations of GnHCl less than 1.5 M, the CD spectrum of yNAP1 in 1.8 M is indicative of a nearly completely unstructured polypeptide. The presence of higher amounts of GnHCl (4 M) leads to a spectrum consistent with complete denaturation. The strong absorbance of GnHCl at wavelengths less than 200 nm precluded a rigorous, quantitative analysis of secondary structure in the presence of denaturant. However, ellipticity at 208 and 222 nm correlate with the proportion of α-helix, and changes in $[\Theta]_{222}$ can be expressed as loss or gain in α-helical content (Fasman,G.D., *CD and the Conformational Analysis of Biomolecules*, 1996). This type of analysis for yNAP1 in the absence of

denaturant yields an α-helical content of ~31 %, similar to that obtained by the more rigorous analysis. Analysis of the intensity at 222 nm for increasing amounts of GnHCl is shown in Figure 3.8B. The $[\Theta]_{222}$ data show a biphasic behavior as GnHCl is increased. The first step, between 0.0 and 1.5 M GnHCl, corresponds to a loss of 40% of yNAP1's helical content (to ~18%). A much more striking loss of negative ellipticity is seen as GnHCl is further increased to 1.8 M. The slight (0.3 M) increase in denaturant yields a net loss in α-helical content of 90% (to ~3%) relative to the native protein. The changes in the CD spectra correlate well with the changes in the sedimentation coefficient observed as a function of GnHCl concentration (Figure 3.7).

3.5 Discussion:

The results of the biochemical and biophysical techniques described above shed light on the structure of yNAP1 in solution. The oligomeric structure of yNAP1 reveals a potential mechanism with which yNAP1 may function in the assembly of histone proteins onto DNA.

The profound change in the gel filtration elution profile when the buffer contained high salt was a significant advancement in our understanding of yNAP1 oligomerization. yNAP1's anomalously fast elution is likely due to either the asymmetry of the protein, or repulsive interactions with the gel filtration media due to the high negative charge of yNAP1 (calculated pI of 4.23). It is equally likely that both these factors contribute. Nevertheless, we

demonstrate by sedimentation equilibrium that the relatively homogeneous, concentration-independent species were yNAP1 dimers (Table 3.2).

The ability to regulate the polydispersity of yNAP1 by controlling the ionic strength of the solvent allowed us to utilize analytical ultracentrifugation to study yNAP1 dynamics in solution, and to determine its fundamental oligomerization state. Sedimentation velocity analysis of yNAP1 in 500 mM salt led to a polydisperse population of 4.7 S. We initially believed this to be a yNAP1 monomer. However, modeling using the monomeric molecular weight failed to yield a hydrodynamic shape or dimension consistent with a 4.7 S monomer. However, using the dimer molecular weight we were able to achieve a model for the 4.7 S species: an ellipsoid of axial ratio 1.8. The S value is smaller than that expected for a 98 kDa sphere (4.9 S). The asymmetric nature of yNAP1 is consistent with the anomalously large Stokes radius revealed by calibrated gel filtration (55.6 Angstroms). The width of the boundaries is also consistent with a protein having a large diffusion coefficient (Demeler *et al.*, 1997). The results of the non-linear regression analysis performed within SEDFIT yielded a range of apparent frictional ratios from 1.5 to 2.5, consistent with the asymmetric nature of the yNAP1 returned from modeling. Limited proteolysis and CD spectroscopy of yNAP1 (McBryant, et al., 2003 submitted) reveals a protease sensitive N-terminus, a well structured central region (aa 74-365), and a C-terminal domain (aa 365-417) which retains histone binding activity though devoid of secondary structure. Taken together, the hydrodynamic properties could result from the modular nature of

yNAP1, as well as the preponderance of unstructured amino acids (~33%), giving an overall elongated/extended shape to the molecule.

Equilibrium ultracentrifugation of yNAP1 in high salt over a >25-fold range in protein concentration led to weight average molecular weights of 82-106 kDa (mean 93.4) consistent with a 98 kDa yNAP1 dimer. Together with the sedimentation velocity analysis of the same range of protein concentrations, the concentration dependence of association was thus abrogated by the presence of high ionic strength. This leads to a relatively homogeneous distribution regardless of solute concentration. yNAP1 is maximally heterogeneous at ionic strengths near physiologic levels (50-100 mM). Interestingly, the loss of heterogeneity seen at high salt (≥ 200 mM) is also seen, to a lesser extent, at very low salt (≤10 mM) (see Figure 3.3C). The acidic character of yNAP1 may play a role in this phenomenon. It is likely that high ionic strength disrupts required intermolecular hydrogen bonds and salt bridges, while low ionic strength leads to charge-charge repulsion between yNAP1 dimers, both leading to a less polydisperse population. Consistent with this, permanent protein-protein interfaces, such as those found in homodimers, are generally rich in hydrophobic side chains (Jones and Thornton, 1996), and are thus less sensitive to disruption by increased ionic strength. The side chains found at the protein-protein interface of 'non-obligate' (more transient) complexes are more likely polar in nature, and are thus more easily disrupted by ionic strength. Likewise, intermolecular hydrogen bonds and salt bridges are more prevalent in non-obligate

complexes, while homodimers generally contain few, if any, salt bridges (Kleanthous, C., in *Protein-Protein Recognition*, 2000). It is reasonable, therefore, that polydispersity due to non-obligate, electrostatic interactions would be readily abrogated by high salt. This appears to be the case for yNAP1.

Sedimentation velocity at a range of protein concentrations led to broad and smoothly curved boundaries. The shape of the boundaries exhibited upon sedimentation velocity is consistent with that expected for a rapidly reversible association (Demeler *et al.*, 1997). Inspection of the extrapolation plots returned from van Holde-Weischet analysis of the sedimentation boundaries, where S values at each position on the boundary are extrapolated out to infinite time, failed to reveal any distinct species (data not shown). Both these observations are consistent with a rapid, self-association equilibrium on the time scale of the experiment. Additionally, the change in mass distributions with concentration in the c(m) analyses (at 75 mM NaCl), and the increase in Mw with increasing concentration of protein (Figure 3.6) indicate that higher-order oligomers are continuously being formed at the expense of smaller oligomers, consistent with the mass action law of equilibrium. Similarly, dilution, as seen for the analysis of concentration dependence of S at 75 mM NaCl (Figure 3.3D), leads to a progressive decrease in the range of S values returned.

Even at high protein concentration, the S (20,W) of any individual sample show only a 1.5-fold range of values. For example, yNAP1 at 25 μM protein

(75 mM NaCl) yields a range of S values from 8 to 12. The dimerization of a species with an S value of 'N' will usually result in a species with S = 1.5 N (van Holde, K., *The Proteins*, 1975). Thus, the limited S value ranges seen herein likely represents an equilibrium between no more than two oligomeric species. This, however, assumes that no profound changes in the molecular shape occur upon oligomerization. The rapidity of the equilibrium precludes unequivocal identification of the larger components by sedimentation velocity. Further, the low resolution of c(M) analyses when associating species are relatively close in molecular weight precludes precise identification of the mass values for these exchanging species.

The insights into yNAP1 oligomerization gained by sedimentation velocity experiments led to our ability to accurately apply and assess the validity of sedimentation equilibrium-derived association models. Self-association of yNAP1 is best described as a rapid, concentration dependent, stepwise assembly of dimers into tetramers into hexamers. No further oligomerization above the hexamer is seen at the concentrations utilized herein, and the hyperbolic shape of the plot of Mw versus loading concentration agrees with this. This model for self-association is consistent with the notion that many protein hexamers are organized as trimers of dimers (Dong *et al.*, 1995). It is important to note that thermodynamic non-ideality due to high solute concentration can lead to an underestimation of the Mw of the largest species in an associative reaction (*Analytical Ultracentrifugation in Biochemistry and Polymer Science*, Chapter 14, p 254). However, the self-association of

yNAP1 appears complete at ~25 μM, thus this effect may not be relevant for the association reaction described herein.

The characterization of the yNAP1 homodimer as the 'obligate' fundamental unit in the self-assembly pathway led us to investigate what conditions were required to reveal the subunits of the dimer. A biphasic change in the sedimentation property of yNAP1 is seen, with a loss of heterogeneity at ~1M GnHCl, and a loss of the 4.7 S 'fundamental' species at ≥1.8 M GnHCl (Figure 3.7). The apparent 3-state denaturation of yNAP1 by GnHCl (Figure 3.8B) therefore involves 2 separate molecular events. First, a loss of intermolecular contacts between yNAP1 higher-order oligomers occurs at 1.0 M GnHCl, yielding a monodisperse population of dimers. This is likely to be mechanistically similar to the effect of high NaCl concentrations. Next, at ≥1.8 M GnHCl, a nearly complete loss of secondary structure occurs, and a monodisperse population of 2.5 S species is seen. Thus, a wholesale loss of secondary structure is required to separate the dimer subunits. Perhaps not coincidentally, a survey of the secondary structure content of 28 homo-dimeric proteins revealed that over one-half (53%) of the interface residues were classified as α-helix (Jones, S and Thornton, J.M., 1995). Thus the concomitant loss of dimerization and α-helical content may be linked, and the dimers may be dependent on each other for proper folding. The loss of higher oligomers (non-obligate) merely required either sufficient ionic strength/desolvation provided by the denaturant to buffer the intermolecular electrostatic attractions between yNAP1 dimers, or sufficient denaturant to

disrupt the secondary structure required for higher-order protein-protein contacts.

It was presumed that the two species seen by native-gel electrophoresis were monomer and dimer (Figure 3.1A). Gel electrophoresis and mass spectrometry of cross-linked yNAP1 (Figures 3.2B and C) indicated that yNAP1 dimers were the predominant species. Our studies using denaturant, however, revealed a requirement for 1.8 M GnHCl to disrupt the yNAP1 dimer (Figure 3.7), and this was commensurate with nearly complete denaturation of the polypeptide (Figure 3.8). We now believe this inconsistency can best be explained by reconsideration of our initial presumption regarding the native PAGE species. If the species are instead presumed to be dimer and tetramer [at ~10 μM there appears to be species consistent with yNAP1 tetramers (Figures 3.3D, 3.4, Table 3.2)], then the two new species seen upon native PAGE of cross-linked yNAP1 would likely be tetramers and hexamers. Cross-linking/spectrometry failed to reveal the presence of these larger complexes due to the loss in sensitivity of mass spectrometry at molecular weights above 100 kDa.

Previous studies have detailed the histone binding activity of yNAP1 (McBryant, *et al*, 2003, submitted, Nakagawa, *et al*, 2001, McQuibban, *et al*, 1998). The histone components of the nucleosomes show little similarity with regard to their amino acid sequence, though their overall amino acid content (Sullivan *et al.*, 2002) and secondary structure (Arents and Moudrianakis, 1995) are highly conserved. Each pair of histone molecules associates

through contacts between the longest helices (α2) of the canonical histone-fold motif, oriented head to tail (Arents and Moudrianakis, 1995). The two adjacent (H3-H4) dimers are linked through the formation of a four-helix bundle between the second of two helix-strand-helix motifs in H3 molecules (Arents and Moudrianakis, 1995; Luger *et al.*, 1997). In each of these complexes, two opposing faces are solvent exposed per pair of histone folds. Further, the tertiary structures of the (H2A-H2B) dimer and one-half of the $(H3\text{-}H4)_2$ tetramer are essentially super-imposable (Arents *et al.*, 1991; Luger *et al.*, 1997; Sullivan *et al.*, 2002). These symmetries may be important for binding by chromatin assembly factors and other chromatin modifying enzymes (Akey and Luger, 2003). The stoichiometries of yNAP1-histone complexes were recently determined to be two yNAP1 molecules per dimer, and four per tetramer (McBryant, *et al.*, 2003 submitted). It is easy, therefore, to envision a model where each subunit of the yNAP1 dimer makes contact with one of two available faces. It is also apparent that oligomerization by yNAP1 above that of the dimer would lead to greater histone binding capacity, consistent with that seen by the *Xenopus* chaperone nucleoplasmin (Dutta, et al 2001), and the *Drosophila* nucleoplasmin like protein NLP (Namboodiri *et al.*, 2003), both of which are pentameric. This functional gain may facilitate the rapid deposition of nucleosomal histones onto the newly synthesized DNA strands behind the replication machinery. Alternatively, perhaps further oligomerization of the yNAP1 obligate dimers acts to buffer the intrinsic

negative charge of yNAP1 molecules in the absence of their basic binding partners.

Altogether, these observations stress the importance of yNAP1 oligomers in the binding of histone complexes, and shed light on an important chromatin assembly factor utilized by numerous research groups investigating chromatin organization and dynamics.

3.6 Acknowledgements:

The authors acknowledge Borries Demmeler and Peter Schuck for the use of their analytical software and technical assistance. We thank Andy Vendel for assistance with CD measurements. We also thank Jeffrey Hansen for his input and critical reading of the manuscript.

Chapter 4

Supplemental Studies on the Conformational Aspects of the Yeast Nucleosome Assembly Protein 1

This chapter will contain experiments performed in the course of the investigations described in Chapters 2 and 3, which were not included in the prepared manuscripts. These experiments pertain to the structural properties of yNAP1 investigated using a spectroscopic method (CD). The experiments described herein will contain: a brief abstract outlining the background for the experiment, including the rationale, an experimental procedures section, the experiment, and a brief results/discussion section. Rather than being heavily annotated, I instead refer readers to relevant sections of the Introduction (Chapter 1), and the prepared manuscripts (Chapters 2 and 3) for in-depth background information.

4.1 yNAP1 structural background:

Chapter 3 describes investigations into the physical nature of the yNAP1 protein, including its secondary structure propensities. Specifically, circular dichroism (CD) spectroscopy was performed on the full-length protein to allow analysis of the nature and proportions of the secondary structural features. This revealed that yNAP1 consists of nearly equal fractions of α-helix, β-sheet and turn, and unstructured residues. This is roughly consistent with secondary structure predictions (data not shown). Chapter 3 also details the significant effect on yNAP1 polydispersity due to changes in ionic strength. Specifically, the presence of NaCl at concentrations greater than 200 mM led to a loss of 'higher-order' oligomerization above the fundamental homo-dimer. While we suggest that the presence of high salt may have led to a 'buffering' of either the positive or negative charge on yNAP1 required for higher oligomerization, we reserve the possibility that yNAP1 undergoes a conformational change in high salt. This change might result in disruption of the secondary structures required for self-association of the dimers. If this is the case, then the binding of small, cationic (basic) polypeptides might induce the same changes upon complex formation with yNAP1, and be detectable by CD.

Many polypeptides bind metal atoms in order to stabilize their secondary or tertiary structure, or to act as a functional group to facilitate the activity of the protein. The divalent ions Zn^{2+} and Mg^{2+} are common metals involved in the structural stability and catalysis of polypeptides. The zinc ion is often

chelated within proteins by forming a bridge between cysteine and histidine residues, located either near to or distant from each other in the primary sequence of the protein (for review see Matthews and Sunde, 2002). Such metalo-proteins are generally considered as being limited to proteins with DNA binding activity. However, their role in cellular processes has extended to involve protein-protein, protein-membrane, and protein-chromatin interactions (Urnov, 2002). yNAP1 contains 5 cysteine and 4 histidine residues, and thus may bind Zn^{2+} in order to achieve its native, *in vivo* conformation. yNAP1 is ~33 % unstructured, which led us to hypothesize that the binding of Zn^{2+} may lead to a conformational change.

Chapter 2 describes CD spectroscopic measurements on yNAP1 and a series of deletion mutants, in order to ascertain their structural integrity, compared to the full-length protein. This analysis revealed that the extreme C-terminus of yNAP1, (amino acids 302-417), which was stable to trypsin proteolysis, retained basic protein binding activity though devoid of measurable secondary structure. We suggest that trypsin cleavage occurrs on a solvent exposed loop between residues 293 and 302, because there are additional trypsin cleavage sites towards the C-terminus from these residues that are not accessible. Because of this, we deduced that yNAP1 is a single 'domain' polypeptide between residues 74 and 417. However, what has not been addressed is if residues 302-417, which are devoid of secondary structure on their own, assume any secondary structure within the context of the full-length protein. Interestingly, a GST pull-down utilizing GST-302-417

and His6-tagged 74-293 was able to detect a direct interaction between the two (data not shown). Thus, it appeared likely that the two polypeptides could form a complex. Thus, we sought to determine if the unstructured, acidic C-terminus of NAP1, shown to contribute to non-specific, basic protein binding (Chapter 2), is unstructured in the context of the full-length protein.

From the above observations a few hypotheses were drawn regarding structure-function relationships of yNAP1. The first: yNAP1 may undergo a significant alteration in secondary structure when exposed to high ionic strength. This was addressed by comparing the CD spectra of identical concentrations of yNAP1 in 75 and 500 mM NaCl (Figure 4.1). The second hypothesis: yNAP1 may undergo significant alterations in secondary structure when in complex with basic polypeptides. This was addressed by comparing the CD spectra of yNAP1 in the presence and absence of the (H2A-H2B) dimer and the small, basic *Xenopus* sperm peptides, protamines (Figures 4.2, 4.3). The third hypothesis: The presence of the divalent cation Zn^{2+} may lead to a significant alteration of the secondary structure of yNAP1. This was tested by a comparison of the spectra of yNAP1 in the presence and absence of $ZnCl_2$ (Figure 4.4). The final hypothesis: The C-terminal region of yNAP1, while nearly completely unstructured in isolation, may, in the context of the full-length protein, assume some secondary structure. This was addressed by comparing the individual CD spectra of the two recombinant proteins that represent the two proteolysis products with the spectrum of the two together (Figure 4.5).

4.2 Experimental Procedures:

Circular Dichroism: CD spectra were collected on a Jasco 720 spectropolarimeter at 5° C. Fifteen to twenty spectra were obtained and averaged for each polypeptide in 20 mM NaH_2PO_4 (pH 7.6), 75 mM NaCl (except where specified otherwise, as for the spectra in 500 mM NaCl). The parameters for the histones (number of residues, molecular weights, molar extinction coefficients) were derived from the *S. cerevisiae* sequences retrieved from Pubmed. Histone isoforms '.1' were used. As it is difficult to accurately quantitate the molar concentration of the protamines (they are heterogeneous polypeptides which absorb very weakly in the near UV), the weight-percent concentration of yNAP1 at 10 μM was determined (~.05%), and a similar concentration of the protamines were used. CD measurement of yNAP1 and its derivatives, as well as the (H2A-H2B) dimer, extended from 260 to 198 or 200 nm. The molar ellipticity [Θ] was obtained by normalization of the measured ellipticity (Θ, in mdeg), using [Θ] = Θ *100 / (n*l*c), where n is the number of residues (430), c is the total concentration in mM and l is the cell path-length in cm (Adler *et al.*, 1973). Experiments which contained a mixture of components which exhibit circular dichroism (polypeptides) are baseline corrected only, not normalized for concentration. This still allows direct comparisons of spectra to ascertain whether the observed spectrum of the mixed components differs significantly from that of the calculated spectra. The calculated spectrum originates from the combined, buffer subtracted

spectra of the individual components. Any significant deviations between the observed and calculated spectra (beyond those expected due to errors in concentration (usually < 7%)) indicate a conformational change in one or both of the absorbing species.

4.3 Results and Discussions:

4.3A Ionic strength induced no conformational change in yNAP1.

Figure 4.1 shows the CD spectra of equivalent concentrations of yNAP1 dialyzed into a buffer containing either 75 or 500 mM NaCl. There is an increase in the negative CD signal at 208 and 222 nm of ~12%, indicating that the presence of high salt does induce some measure of α-helical secondary structure. It is possible, however, that the difference in the intensity of the 500 mM NaCl sample is due to inaccuracies in the measurement of yNAP1 concentration. The intensity of the signal in CD spectroscopy is extremely sensitive to changes in concentration, and the similarity in the overall shape of the two spectra possibly indicates a change in the intensity, rather than a change in conformation. A true conformational change would perhaps lead to a change in the shape of the spectrum, for example, altering the ratio of the negative peaks at 208 and 22 nm.

Thus, while there is a change in the spectrum of yNAP1 in high salt, and that change is greater than the expected error due to measuring of the protein, the data are not conclusive with regard to a true conformational change. This could be more quantitatively analyzed by preparing 3 or more

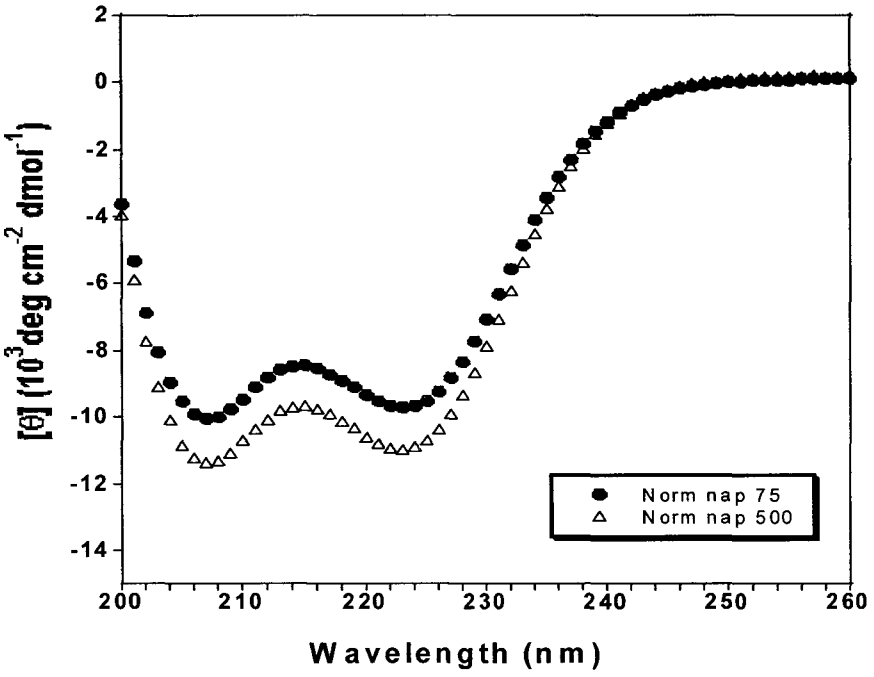

Figure 4.1: CD spectra of yNAP1 at 75 and 500 mM NaCl. CD spectra of full-length yNAP1 shows a minor conformational change due to ionic strength.
10 μM purified, dialyzed (75 mM and 500 mM NaCl) yNAP1 was subject to CD spectroscopy. The data was buffer subtracted and normalized on a per-residue basis.

samples at a variety of protein concentrations for each concentration of NaCl. Upon collection of the spectra, the data could be buffer subtracted and normalized for concentration, after which the spectra for each salt concentration should overlap. The average of the spectra at different protein concentrations could be determined, and a comparison of the average spectra for 75 and 500 mM NaCl might more qualitatively determine the difference between them. This result was not pursued further at the time because other experiments were judged to be of higher priority. However, the simplicity of the method makes it highly amenable to a future investigation.

4.3B: No Conformational change induced in yNAP1 by a structure specific ligand (H2A-H2B).

We next asked if any structural changes might be invoked in yNAP1 in the presence of a structure-specific interacting polypeptide, the (H2A-H2B) dimer. Figure 4.2 shows the observed CD spectrum of yNAP1 in the presence of the histone dimer (obs nap+dimer), and the calculated spectrum of yNAP1 plus the dimer (calc nap+dimer). Again, within the error range of the method, no changes in the CD spectra are seen, indicating no gross conformational change induced in yNAP1 in the presence of its natural protein ligand, the (H2A-H2B) dimer.

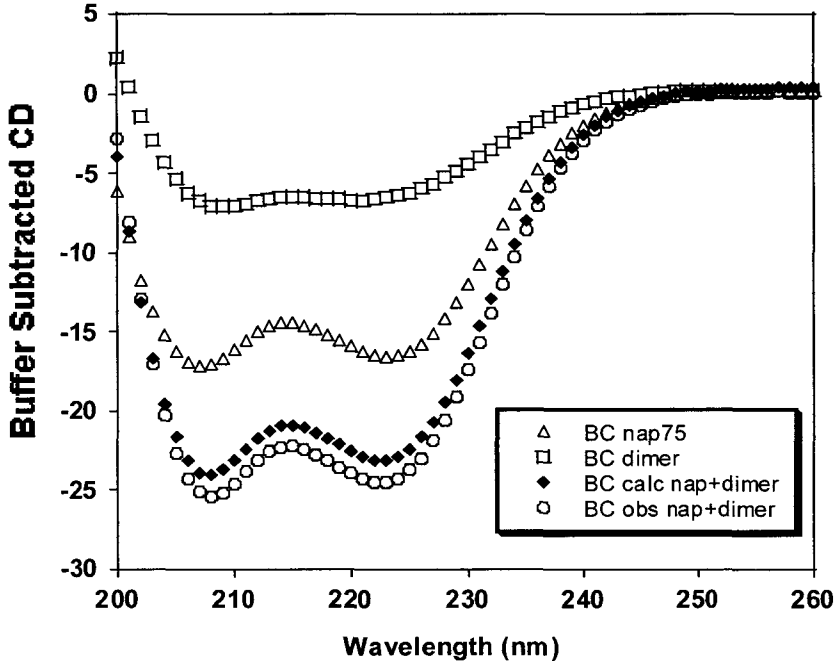

Figure 4.2: CD spectrum of yNAP1 and (H2A-H2B). CD spectra of yNAP1 in the presence and absence of the (H2A-H2B) histone dimer indicates no significant conformational changes upon mixing. Reference spectra for 10 μM yNAP1 and 5 μM dimer were collected separately. The spectra of both the components (obs nap+ dimer) contained the same concentrations of each polypeptide. The calculated spectrum is the sum of the two components. All data were buffer subtracted.

4.3C No conformational change is induced in yNAP1 by a basic peptide.

Figure 4.3 shows the CD spectra of yNAP1 in the presence and absence of the basic polypeptide protamines, and the calculated spectrum of yNAP1 plus the protamines. These small cationic peptides would likely interact with yNAP1 though a non-specific interaction mediated by the acidic C-terminal domain (or other exposed acidic patches) as described for histone H1 in Chapter 2. These basic peptides appear relatively unstructured on their own, and a comparison of the observed spectrum of yNAP1 in the presence of these peptides (obs nap+prot), and the calculated spectrum of yNAP1 plus the peptides (calc nap+prot), reveals no gross changes in the shape or intensity of the spectra. This indicates that no conformational changes are induced within yNAP1 in the presence of protamines.

4.3D Zn^{2+} induces no conformational change in yNAP1.

Figure 4.4 shows the CD spectrum of yNAP1 in the presence and absence of Zn^{2+}. The presence of 40 μM $ZnCl_2$ had no affect on the secondary structure of yNAP1, indicating that it likely does not bind this divalent cation or its binding enacts no alterations to the secondary structure. This does not preclude the possibility, however, that yNAP1 binds other divalent cations (Mg^{2+}, Mn^{2+}, etc.).

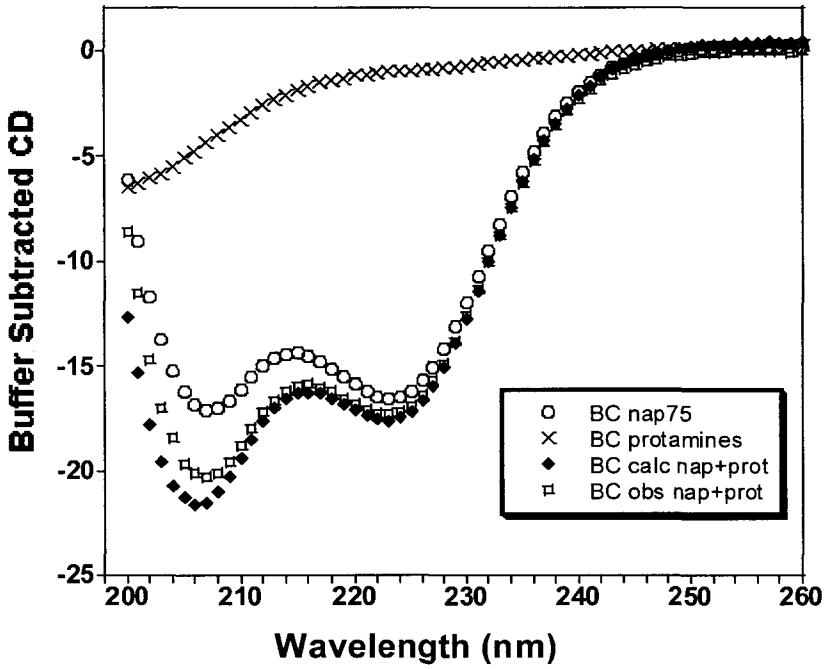

Figure 4.3: CD spectrum of yNAP1 and protamine. Reference spectra of 10 μM yNAP1 and .05 % protamine were collected separately.The spectra of both the components (obs nap+ prot) contained the same amounts of each molecule. The calculated spectrum is the sum of the two components. All data was buffer subtracted.

.

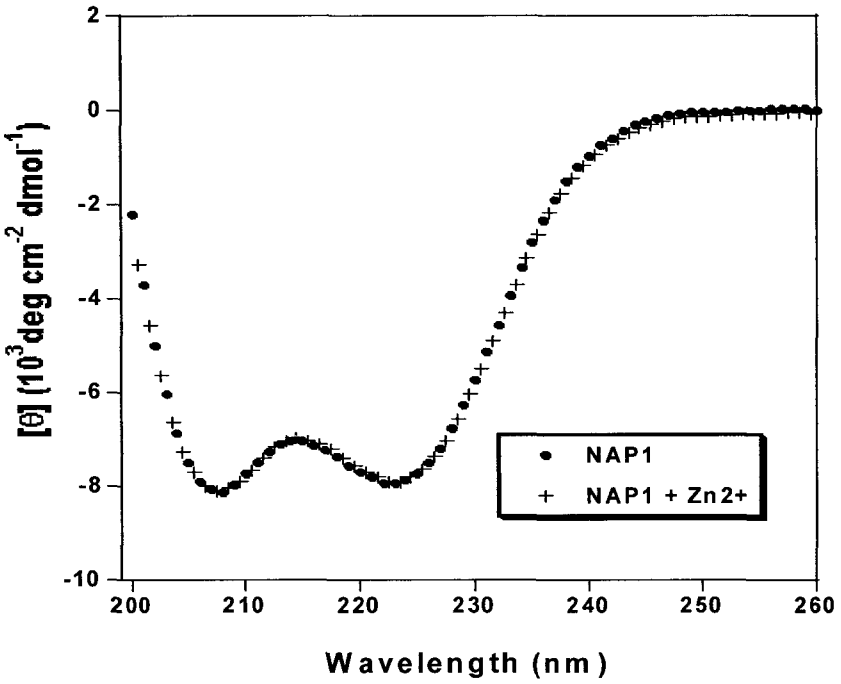

Figure 4.4: CD spectra +/- ZnCl2. CD spectra of yNAP1 shows no secondary structure changes upon addition of zinc. Shown are the CD spectra of 10 μM yNAP1 in the presence and absence of 40 μM $ZnCl_2$. The data was buffer subtracted and normalized on a per-residue basis.

4.3E Conformation of the C-terminus of yNAP1

Figure 4.5 shows the CD spectra of amino acids 74-293, 302-417, and the observed and calculated spectra of equivalent concentrations of both. The spectrum of 302-417 is indicative of a largely unordered polypeptide, while that of 74-293 retains a significant proportion of α-helix (~15%, Chen *et al.*, 1972). However, the observed spectrum of an equimolar mixture of the two components (observed) deviates significantly from that of the calculated spectrum determined by adding the spectra of the two separate polypeptides. The large negative peak at ~200 nm, indicative of a largely unstructured polypeptide, is not observed. Instead, a well-defined peak of negative intensity at 208 nm is observed. This result possibly indicates that complex formation between the two components occurred, resulting in an increase in the secondary structure of one or both of the components. Thus, while the unstructured acidic C-terminus of yNAP1 retains the ability to bind histones and non-histone basic proteins on its own, it is more structured in the context of the full length protein. This finding may alter our interpretation of how yNAP1 interacts with its binding partners, as it may contribute a structure dependent AND electrostatic attraction, as discussed in Chapter 2.

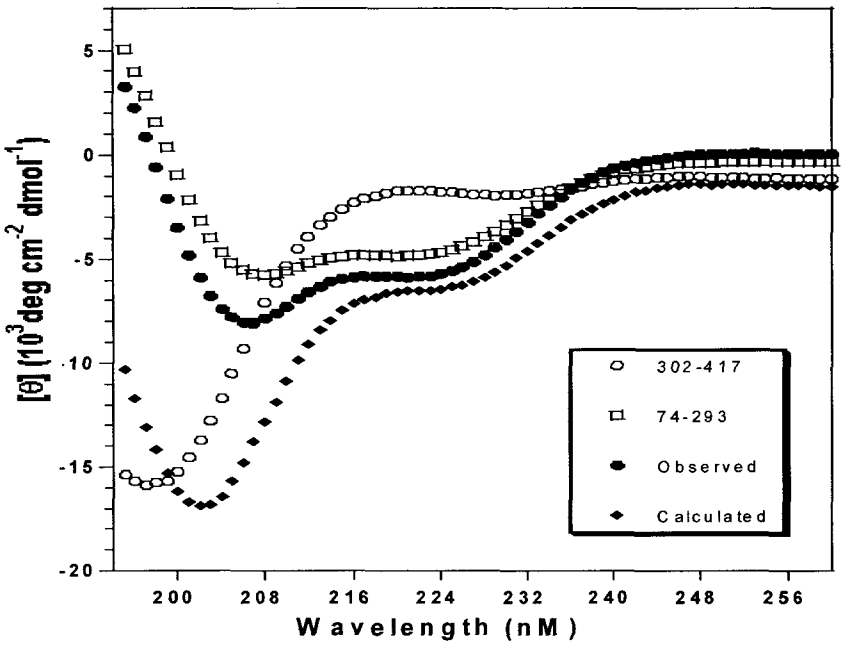

Figure 4.5: CD spectra of yNAP1 deletion constructs. These spectra show binding and the induction of secondary structure. 10 μM of each yNAP1 deletion was subject to CD spectroscopy, as was a mixture of 10 μM of both the components (observed). The calculated spectrum is the sum of the two components, normalized for concentration. The data was buffer subtracted and normalized on a per-residue basis.

4.3F Summary of CD experiments

The results of these analyses reveal that while a subtle change in the conformation of yNAP1 may be induced upon the addition of high salt, no gross changes are seen upon complex formation with either a non-specific, electrostatic binding ligand (protamine), or a structure-specific binding ligand (H2A-H2B). We had hoped that the relatively large proportion of unstructured residues within yNAP1 would undergo a transition and adopt a more ordered conformation upon interaction with these cations. However, it appears that the unstructured residues within yNAP1 do not become more ordered upon interaction with positively charged molecules, specific or non-specific. We reserve the possibility that the secondary structure analysis performed on yNAP1 utilizing a CD spectrum extending into the far UV overestimated the proportion of unstructured residues within yNAP1. Regardless, we hope that the efforts currently being extended towards solving the high-resolution X-ray crystal structure of yNAP1 will shed some light on the domains required for histone-fold specific and non-specific, basic protein binding. Additionally, these studies will also likely reveal regions that are devoid of secondary structure, and what role they play in the diverse functions in which yNAP1 participates. A high resolution structure will also reveal the domain(s) necessary for the formation of the homo-dimer, and what region(s) are necessary for the formation of the higher order complexes investigated in Chapter 3. This will inevitably lead to a great number of interesting and

challenging experiments to further investigate the structure-function relationships within yNAP1 (see Chapter 6).

Chapter 5

Supplemental Studies on the Histone Binding Properties of the Yeast Nucleosome Assembly Protein 1

This chapter will contain experiments performed in the course of the investigations described in Chapters 2 and 3, which were not included in the prepared manuscripts. These experiments pertain to its histone binding activity and utilize direct binding assays (GST pull-down) and CD spectroscopy. The experiments described herein will contain: a brief abstract outlining the background for the experiment, including the rationale, an experimental procedures section, the experiment, and a brief results/discussion section. Rather than being heavily annotated, I instead refer readers to relevant sections of the Introduction (Chapter 1), and the prepared manuscripts (Chapters 2 and 3) for in-depth background information.

5.1 Background on protein binding by yNAP1

Chapter 2 describes the ability of yNAP1 to bind recombinant and native core histones, and the non-histone fold protein H1. These studies use the highly purified, well characterized histone pairs (H2A-H2B) and $(H3\text{-}H4)_2$. Previous studies on NAP1 have utilized native histone preparations which contain a variety of histone variants and post-translational modifications (Fujii-Nakata *et al.*, 1992; Ishimi *et al.*, 1987; Ito *et al.*, 1996; McQuibban *et al.*, 1998). The McQuibban study determined the binding preference of yNAP1 by performing a Far-Western blot, in which individual, SDS-PAGE separated histones were 'refolded' on a membrane. This preceded the binding of radio- or fluorescently labeled yNAP1 and detection of complexes by PhosphorImage analysis. This method determined that H2B had the highest, and H4 the lowest affinity for yNAP1. We argue in Chapters 1 and 2, however, that the histone proteins are not properly folded in the absence of their complementary histone, and only in the context of the histone 'handshake' conformation are the valid yNAP1 contacts and affinities revealed. We sought, therefore, to further investigate the interaction of yNAP1 with purified, recombinant individual histones (Figures 5.1 and 5.2).

While yNAP1 has been shown to bind to the core histone proteins, it has also been shown that yNAP1 binds the linker histones H1 and H5 and the non-histone, DNA binding and chromatin associated proteins HMG1 and 2 (though HMG 14 did not bind) (McQuibban *et al.*, 1998). A Far-Western blot was again used to determine yNAP1 binding affinities, and, as discussed

above, this assay does not necessarily monitor the binding of proteins in their native conformation. Chapter 2 describes how yNAP1 binds the histone-fold-lacking, basic protein H1 in solution, and determines that this binding is possibly a result of electrostatic interactions with the acidic C-terminus of yNAP1 (amino acids 302-417). We sought to determine if irrelevant protein binding by yNAP1 was one of its intrinsic properties, or if yNAP1 will only bind basic proteins that are relevant to the chromosomal milieu. We thus determined if yNAP1 would bind another histone-fold lacking protein, the cyclic-AMP response element binding protein (CREB) (Quinn, 2002). CREB contains a basic leucine zipper domain. We hypothesized that this domain, when not in contact with DNA, would act as a non-specific binding substrate for yNAP1 (Figure 5.1).

Chapter 2 describes how the isolated, acidic C-terminus of yNAP1 was unstructured in solution, though retained the ability to bind the core histones and the non-histone protein H1. This region of yNAP1 (amino acids 302-417) contains the two most highly conserved regions within the NAP family, as well as the largest acidic domain (see Figures 1.8A, 1.8B). We sought to determine if the histone binding by 302-417 was due to the conserved regions between residues 302 and 365 or the acidic region (amino acids 365-403). We prepared a GST-fusion protein containing residues 302-365 and tested it for binding to the histone complexes (Figure 5.2)

5.2 Experimental procedures:

The purified, lyophilized, core histones were a generous gift of Cindy White. The four core histones were separately dialyzed extensively into a mild buffer of neutral pH (7.6) and moderate ionic strength (75 mM NaCl). Their concentrations were determined by the Beer-Lambert law, using their absorbance and extinction coefficients at 276 nm. CD spectroscopy was performed essentially as described in Chapter 3. Recombinant protein expression/purification and GST pull-downs were performed essentially as described in Chapter 2. CREB protein was a generous gift of Jeanne Mick.

5.3 Results and Discussion:

5.3A Binding of individual histones to yNAP1

The individual histone proteins (lyophilized peptides) were dialyzed extensively into a buffer of neutral pH (7.6) and moderate ionic strength (75 mM NaCl) and tested for their ability to bind yNAP1 (Figure 5.1, lanes 1-12). This experiment shows that yNAP1 does bind the individual histones, though no clear preference is indicated. What is also evident is that histones H3 and H4 bind nearly as well to the negative control protein GST as to GST-yNAP1 (see lanes 8 and 11).

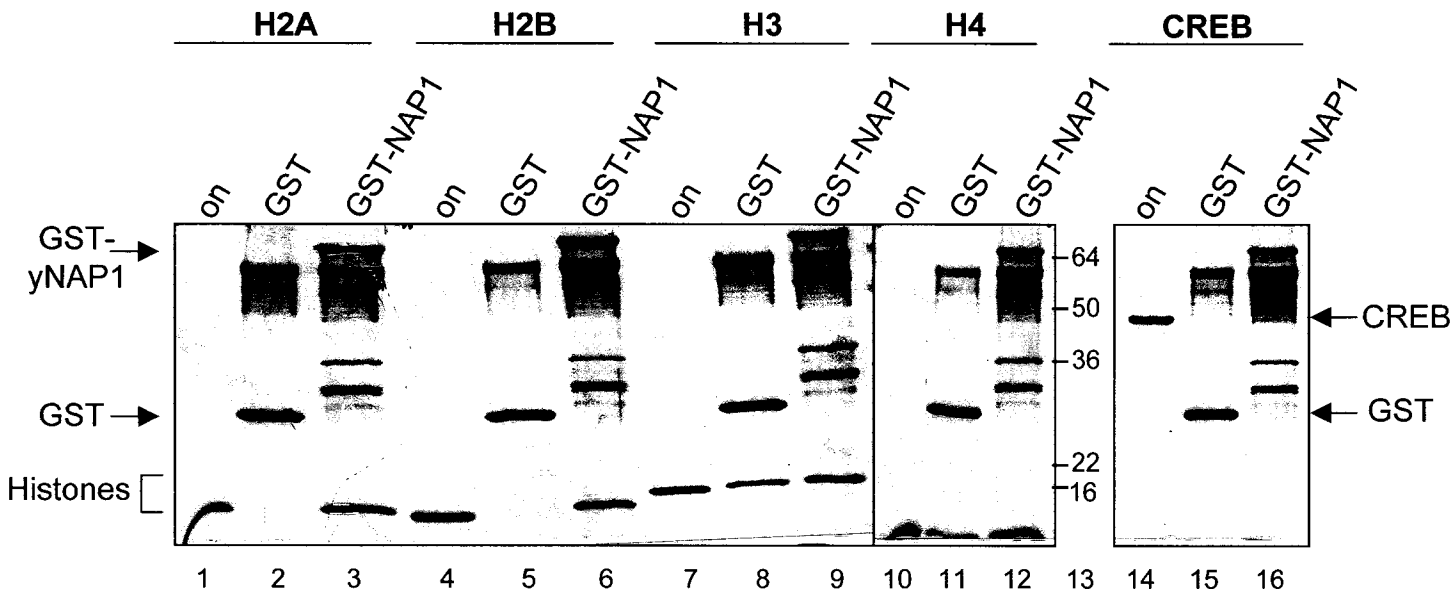

Figure 5.1: Binding of individual histones and the basic protein CREB by yNAP1.
100 pMoles of bead-bound GST or GST yNAP1 were incubated with 100 pmoles of the individual histones and the basic protein CREB. The protein complexes were separated by SDS PAGE and detected by Coomassie staining. 20% of each histone and CREB onput is shown (lanes 1, 4, 7,10, and 14). Lanes 2, 5, 8, 11, and 15 are controls for non-specific binding (GST alone). Lanes 3, 6, 9, 12 and 16 show binding of the histones H2A, H2B, H3, H4 and CREB by yNAP1. Lane 13 shows the positions of the molecular weight markers (kDa). The positions of the proteins are located at left and right. The smearing in the lanes containing GST and GST yNAP1 is an artifact of loading beads onto the gel.

These complexes were washed with buffer containing 250 mM NaCl prior to gel electrophoresis, thus the non-specific binding to GST is relatively robust. No such controls were utilized in the McQuibban study, and the washes were performed with a less stringent buffer. This suggests that the binding shown by Figure 5.1 and that described in the McQuibban study are likely non-specific in nature, and the preference that this group reports is unlikely to be physiologically valid. What this experiment doesn't reveal, however, is the structural nature of the individual histones in these binding reactions.

5.3B CD spectroscopy of individual histones

These same polypeptides were subjected to CD spectroscopy to determine their secondary structure content (Figure 5.2). The data from the CD analysis were rigorously analyzed for secondary structure components (Sreerama and Woody, 2000). While the X-ray structures of the histone octamer and the nucleosome core particle reveal the histones to be almost entirely α-helical, the secondary structure analysis of the individual histones revealed H2A and H2B to be all β-sheet, while H3 and H4 were a mixture of α-helix and β-sheet. Thus, the individual histones do not adopt their native conformation. It is unlikely that any binding assay using individual histones will reflect the preferences and affinities of the folded histone pairs. Therefore, the experiments from which the conclusions of the McQuibban study were drawn need to be considered when analyzing this report.

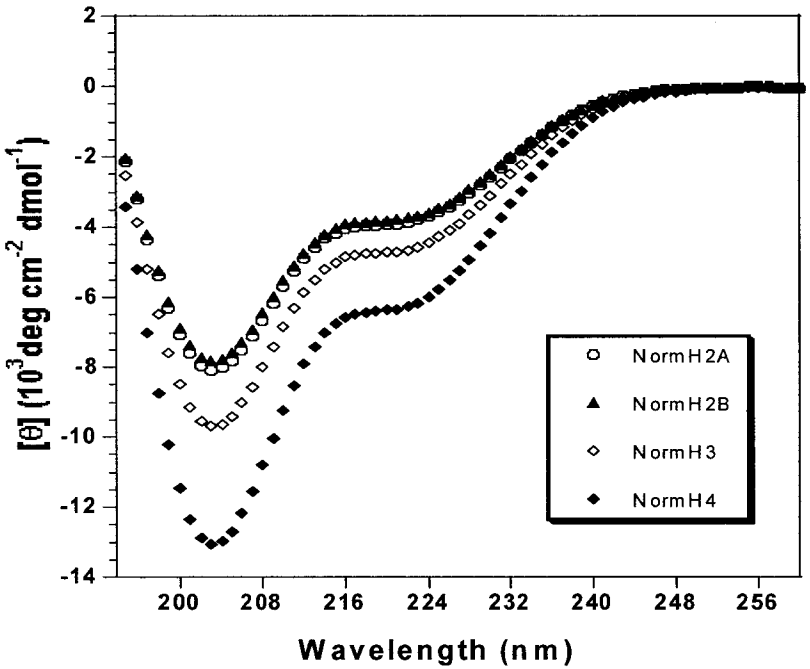

Figure 5.2: CD spectra of histones. CD spectra of the individual histone proteins show their lack of secondary structure. 10 μM of purified, dialyzed histones were subject to CD spectroscopy. The data was buffer subtracted and normalized on a per-residue basis.

5.3C CREB binding by yNAP1

We next asked if yNAP1 would bind the non-histone protein CREB. Figure 5.1, lanes 14-16 show that yNAP1 does not bind this basic protein, thus the binding of H1 described herein (Chapter 2) is not the result of yNAP1 having a 'general' affinity for basic polypeptides. It is also possible that NAP1 may function in the deposition onto or removal of histone H1 from chromatin, though the role of yNAP1 in H1 dynamics has not been investigated to date.

5.3D Histone-pair binding by residues 302-365 of yNAP1

We next analyzed a small region of the C-terminus of yNAP1 (amino acids 302-365) to determine if this most conserved region, or the most acidic region, is responsible for histone binding. Figure 5.3 shows amino acids 302-365 binding to the histone complexes.

5.4 Summary and conclusions.

In this chapter we demonstrate that while yNAP1 does bind the isolated histone proteins, it appears not to discriminate between them. These experiments were performed in order to rationalize the differences in our results (Chapter 2) from those of a previous analysis of yNAP1 (McQuibban *et al.*, 1998). Our demonstration that yNAP1 binds unstructured, basic polypeptides is not surprising. In Chapter 2 we demonstrate that the acidic C-terminus of yNAP1 (aa 366-417) can, on its own, interact with histone H1, and interacts with the unstructured, basic N-terminal tails of the core histones.

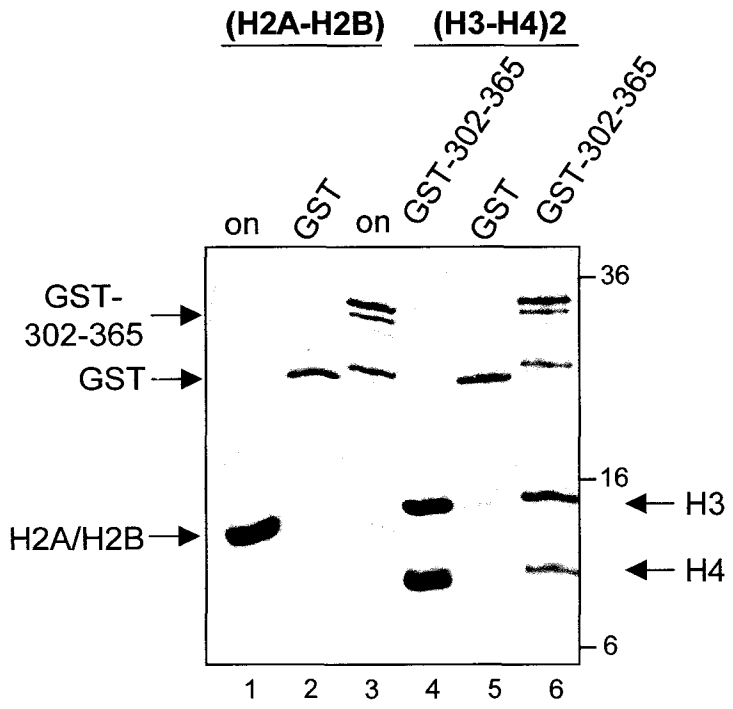

Figure 5.3: yNAP1 302-365 binds the histone pairs. Histone binding by the conserved domain of yNAP1 (aa302-365).100 pMoles of bead-bound GST or GST 302-365 was incubated with 100 pMoles of the histone pairs. The protein complexes were separated by SDS PAGE and detected by Coomassie staining. 20% of each histone onput is shown (lanes 1 and 4). Lanes 2 and 5 are controls for non-specific. Binding (GST alone). Lanes 3 and 6 show binding of the histone pairs by yNAP1 amino acids 302-365.The positions of the proteins are indicated, and the positions of MW markers are shown at right (kDa).

A comparison of the primary sequences of histones from yeast and *Xenopus* reveals that H2B, shown to have the highest affinity for yNAP1 (McQuibban *et al.*, 1998), is more enriched with lysine side chains than the other histones (6-8 more on average). Additionally, histone H4 is ~103 amino acids in length, whereas the others are 131-136 amino acids long. Thus, rather than measuring the affinities towards individual histone structures, the McQuibban study may have revealed only electrostatic attractions between small, unstructured basic polypeptides and the acidic yNAP1 molecule.

In Chapter 2 we suggested that the acidic region (amino acids 356-403) contributes an electrostatic attraction towards the basic histone molecules, and thus acts as a non-specific binding domain. We also demonstrated that the acidic C-terminus binds the unstructured N-terminal tails of the histones (Chapter 2). This conclusion was drawn from data utilizing constructs containing residues 302-417. This construct contains both the highly conserved regions and the largest acidic region.

Therefore, we must now consider the possibility that two histone-binding domains are located in the C-terminus. We can infer from the remarkable level of conservation of amino acids 310-320 and 354-364 that they play an important role in yNAP1 structure and/or function. If one or both of these domains do form a histone-binding platform, the acidic region may serve as an electrostatic 'net' to bring the basic histone proteins into the vicinity of these conserved regions. Rather than functioning as a 'reservoir' for histones,

as suggested in Chapter 2, the acidic domain might rapidly capture histones and enhance the affinity of yNAP1 towards histones.

We also must consider, however, that this small construct, with two regions rich in hydrophobic side-chains flanking a short acidic domain, does not behave in isolation as it does in the context of the full-length protein. Caution must be exercised when analyzing deletion mutants, as a single domain or region may not function in isolation as it might in the context of the full-length protein. It is likely that the high-resolution X-ray structure of yNAP1 will reveal much about the positions of these regions in the context of the protein, and that this will reveal the true mechanism for histone binding by yNAP1.

Chapter 6

Summary of Results and Future Directions for yNAP1 investigations

The goal of this chapter is to provide the reader with a clear sense of what was learned from the results presented herein regarding histone binding and yNAP1 structure-function relationships, and what remains to be learned regarding yNAP1. Future investigations will be facilitated by the fact that yNAP1 is a relatively simple protein (biochemically) to work with. It is easily prepared in large quantities and is stable at high concentrations (mM). With the purified histone components and pre-formed nucleosomes and nucleosomal arrays available within the Department of Biochemistry and Molecular Biology at CSU, there are a number of straightforward and ready-made experiments leading to publications that could follow from this work.

6.1 Summary of Dissertation Results: Implications Towards yNAP1/Histone Complexes.

The results presented in Chapter 2 indicate a clear preference for yNAP1 towards the tetramer over the dimer. This preference is independent of the method of preparation (native or recombinant) or organism from which the histones were obtained. The preference towards the tetramer appears to be due to electrostatic binding of the histone N-terminal tails of H3 and H4 by the C-terminal acidic region of yNAP1. Non-specific, basic protein binding appears also to be mediated by this same acidic domain. Finally, the stoichiometry of the yNAP1/histone complexes was determined to be one yNAP1 molecule per histone-fold. This equates to two yNAP1 molecules binding to each (H2A-H2B) dimer, and four to each $(H3\text{-}H4)_2$ tetramer.

Chapter 3 demonstrates that yNAP1 is a dimer, which likely self-associates into larger species (tetramer and hexamer) in a concentration-dependent manner. Formation of these larger oligomers is regulated by ionic strength.

Taken together, the stoichiometries of the yNAP1/histone complexes and that of yNAP1 itself have important implications towards the mechanism with which yNAP1 binds histones. The two histone-fold dimers (H2A-H2B and H3-H4) have a two-fold symmetry. That is, they each expose two nearly identical faces (surfaces) which are available for interaction by histone binding factors (Figure 6.1). These surfaces are not involved directly in histone-DNA

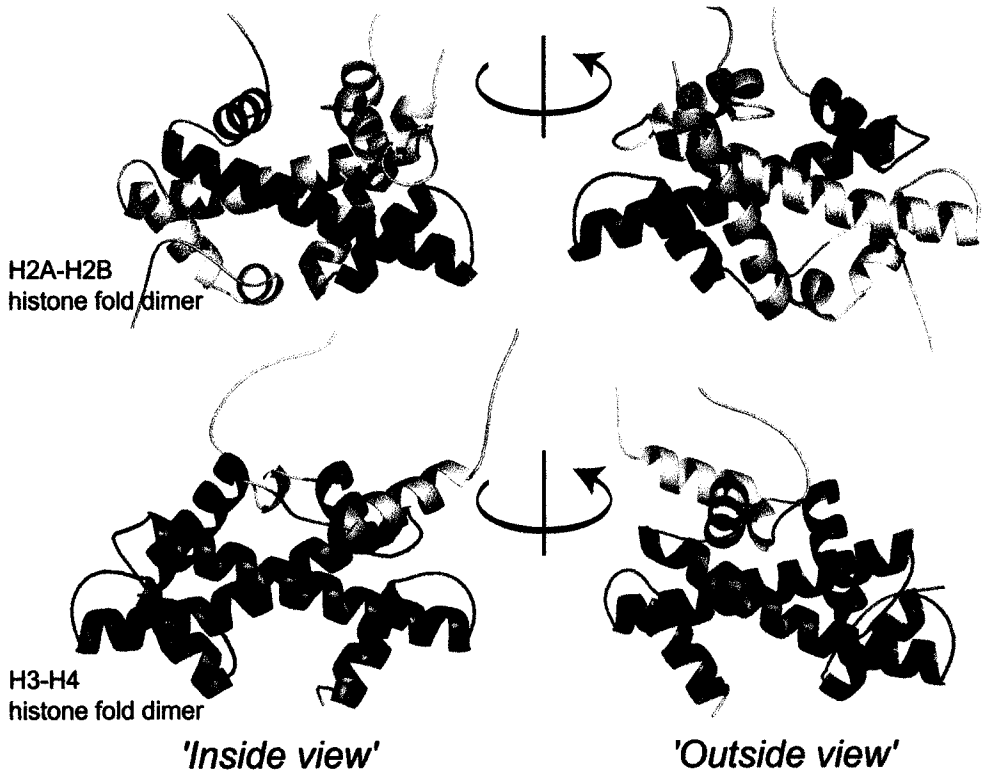

Figure 6.1: Conservation of the histone pairs and their exposed faces . Ribbon diagrams of the H2A (yellow) and H2B (red) dimer, and the H3 (blue) and H4 (green) dimer. The H2B α-C helix and the H3 α-N helix are shown in tan. One half of the (H3-H4)2 tetramer is shown for clarity, and to highlight the remarkable similarity between the two histone-fold dimers. Figure provided by U.M. Muthurajan.

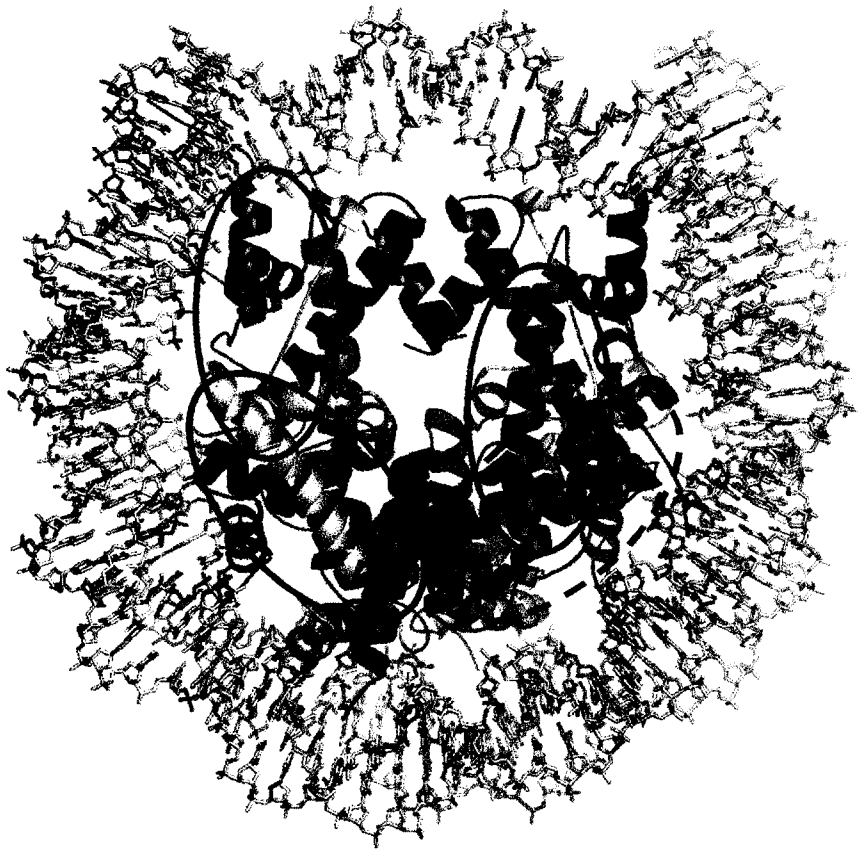

Figure 6.2: Exposed faces within the nucleosome core particle. The structure of the nucleosome core particle reveals likely interaction surfaces for yNAP1. Viewed from one face of the disk-shaped core particle, one can easily see the exposed face of the nearest (H2A-H2B) dimer (circled in black), and the exposed faces of the two (H3-H4) dimers (circled in red) on this side of the disk. Note: the H3 long helix at left is partially truncated in this figure to better see the exposed H2A long helix. Identical interaction surfaces for the distant (H2A-H2B) dimer (dashed black circle) and two for the distant face of $(H3\text{-}H4)_2$ (not indicated) exist on the opposite face of the nucleosome. Figure provided by U.M. Mutharajan.

interactions necessary for the stability of the nucleosome. Further, these surfaces remain largely exposed even when the histone sub-complexes are restrained within a nucleosome (Figure 6.2). These surfaces would be ideal interaction surfaces for a protein needing to bind to the histone sub-complexes and still be able to deposit them within the constraints of the nucleosome.

yNAP1 also has a two-fold symmetry, that is, forms dimers at physiologic ionic strength and within a reasonably physiologic range of concentrations (nano-molar to low micro-molar). It is easy, therefore, to speculate on the mechanism of histone binding by yNAP1 and to envision the types of complexes that are formed by yNAP1 and histone sub-complexes. Each yNAP1 dimer is capable of interacting with the (H2A-H2B) dimer, or with one-half of the $(H3\text{-}H4)_2$ tetramer. A model for these complexes is shown in Figure 6.3.

As one yNAP1 molecule will likely interact with the opposing faces of the histone-fold pairs, a hinge-like structure between two yNAP1 monomers could allow for simultaneous binding to these faces. The yNAP1/histone complex would also have to leave the histone surfaces required for DNA interactions free, in order for yNAP1 to deposit the histone sub-complex into a stable DNA/histone complex. It is also possible that some portion of yNAP1 acts to mimic the DNA gyres and/or charge yet has a lower affinity toward the histone than that of the DNA/histone complex.

Figure 6.3: Models of yNAP1 / histone complexes. The two-fold symmetry of the histone sub-complexes and the oligomeric state of yNAP1 implies a likely mechanism and stoichiometry of the complexes. Two molecules of a yNAP1 dimer interact with an (H2A-H2B) dimer (above), while two yNAP1 dimers (or one tetramer) interact with an $(H3\text{-}H4)_2$ tetramer (below).

The order of these affinities/stabilities would likely be: DNA/tetramer+dimers (nucleosome) > hexasome > tetrasome > yNAP1/tetramer > yNAP1/dimer. This order of affinities would be required to allow for deposition, and are consistent with those inferred by an earlier mechanistic study of NAP1 (Nakagawa, *et al.*, 2001).

It is unclear at this point what the role of higher-oligomerization by yNAP1 is in histone binding and nucleosome assembly. Perhaps the symmetries and histone interaction surfaces revealed though X-ray crystallography will ultimately determine whether these larger aggregate states contribute to the function of yNAP1, or are, sadly, merely an artifact of the concentrations and methodology used to study the self-association properties.

6.2 Future Directions for yNAP1 Investigations

6.2A Histone Binding Preferences and Affinities

Early investigations have studied NAP1 / histone binding using native preparations of histone proteins (Fujii-Nakata *et al.*, 1992; Ishimi *et al.*, 1987; Ito *et al.*, 1996; McQuibban *et al.*, 1998). These contain a number of different histone isoforms that likely contain a variety of post-translational modifications. It is possible that NAP1 behaves differently towards histone variants, and that the binding affinities/preferences towards histones are altered due to post-translational modifications of histone amino acid side-chains. Our use of recombinant preparations from two different organisms (yeast and *Xenopus*), and the direct comparisons between native and

recombinant preparations (yeast and *Drosophila*) has laid a foundation for our understanding of these effects. However, much remains to be learned with regard to the binding of histones by yNAP1.

6.2A.1 Labeling Woes

Most importantly, a reliable assay must be achieved in order to determine rigorous, quantitative binding constants for NAP1 / histone complexes. This will mandate using a labeled protein in order to detect complexes at nano-molar concentrations, the likely range of the dissociation constants (Kd's). Our inability to generate functionally competent, isotopic or fluorescently labeled yNAP1 has precluded such determinations.

dNAP1 is readily phosphorylated by CKII (Li *et al.*, 1999), and we have found that it is also an excellent substrate for protein kinase A (PKA) (data not shown). However, γ ^{32}P-ATP phosphorylation by PKA yields a protein that migrates irregularly on a native acrylamide gel, and is likely not functional for such binding assays. While the protocol for PKA labeling calls for incubation at 37 °C for 60 minutes, we modified the protocol to lower temperature (22 °C) and shorter incubations (15 minutes). This yields high-specific activity protein, but again shows aberrant migration on native PAGE. Perhaps there is a different protocol that would yield a better behaved, labeled protein.

We also utilized the *in vitro*, rabbit reticulocyte lysate (TNT, Promega) method for the preparation of ^{35}S-Met labeled yNAP1. This method incorporates radio-labeled sulfur at methiones within the protein during a coupled transcription-translation process, a very innocuous modification.

However, labeled protein derived from this assay also appears to migrate irregularly on native PAGE, and thus is not viable for binding assays. Modification of the protocol to lower temperature and shorter incubations yielded similar results. Perhaps NAP1 requires some component of a bacterial or eukaryotic cell to fold properly or there is a component within the reticulocyte lysate which disrupts the protein. Further, the presence of large amounts of unincorporated labeled amino acid obscured the bands. Perhaps an additional purification step (a small ion exchange column) would eliminate these contaminates.

It appears unlikely at this time, however, that this is a viable method for achieving functional labeled protein.

Young Jun Park has made several attempts to fluorescently label yNAP1 (K. Luger lab, personal communications). N-terminal, C-terminal and internal, cysteine-directed labeling has failed to yield protein which migrates normally on a native PAGE. While these methodologies are often acid/base catalyzed, more mild methods have altered the mobility or the structure of yNAP1 such that the protein is not functional for binding assays. However, there does seem to be further avenues to explore, and these will likely be pursued by Park in the coming months (Summer, 2003). There is such a variety of fluorescent labels and methods that it seems likely that a functional, fluorescently labeled protein can be achieved.

It is interesting to note that a recent analysis of yNAP1-histone binding used fluorescently labeled yNAP1 (McQuibban *et al.*, 1998). This may be

another reason to discount the author's results regarding histone binding affinities and preferences.

6.2A.2 Comparative Affinities for Different Histones

Once we have a method for labeling yNAP1, we can perform EMSA's, and possibly fluorescence resonance energy transfer (FRET) assays, where the energy from one fluorophore (donor) is transferred to another fluorophore on a separate molecule (acceptor). Quantitation of this transfer can allow the preparation of binding curves and a rigorous determination of binding constants. Using one or both of these assays, we can determine absolute binding constants for yNAP1 and the (H2A-H2B) dimer and $(H3\text{-}H4)_2$ tetramer. Such assays will also confirm the stoichiometries determined from EMSA's by Coomassie staining (Chapter 2). With this in hand, we can continue and explore the affinities of yNAP1 for the recombinant histone pairs from a variety of organisms, such as yeast, *Drosophila*, *Xenopus*, and humans. We can also compare the affinities of core histone pairs containing histone variants, such as those incorporated in specialized chromatin domains (Ahmad and Henikoff, 2002).

6.2A.3 N-terminal Histone Tail Modifications

Perhaps the most exciting avenue to pursue is the affect of histone modifications on yNAP1 binding. To date, no correlation between the two has been determined. We have shown that yNAP1 specifically binds to the N-terminal tails of H3 and H4 (Chapter 2), it is likely that modification of these residues by acetylation, methylation and/or phosphorylation will alter NAP1's

affinity towards the histone complexes. Perhaps the most interesting of these modifications is acetylation by the primary cytoplasmic acetyltransferase in yeast, HAT1 (Parthun *et al.*, 1996). This enzyme specifically acetylates histone H4 at lysine 12, one of the conserved, chromatin-assembly specific modifications (see section 1.3). It will be very interesting to determine if this simple modification alters the affinity or specificity of yNAP1 towards $(H3\text{-}H4)_2$.

In addition to this modification, there are a number of site-specific and general histone tail modifying enzymes available in the department and from collaboratory and commercial sources. A number of yeast and higher eukaryote acetyltransferases, methyltransferases and kinases are available, which could be used alone and in concert to analyze yNAP1 binding to modified histone pairs and isolated N-terminal tails (GST-fusions or peptides).

6.2A.4 Tailless Histone Binding

Finally, we have described how the deletion of the N-terminal tails of the four core histones leads to a loss of the preference of yNAP1 for the tetramer over the dimer (Chapter 2). We hypothesized that the binding of yNAP1 to the N-terminal tails of H3 and H4 led to this preference, due to the remarkable similarity between the folded, globular domains of the tetramer and dimer (see section 1.2). It is thus of great interest to determine the relative binding constants of yNAP1 towards the full-length and N-terminally deleted histone pairs to quantitatively validate our hypothesis.

6.2A.5 Mechanism of Histone Binding by yNAP1

In Chapter 2 we describe two independent histone binding modes by yNAP1. The first is the histone-fold specific binding located between amino acids 74 and 365. Binding may be mediated by one or both of the conserved regions between residues 302 and 365 (or other regions of the polypeptide). Consistent with this, Chapter 4 describes how a small construct of yNAP1 (amino acids 302-365) retains histone binding. This region could possibly confer the stoichiometry of the yNAP1 / histone complexes (Chapter 2). The second is crudely determined to be contained within residues 302-417. Chapter 2 describes how the C-terminal, acidic domain located between amino acids 365 and 403 is likely responsible a 'non-specific' binding of basic proteins. This hypothesis is largely drawn from experiments showing that deletion of the large C-terminal acidic domain abrogates yNAP1 binding of the basic, histone fold-lacking protein H1 (Chapter 2).

Titrations of histones beyond the fundamental stoichiometries (2:1 (yNAP1:H2A-H2B) and 4:1 (yNAP1: $(H2A\text{-}H2B)_2$) leads to the formation of larger complexes, perhaps due to non-specific, ancillary binding by the acidic domain (Chapter 2). Alternatively, this domain may serve as a histone protein reservoir, maintaining a greater number of histone molecules in the regions of active chromatin assembly, as appears to be the case for the C-terminal acidic portion of Np and dNLP (Dutta *et al.*, 2001; Namboodiri *et al.*, 2003)

Together, these observations have led us to believe that the two binding activities within yNAP1 are mechanistically different, and thus may perform different functions in the context of chromatin assembly. It is also possible, however, that the electrostatic attraction afforded by the acidic region seems to enhance binding of histones by the more central region. The ability of the C-terminally deleted construct to function in a super-coiling (chromatin assembly) assay as well as the full length protein is thus a consequence of the large amount of yNAP1 utilized and the extensive incubation period (16 hours) (Chapter 2). Thus, we believe that the histone-fold specific binding is due to one or both of the highly conserved regions (residues 311-319 and/or residues 352-363), while there is an ancillary, general basic protein binding activity by the large, C-terminal acidic domain (residues 365-403).

This discrepancy could likely be resolved by comparing the binding constants and curves of full-length yNAP1 and the construct lacking the acidic region (aa 74-417). If the acidic domain aids in binding by the central region, then the dissociation constant of full length yNAP1 will be lower (higher affinity) than that of the deletion construct. If, however, there are two distinct domains for histone binding, then the resulting binding curves from a titration of histones will be bi-phasic, with the histone-fold specific binding yielding a lower Kd than the subsequent ancillary binding due to the C-terminal acidic domain. Such a mechanistic analysis will greatly enhance our understanding of the different functional domains within yNAP1, and expand our understanding of yNAP1 function in chromatin assembly.

6.3 Further Analysis of yNAP1 Chromatin Assembly: What is the Role of the C-terminal Acidic Domain?

In Chapter 2 and section 5.3D, we describe two independent histone binding domains within yNAP1. We hypothesize that there is a primary binding site for histones between amino acids 302 and 365, perhaps involving one or both of the highly conserved regions, and an ancillary binding activity due to the large, acidic domain between residues 365 and 403. This ancillary binding activity may act as a reservoir for histones, and enhance the chromatin assembly activity of NAP1. Alternatively, it may function to enhance the specific binding of histones by contributing an electrostatic attraction.

In vitro chromatin assembly reactions using yNAP1 are typically incubated overnight (+/- 16 hours) prior to processing and gel-electrophoresis. It is likely that this is much longer than is required, as shorter incubation times have been reported, with similar results (S.M. Price, P.J. Laybourn, personal communication). We believe that using select deletion mutants of yNAP1 and a time course of chromatin assembly can determine whether the C-terminal acidic region of yNAP1 facilitates chromatin assembly.

We can design a direct kinetic analysis of the N-terminal deletion of yNAP1 (amino acids 74-417), which assembles chromatin as well as the full-length protein (Fujii-Nakata, *et al*, 1996 and Chapter 2), and the construct lacking the C-terminal acidic domain (amino acids 74-365). By assembling a bulk plasmid chromatin assembly reaction containing equal moles of these polypeptides, and removing and quenching aliquots at specific time intervals,

we can determine to what extent this acidic domain cooperates with the central region in facilitating chromatin assembly. Such an assay would be or great benefit to those who use chromatin assembled plasmid DNA to study transcription, as the use of a shorter incubation time would expedite the accumulation of data.

6.4 Structural Aspects of yNAP1

To date there have been two high-resolution structures of histone chaperones/chromatin assembly factors (nucleoplasmin (Dutta, *et al*, 2001), and NLP (Namboodiri, *et al.*, 2003)). Unfortunately, the high similarity between the two structures, and the lack of similarity of these factors to the NAP-type factors, has not revealed much regarding chromatin assembly and histone binding. There is currently an effort underway to determine the X-ray structure of yNAP1 (Y.J. Park, K. Luger lab). This effort has resulted in crystals that diffract to a high resolution, though difficulties in the phasing process have hampered the acquisition of an electron density map. The high-resolution structure would lead to a number of very exciting new experimental avenues.

6.4A Oligomerization domains of yNAP1

The oligomerization domain of yNAP1 which leads to the formation of the homo-dimer would be revealed. The structure would likely reveal the inter- and intra-molecular contacts required for the dimerization, and might be amenable to future biochemical or biophysical studies. The structure also might reveal the surface involved in the inter-molecular contacts involved in

high-order oligomerization, and the identity of the highest oligomerization state as well. This was explored in the analyses described in Chapter 3, however was not absolutely defined. Disruption of the oligomerization above and beyond the dimer, perhaps by select point mutagenesis, would likely yield significant insight into the role of higher oligomerization with regards to histone binding and the kinetics of chromatin assembly.

6.4B Histone binding domains on yNAP1

Additionally, the structure would likely reveal a hydrophobic and acidic binding platform for the histone fold. The complementarities of these two surfaces could reveal the mechanism of binding, and could lead to interesting mutational analyses on both the yNAP1 surface and the opposing surface(s) on the histone fold. Finally, the localization and availability of the C-terminal acidic region might be determined. When considered together with the deletion analysis (Chapter 2) and the kinetic analysis (section 6.5), the structure would likely be very informative with regard to this relatively enigmatic domain. A more mechanistic interpretation of our earlier results might be seen, and would likely lead to other interesting experimental opportunities.

6.4C Co-crystal structures

While the determination of a *de novo* structure is extremely challenging, often requiring years of concerted effort, having the atomic coordinates in hand can be a powerful tool towards building atomic models for larger complexes. With the atomic model for yNAP1, we can proceed to determine

the co-crystal structure of yNAP1 and its natural binding partners, the histone dimer and tetramer. These structures would reveal the contacts specifically involved in complex formation, and would yield insight into the mechanism behind the preferential binding of $(H3\text{-}H4)_2$ over (H2A-H2B). The co-crystal structure could also determine whether a single histone complex makes simultaneous contacts with both the binding domains on yNAP1. These experiments are currently being pursued by Y.J. Park in Karolin Luger's laboratory.

However, other binding partners for NAP1 exist, and the determination of an X-ray structure would reveal much about the structure-function relationships of yNAP1. Specifically, yNAP1 has been shown to form biologically meaningful complexes with components of the cell-cycle machinery, as revealed by biochemical and genetic methodologies (see section 1.10). It would be very interesting to determine the binding domains on yNAP1 responsible for these interactions, and how these interactions might modulate the histone binding and chromatin assembly activities of yNAP1.

6.5 General Laboratory Properties of yNAP1

6.5A Oligomerization Behavior of yNAP1: Implications towards chromatin assembly reactions.

Chapter 2 describes the oligomerization states of yNAP1. yNAP1 appears to be an obligate dimer, in that it does not appear to dissociate into monomers without undergoing some degree of denaturation. Unless experiments are

performed at concentrations above ~10 uM, there will be little or no higher oligomers. However, the conversion from tetramers and hexamers to the dimeric form may be slow, so extensive dialysis at low concentrations may be necessary if this is an issue. There is little worry of yNAP1 losing function following extensive dialysis at 4 °C as CD has been performed on samples left on ice at 4 °C for many days, with no apparent change in the secondary structure content. However, there is some evidence that yNAP1 is particularly sensitive to temperature, as a preliminary melting curve revealed an apparent Tm of ~37 °C. This melting was fully reversible however, though this 'renatured' protein was not assayed for chromatin assembly or histone binding activity.

From 'back of the envelope' calculations of the concentrations of yNAP1 used in chromatin assembly assays, at 8:1 yNAP1 to histone ratios (mass) the net concentration of yNAP1 is ~100-500 nano-molar. Of course the amount varies as the ratio of histone to DNA changes, as the yNAP1 and histones are mixed together prior to dilution in the final, DNA containing reaction. At these concentrations, yNAP1 is undoubtedly dimeric, thus its function does not seem to depend on the higher oligomerization. However, some of my early cross-linking experiments have shown that more large yNAP1 complexes are formed in the presence of trace amounts of histones (10:1 yNAP1 to histone dimer). Thus, one must consider that oligomerization of yNAP1 may be facilitated by the presence of histones.

6.5B Expression and Purification of yNAP1 and Derivatives

I have used the protocol from the Kadonaga lab (Univ. CA, San Diego) as a starting point for the expression and purification of yNAP1 and deletion mutants. However there are some deviations I have used which can facilitate the acquisition of large amounts of pure protein. Young Jun Park in the Luger laboratory has also expressed and purified many of the larger constructs I cloned (His-6 74-417and 74-365), thus he might also be a good resource for recommendations.

I have not found it necessary to begin the first cultures following transformation immediately following the overnight growth on LB plates. The levels of expression of yNAP1 and derivatives seems to not suffer from storing the plates at 4 °C for a few (1-3) days. I have never made a glycerol stock of yNAP1 in DE3 cells, as this has always seemed somewhat lazy and, in general, bad practice. That does not preclude the possibility that expression would not suffer, however. The ammonium sulfate precipitation requires a solution of 4M $AmSO_4$. This solution must be brought to pH 7.0 or the solution will remain cloudy. If you filter this solution (0.45 µm) it will store well on your bench for many months. I have always grown 4-6 liters of culture, proceeded through the dialysis into A100 (following AmSO4 precipitation), and then frozen 2 liters worth of the supernatent in aliquots at –70 °C. These can then be thawed and loaded onto the Q-Sepharose column at your convenience. I learned to be generous with the protease inhibitors (PMSF and benzamidine) during the purification, as yNAP1 is prone to degradation. Indeed, some level of degradation is inevitable, but can be

minimized by using the indicated amounts and putting them into the buffers immediately before yNAP1. The half-life of PMSF is measured in minutes in aqueous buffers, so a fresh addition is absolutely required. Following the Q-Sepharose column the protocol suggests that you measure the conductivity of the peak fractions and dilute them to 150 mM NaCl. However, I have found that the elution is so consistent from one batch to the next that I assume the NaCl concentration is 410 mM, and thus dilute with A 0M to 150 mM. I have not seen any loss in yield from this shortcut.

The Mono-Q column wash steps can be adjusted to optimize the yield or the purity, depending on your needs. Specifically, the step prior to elution at 500 mM can be modulated up or down from 325 mM NaCl to gain purity or quantity, respectively. The peak from this column is very concentrated, often more than 150 µM. As described above, this should be extensively dialyzed to lower salt and concentration (2-3 days) to eliminate the higher band upon native PAGE. The protein can be stored on ice in the refrigerator or in aliquots at –70 °C, provided there is glycerol in the buffer (>5%).

Some comments on the deletion mutants. I generally screened a series of clones from the initial ligation-transformation mixture to get a clone that expresses well. These clones are in a library in the Luger lab. As described in Chapter 2, His6 74-293 and 74-353 are insoluble, though can be purified following solubilization of the pellets in 8 M urea. 74-353 is not entirely insoluble, and I have compared the protein obtained by native and denaturing purification for histone binding and chromatin assembly, and they are similar.

The GST fusions of these two clones are also insoluble, and I never tried to rescue them, for reasons that should be obvious. His6 302-417 expresses and purifies well, though it always seemed that the recognition of the His6 tag by the antibody (H-15) was poor. Using a similar number of moles of this and any other construct seemed to result in weaker bands following a western blot. The GST-302-365 clone was very prone to proteolysis, as can be seen from Figure 5.3, and the yields are usually quite low.

6.6 Summary

Considering the inter-species homology, and the variety of activities in which NAP1 is involved, our knowledge of the functional, mechanistic and structural aspects of the protein are limited. Early biochemical investigations revealed little about the mechanism and structure/function relationships, and the work presented herein gives the first clear insight into the mechanism of histone binding (Chapter 2) and the structure of yNAP1 (Chapter 3). Much remains to be done, and hopefully the coming months and years will add to our knowledge of the function and structure of the ubiquitous histone chaperone and chromatin assembly factor NAP1.

References

Adler, A.J., Greenfield, N.J. and Fasman, G.D. (1973) Circular dichroism and optical rotatory dispersion of proteins and polypeptides. *Methods Enzymol*, 27,675-735.

Ahmad, A., Takami, Y. and Nakayama, T. (1999) WD repeats of the p48 subunit of chicken chromatin assembly factor-1 required for in vitro interaction with chicken histone deacetylase-2. J *Biol Chem*, 274, 16646-53.

Ahmad, K., and Hennikoff, S. (2002) Histone H3 variants specify modes of chromatin assembly. *Proc Natl Acad Sci USA*, **99**, 16477-16484.

Akey, C.W. and Luger, K. (2003) Histone chaperones and nucleosome assembly. *Curr Opin Struct Biol*, 13, 6-14.

Altman, R. and Kellogg, D. (1997) Control of mitotic events by Nap1 and the Gin4 kinase. *J Cell Biol*, 138, 119-130.

An, W., Palhan, V.B., Karymov, M.A., Leuba, S.H. and Roeder, R.G. (2002) Selective requirements for histone H3 and H4 N termini in p300- dependent transcriptional activation from chromatin. *Mol Cell*, 9, 811-821.

Annunziato, A.T. and Hansen, J.C. (2000) Role of histone acetylation in the assembly and modulation of chromatin structures. *Gene Expr*, 9, 37-61.

Arents, G. and Moudrianakis, E.N. (1995) The histone fold: a ubiquitous architectural motif utilized in DNA compaction and protein dimerization. *Proc Natl Acad Sci* U S A, 92, 11170-11174.

Arents, G., Burlingame, R.W., Wang, B.C., Love, W.E. and Moudrianakis, E.N. (1991) The nucleosomal core histone octamer at 3.1 A resolution: a tripartite

protein assembly and a left-handed superhelix. *Proc Natl Acad Sci* U S A, 88, 10148-10152.

Asahara, H., Tartare-Deckert, S., Nakagawa, T., Ikehara, T., Hirose, F., Hunter, T., Ito, T. and Montminy, M. (2002) Dual roles of p300 in chromatin assembly and transcriptional activation in cooperation with nucleosome assembly protein 1 in vitro. *Mol Cell Biol*, 22, 2974-2983.

Ausio, J. and van Holde, K.E. (1986) Histone hyperacetylation: its effects on nucleosome conformation and stability. *Biochemistry*, 25, 1421-1428.

Ausio, J., Dong, F. and van Holde, K.E. (1989) Use of selectively trypsinized nucleosome core particles to analyze the role of the histone "tails" in the stabilization of the nucleosome. *J Mol Biol,* 206, 451-463.

Baake, M., Doenecke, D. and Albig, W. (2001) Characterisation of nuclear localisation signals of the four human core histones. *J Cell Biochem*, 81, 333-46.

Baer, B.W. and Rhodes, D. (1983) Eukaryotic RNA polymerase II binds to nucleosome cores from transcribed genes. *Nature*, 301, 482-8.

Bannister, A.J. and Kouzarides, T. (1996) The CBP co-activator is a histone acetyltransferase. *Nature*, 384, 641-3.

Bauer, U.M., Daujat, S., Nielsen, S.J., Nightingale, K. and Kouzarides, T. (2002) Methylation at arginine 17 of histone H3 is linked to gene activation. *EMBO* Rep, 3, 39-44.

Baxevanis, A.D., Arents, G., Moudrianakis, E.N. and Landsman, D. (1995) A variety of DNA-binding and multimeric proteins contain the histone fold motif. *Nucleic Acids Re*s, 23, 2685-91.

Bohm, L. and Crane-Robinson, C. (1984) Proteases as structural probes for chromatin: the domain structure of histones. *Biosci Rep,* 4, 365-386.

Carruthers, L.M. and Hansen, J.C. (2000) The core histone N termini function independently of linker histones during chromatin condensation. *J Biol Chem*, 275, 37285-37290.

Carruthers, L.M., Schirf, V.R., Demeler, B. and Hansen, J.C. (2000) Sedimentation velocity analysis of macromolecular assemblies. *Methods Enzymol*, 321, 66-80.

Chang, L., Loranger, S.S., Mizzen, C., Ernst, S.G., Allis, C.D. and Annunziato, A.T. (1997) Histones in transit: cytosolic histone complexes and diacetylation of H4 during nucleosome assembly in human cells. *Biochemistry*, 36, 469-480.

Chen, Y.H., Yang, J.T. and Martinez, H.M. (1972) Determination of the secondary structures of proteins by circular dichroism and optical rotatory dispersion. *Biochemistry*, 11, 4120-4131.

Cheung, P., Allis, C.D. and Sassone-Corsi, P. (2000) Signaling to chromatin through histone modifications. *Cell,* 103, 263-71.

Cotten, M. and Chalkley, R. (1987) Purification of a novel, nucleoplasmin-like protein from somatic nuclei. *Embo J*, 6, 3945-54.

Davey, C.A., Sargent, D.F., Luger, K., Maeder, A.W. and Richmond, T.J. (2002) Solvent mediated interactions in the structure of the nucleosome core particle at 1.9 a resolution. *J Mol Biol*, 319, 1097-113.

Davie, J.R. (1998) Covalent modifications of histones: expression from chromatin templates. *Curr Opin Genet Dev,* 8, 173-8.

Davies, G.E. and Stark, G.R. (1970) Use of dimethyl suberimidate, a cross-linking reagent, in studying the subunit structure of oligomeric proteins. *Proc Natl Acad Sci U* S A, 66, 651-656.

DeLange, R.J. (1979) The evolution of histones in relationship to recent advances in elucidating chromatin structure. *UCLA Forum Med Sci,* 21, 151-8.

Demeler, B., Saber, H. and Hansen, J.C. (1997) Identification and interpretation of complexity in sedimentation velocity boundaries. *Biophys J,* 72, 397-407.

Dilworth, S.M., Black, S.J. and Laskey, R.A. (1987) Two complexes that contain histones are required for nucleosome assembly in vitro: role of nucleoplasmin and N1 in Xenopus egg extracts. *Cell,* 51, 1009-18.

Dingwall, C. and Laskey, R.A. (1990) Nucleoplasmin: the archetypal molecular chaperone. *Semin Cell Biol,* 1, 11-7.

Dingwall, C., Dilworth, S.M., Black, S.J., Kearsey, S.E., Cox, L.S. and Laskey, R.A. (1987) Nucleoplasmin cDNA sequence reveals polyglutamic acid tracts and a cluster of sequences homologous to putative nuclear localization signals. *Embo J,* 6, 69-74.

Dong, A., Zhu, Y., Yu, Y., Cao, K., Sun, C. and Shen, W.H. (2003) Regulation of biosynthesis and intracellular localization of rice and tobacco homologues of nucleosome assembly protein 1. *Planta*, 216, 561-70.

Dorigo, B., Schalch, T., Bystricky, K. and Richmond, T.J. (2003) Chromatin Fiber Folding: Requirement for the Histone H4 N-terminal Tail. *J Mol Biol*, 327, 85-96.

Dutta, S., Akey, I.V., Dingwall, C., Hartman, K.L., Laue, T., Nolte, R.T., Head, J.F. and Akey, C.W. (2001) The crystal structure of nucleoplasmin-core: implications for histone binding and nucleosome assembly. *Mol Cell*, 8, 841-853.

Earnshaw, W.C., Honda, B.M., Laskey, R.A. and Thomas, J.O. (1980) Assembly of nucleosomes: the reaction involving X. laevis nucleoplasmin. *Cell,* 21, 373-383.

Finch, J.T., Lutter, L.C., Rhodes, D., Brown, R.S., Rushton, B., Levitt, M. and Klug, A. (1977) Structure of nucleosome core particles of chromatin. *Nature*, 269, 29-36.

Fujii-Nakata, T., Ishimi, Y., Okuda, A. and Kikuchi, A. (1992) Functional analysis of nucleosome assembly protein, NAP-1. The negatively charged COOH-terminal region is not necessary for the intrinsic assembly activity. J Biol Chem, 267, 20980-20986.

Georgel, P.T., Palacios DeBeer, M.A., Pietz, G., Fox, C.A. and Hansen, J.C. (2001) Sir3-dependent assembly of supramolecular chromatin structures in vitro. *Proc Natl Acad Sci* U S A, 98, 8584-9.

Georges, S.A., Kraus, W.L., Luger, K., Nyborg, J.K. and Laybourn, P.J. (2002) p300-mediated tax transactivation from recombinant chromatin: histone tail deletion mimics coactivator function. *Mol Cell Biol*, 22, 127-137.

Goodman, R.H. and Smolik, S. (2000) CBP/p300 in cell growth, transformation, and development. *Genes Dev*, 14, 1553-77.

Grayling, R.A., Sandman, K. and Reeve, J.N. (1996) Histones and chromatin structure in hyperthermophilic Archaea. *FEMS Microbiol Rev,* 18, 203-213.

Grunstein, M. (1997) Histone acetylation in chromatin structure and transcription. *Nature*, 389, 349-352.

Hartzog, G.A. and Winston, F. (1997) Nucleosomes and transcription: recent lessons from genetics. *Curr Opin Genet Dev,* 7, 192-8.

Hecht, A., Laroche, T., Strahl-Bolsinger, S., Gasser, S.M. and Grunstein, M. (1995) Histone H3 and H4 N-termini interact with SIR3 and SIR4 proteins: a molecular model for the formation of heterochromatin in yeast. *Cell*, 80, 583-592.

Horn, P.J. and Peterson, C.L. (2002) Molecular biology. Chromatin higher order folding--wrapping up transcription. *Science*, 297, 1824-7.

Hu, R.J., Lee, M.P., Johnson, L.A. and Feinberg, A.P. (1996) A novel human homologue of yeast nucleosome assembly protein, 65 kb centromeric to the

p57KIP2 gene, is biallelically expressed in fetal and adult tissues. *Hum Mol Genet*, 5, 1743-8.

Iizuka, M. and Smith, M.M. (2003) Functional consequences of histone modifications. *Curr Opin Genet Dev*, 13, 154-60.

Ilshimi, Y. and Kikuchi, A. (1991) Identification and molecular cloning of yeast homolog of nucleosome assembly protein I which facilitates nucleosome assembly in vitro. *J Biol Chem,* 266, 7025-7029.

Ishimi, Y., Hirosumi, J., Sato, W., Sugasawa, K., Yokota, S., Hanaoka, F. and Yamada, M. (1984) Purification and initial characterization of a protein which facilitates assembly of nucleosome-like structure from mammalian cells. *Eur J Biochem*, 142, 431-439.

Ishimi, Y., Kojima, M., Yamada, M. and Hanaoka, F. (1987) Binding mode of nucleosome-assembly protein (AP-I) and histones. *Eur J Biochem*, 162, 19-24.

Ishimi, Y., Sato, W., Kojima, M., Sugasawa, K., Hanaoka, F. and Yamada, M. (1985) Rapid purification of nucleosome assembly protein (AP-I) and production of monoclonal antibodies against it. *Cell Struct Funct*, 10, 373-82.

Ishimi, Y., Yasuda, H., Hirosumi, J., Hanaoka, F. and Yamada, M. (1983) A protein which facilitates assembly of nucleosome-like structures in vitro in mammalian cells. *J Biochem* (Tokyo), 94, 735-44.

Ito, T., Bulger, M., Kobayashi, R. and Kadonaga, J.T. (1996a) Drosophila NAP-1 is a core histone chaperone that functions in ATP- facilitated assembly of regularly spaced nucleosomal arrays. *Mol Cell Biol,* 16, 3112-3124.

Ito, T., Tyler, J.K., Bulger, M., Kobayashi, R. and Kadonaga, J.T. (1996b) ATP-facilitated chromatin assembly with a nucleoplasmin-like protein from Drosophila melanogaster. *J Biol Chem,* 271, 25041-25048.

Ito, T., Ikehara, T., Nakagawa, T., Kraus, W.L. and Muramatsu, M. (2000) p300-mediated acetylation facilitates the transfer of histone H2A-H2B dimers from nucleosomes to a histone chaperone. *Genes Dev,* 14, 1899-1907.

Ito, T., Tyler, J.K. and Kadonaga, J.T. (1997) Chromatin assembly factors: a dual function in nucleosome formation and mobilization? *Genes Cells*, 2, 593-600.

Jenuwein, T. and Allis, C.D. (2001) Translating the histone code. *Science*, 293, 1074-80.

Jones, S. and Thornton, J.M. (1996) Principles of protein-protein interactions. *Proc Natl Acad Sci* U S A, 93, 13-20.

Karantza, V., Freire, E. and Moudrianakis, E.N. (1996) Thermodynamic studies of the core histones: pH and ionic strength effects on the stability of the (H3-H4)/(H3-H4)2 system. *Biochemistry*, 35, 2037-2046.

Kaufman, P.D. (1996) Nucleosome assembly: the CAF and the HAT. *Curr Opin Cell Biol*, 8, 369-73.

Kaufman, P.D., Kobayashi, R., Kessler, N. and Stillman, B. (1995) The p150 and p60 subunits of chromatin assembly factor I: a molecular link between newly synthesized histones and DNA replication. *Cell,* 81, 1105-14.

Kelley, R.I. (1973) Isolation of a histone IIb1-IIb2 complex. *Biochem Biophys Res Commun*, 54, 1588-1594.

Kellogg, D.R. and Murray, A.W. (1995a) NAP1 acts with Clb1 to perform mitotic functions and to suppress polar bud growth in budding yeast. *J Cell Biol,* 130, 675-685.

Kellogg, D.R., Kikuchi, A., Fujii-Nakata, T., Turck, C.W. and Murray, A.W. (1995) Members of the NAP/SET family of proteins interact specifically with B- type cyclins. *J Cell Biol,* 130, 661-73.

Kimura, H. and Cook, P.R. (2001) Kinetics of core histones in living human cells: little exchange of H3 and H4 and some rapid exchange of H2B. *J Cell Biol,* 153, 1341-1353.

King, R.W., Jackson, P.K. and Kirschner, M.W. (1994) Mitosis in transition. Cell, 79, 563-71.

Kingston, R.E. and Narlikar, G.J. (1999) ATP-dependent remodeling and acetylation as regulators of chromatin fluidity. *Genes Dev,* 13, 2339-2352.

Kireeva, M.L., Walter, W., Tchernajenko, V., Bondarenko, V., Kashlev, M. and Studitsky, V.M. (2002) Nucleosome remodeling induced by RNA polymerase II: loss of the H2A/H2B dimer during transcription. Mol Cell, 9, 541-552.

Kleinschmidt, J.A., Dingwall, C., Maier, G. and Franke, W.W. (1986) Molecular characterization of a karyophilic, histone-binding protein: cDNA cloning, amino acid sequence and expression of nuclear protein N1/N2 of Xenopus laevis. *Embo J*, 5, 3547-52.

Kleinschmidt, J.A., Seiter, A. and Zentgraf, H. (1990) Nucleosome assembly in vitro: separate histone transfer and synergistic interaction of native histone complexes purified from nuclei of Xenopus laevis oocytes. *Embo J*, 9, 1309-18.

Kornberg, R.D. (1974) Chromatin structure: a repeating unit of histones and DNA. *Science*, 184, 868-871.

Kornberg, R.D. and Thomas, J.O. (1974) Chromatin structure; oligomers of the histones. *Science*, 184, 865-868.

Kouzarides, T. (2000) Acetylation: a regulatory modification to rival phosphorylation? *Embo J*, 19, 1176-9.

Krajewski, W.A. and Ausio, J. (1996) Modulation of the higher-order folding of chromatin by deletion of histone H3 and H4 terminal domains. *Biochem J*, 316, 395-400.

Krude, T. and Keller, C. (2001) Chromatin assembly during S phase: contributions from histone deposition, DNA replication and the cell division cycle. *Cell Mol Life Sci*, 58, 665-672.

Kuo, M.H., Zhou, J., Jambeck, P., Churchill, M.E. and Allis, C.D. (1998) Histone acetyltransferase activity of yeast Gcn5p is required for the activation of target genes in vivo. *Genes Dev*, 12, 627-39.

Lachner, M., O'Carroll, D., Rea, S., Mechtler, K. and Jenuwein, T. (2001) Methylation of histone H3 lysine 9 creates a binding site for HP1 proteins. *Nature*, 410, 116-120.

Lankenau, S., Barnickel, T., Marhold, J., Lyko, F., Mechler, B.M. and Lankenau, D.H. (2003) Knockout targeting of the Drosophila nap1 gene and examination of DNA repair tracts in the recombination products. *Genetics*, 163, 611-23.

Laskey, R.A., Honda, B.M., Mills, A.D. and Finch, J.T. (1978) Nucleosomes are assembled by an acidic protein which binds histones and transfers them to DNA. *Nature*, 275, 416-20.

Lebowitz, J., Lewis, M.S. and Schuck, P. (2002) Modern analytical ultracentrifugation in protein science: a tutorial review. *Protein Sci*, 11, 2067-79.

Lee, K.M. and Hayes, J.J. (1997) The N-terminal tail of histone H2A binds to two distinct sites within the nucleosome core. *Proc Natl Acad Sci* U S A, 94, 8959-64.

Liang, P. and MacRae, T.H. (1997) Molecular chaperones and the cytoskeleton. *J Cell Sci*, 110, 1431-1440.

Ling, X., Harkness, T.A., Schultz, M.C., Fisher-Adams, G. and Grunstein, M. (1996) Yeast histone H3 and H4 amino termini are important for nucleosome assembly in vivo and in vitro: redundant and position-independent functions in assembly but not in gene regulation. *Genes Dev*, 10, 686-99.

Litt, M.D., Simpson, M., Gaszner, M., Allis, C.D. and Felsenfeld, G. (2001a) Correlation between histone lysine methylation and developmental changes at the chicken beta-globin locus. *Science*, 293, 2453-5.

Litt, M.D., Simpson, M., Recillas-Targa, F., Prioleau, M.N. and Felsenfeld, G. (2001b) Transitions in histone acetylation reveal boundaries of three separately regulated neighboring loci. *Embo J,* 20, 2224-2235.

Lorch, Y., Zhang, M. and Kornberg, R.D. (1999) Histone octamer transfer by a chromatin-remodeling complex. *Cell*, 96, 389-92.

Luger, K. and Richmond, T.J. (1998a) DNA binding within the nucleosome core. *Curr Opin Struct Biol*, 8, 33-40.

Luger, K. and Richmond, T.J. (1998b) The histone tails of the nucleosome. *Curr Opin Genet Dev,* 8, 140-146.

Luger, K., Mader, A.W., Richmond, R.K., Sargent, D.F. and Richmond, T.J. (1997a) Crystal structure of the nucleosome core particle at 2.8 A resolution. *Nature*, 389, 251-260.

Luger, K., Rechsteiner, T.J. and Richmond, T.J. (1999a) Expression and purification of recombinant histones and nucleosome reconstitution. *Methods Mol Biol,* 119, 1-16.

Luger, K., Rechsteiner, T.J. and Richmond, T.J. (1999b) Preparation of nucleosome core particle from recombinant histones. *Methods Enzymol*, 304, 3-19.

Luger, K., Rechsteiner, T.J., Flaus, A.J., Waye, M.M. and Richmond, T.J. (1997b) Characterization of nucleosome core particles containing histone proteins made in bacteria. *J Mol Biol,* 272, 301-311.

Matthews, J.M. and Sunde, M. (2002) Zinc fingers--folds for many occasions. *IUBMB Life*, 54, 351-5.

McQuibban, G.A., Commisso-Cappelli, C.N. and Lewis, P.N. (1998) Assembly, remodeling, and histone binding capabilities of yeast nucleosome assembly protein 1. *J Biol Chem*, 273, 6582-6590.

Mills, A.D., Laskey, R.A., Black, P. and De Robertis, E.M. (1980) An acidic protein which assembles nucleosomes in vitro is the most abundant protein in Xenopus oocyte nuclei. *J Mol Biol*, 139, 561-8.

Moggs, J.G., Grandi, P., Quivy, J.P., Jonsson, Z.O., Hubscher, U., Becker, P.B. and Almouzni, G. (2000) A CAF-1-PCNA-mediated chromatin assembly pathway triggered by sensing DNA damage. *Mol Cell Biol*, 20, 1206-18.

Morales, V. and Richard-Foy, H. (2000) Role of histone N-terminal tails and their acetylation in nucleosome dynamics. *Mol Cell Biol*, 20, 7230-7.

Mosammaparast, N., Ewart, C.S. and Pemberton, L.F. (2002) A role for nucleosome assembly protein 1 in the nuclear transport of histones H2A and H2B. *Embo J*, 21, 6527-38.

Mosammaparast, N., Jackson, K.R., Guo, Y., Brame, C.J., Shabanowitz, J., Hunt, D.F. and Pemberton, L.F. (2001) Nuclear import of histone H2A and H2B is mediated by a network of karyopherins. *J Cell Biol*, 153, 251-62.

Muthurajan, U.M., Park, Y.J., Edayathumangalam, R.S., Suto, R.K., Chakravarthy, S., Dyer, P.N. and Luger, K. (2003) Structure and dynamics of nucleosomal DNA. *Biopolymers*, 68, 547-56.

Nakagawa, T., Bulger, M., Muramatsu, M. and Ito, T. (2001) Multistep chromatin assembly on supercoiled plasmid DNA by nucleosome assembly protein-1 and ATP-utilizing chromatin assembly and remodeling factor. *J Biol Chem*, 276, 27384-27391.

Namboodiri, V.M., Dutta, S., Akey, I.V., Head, J.F. and Akey, C.W. (2003) The Crystal Structure of Drosophila NLP-Core Provides Insight into Pentamer Formation and Histone Binding. *Structure* (Camb), 11, 175-186.

Nishiyama, N., Sawatsubashi, S., Ishida, M. and Yamauchi, K. (2001) Organization and expression of the Paramecium caudatum gene encoding nucleosome assembly protein 1. *Gene,* 280, 107-14.

Ogryzko, V.V., Schiltz, R.L., Russanova, V., Howard, B.H. and Nakatani, Y. (1996) The transcriptional coactivators p300 and CBP are histone acetyltransferases. *Cell,* 87, 953-9.

Oliva, R., Bazett-Jones, D.P., Locklear, L. and Dixon, G.H. (1990) Histone hyperacetylation can induce unfolding of the nucleosome core particle. *Nucleic Acids Res*, 18, 2739-47.

Pace, C.N., Vajdos, F., Fee, L., Grimsley, G. and Gray, T. (1995) How to measure and predict the molar absorption coefficient of a protein. *Protein Sci*, 4, 2411-23.

Parthun, M.R., Widom, J. and Gottschling, D.E. (1996) The major cytoplasmic histone acetyltransferase in yeast: links to chromatin replication and histone metabolism. *Cell,* 87, 85-94.

Pazin, M.J., Kamakaka, R.T. and Kadonaga, J.T. (1994) ATP-dependent nucleosome reconfiguration and transcriptional activation from preassembled chromatin templates. *Science*, 266, 2007-2011.

Perkins, S.J. (1986) Protein volumes and hydration effects. The calculations of partial specific volumes, neutron scattering matchpoints and 280-nm absorption coefficients for proteins and glycoproteins from amino acid sequences. *Eur J Biochem*, 157, 169-80.

Perry, C.A., Dadd, C.A., Allis, C.D. and Annunziato, A.T. (1993) Analysis of nucleosome assembly and histone exchange using antibodies specific for acetylated H4. *Biochemistry*, 32, 13605-14.

Philpott, A., Krude, T. and Laskey, R.A. (2000) Nuclear chaperones. *Semin Cell Dev Biol,* 11, 7-14.

Pilon, J., Terrell, A. and Laybourn, P.J. (1997b) Yeast chromatin reconstitution system using purified yeast core histones and yeast nucleosome assembly protein-1. *Protein Expr Purif,* 10, 132-40.

Prevelige, P.E., Jr. and Fasman, G.D. (1987) Structural studies of acetylated and control inner core histones. *Biochemistry*, 26, 2944-55.

Quinn, P.G. (2002) Mechanisms of basal and kinase-inducible transcription activation by CREB. *Prog Nucleic Acid Res Mol Biol*, 72, 269-305.

Recht, J. and Osley, M.A. (1999) Mutations in both the structured domain and N-terminus of histone H2B bypass the requirement for Swi-Snf in yeast. *Embo J*, 18, 229-40.

Regnard, C., Desbruyeres, E., Huet, J.C., Beauvallet, C., Pernollet, J.C. and Edde, B. (2000) Polyglutamylation of nucleosome assembly proteins. *J Biol Chem*, 275, 15969-15976.

Richmond, T.J. and Davey, C.A. (2003) The structure of DNA in the nucleosome core. *Nature*, 423, 145-50.

Richmond, T.J., Finch, J.T., Rushton, B., Rhodes, D. and Klug, A. (1984) Structure of the nucleosome core particle at 7 A resolution. *Nature*, 311, 532-537.

Richmond, T.J., Searles, M.A. and Simpson, R.T. (1988) Crystals of a nucleosome core particle containing defined sequence DNA. *J Mol Biol*, 199, 161-70.

Roark, D.E., Geoghegan, T.E. and Keller, G.H. (1974) A two-subunit histone complex from calf thymus. *Biochem Biophys Res Commun*, 59, 542-547.

Rodriguez, P., Munroe, D., Prawitt, D., Chu, L.L., Bric, E., Kim, J., Reid, L.H., Davies, C., Nakagama, H., Loebbert, R., Winterpacht, A., Petruzzi, M.J., Higgins, M.J., Nowak, N., Evans, G., Shows, T., Weissman, B.E., Zabel, B., Housman, D.E. and Pelletier, J. (1997) Functional characterization of human nucleosome assembly protein-2 (NAP1L4) suggests a role as a histone chaperone. *Genomics,* 44, 253-65.

Rodriguez, P., Pelletier, J., Price, G.B. and Zannis-Hadjopoulos, M. (2000) NAP-2: histone chaperone function and phosphorylation state through the cell cycle. *J Mol Biol*, 298, 225-238.

Roth, S.Y., Denu, J.M. and Allis, C.D. (2001) Histone acetyltransferases. *Annu Rev Biochem*, 70, 81-120.

Rundlett, S.E., Carmen, A.A., Suka, N., Turner, B.M. and Grunstein, M. (1998) Transcriptional repression by UME6 involves deacetylation of lysine 5 of histone H4 by RPD3. *Nature*, 392, 831-5.

Schuster, T., Han, M. and Grunstein, M. (1986) Yeast histone H2A and H2B amino termini have interchangeable functions. *Cell*, 45, 445-51.

Shibahara, K. and Stillman, B. (1999) Replication-dependent marking of DNA by PCNA facilitates CAF-1-coupled inheritance of chromatin. *Cell,* 96, 575-85.

Shibahara, K., Verreault, A. and Stillman, B. (2000) The N-terminal domains of histones H3 and H4 are not necessary for chromatin assembly factor-1-mediated nucleosome assembly onto replicated DNA in vitro. *Proc Natl Acad Sci* U S A, 97, 7766-7771.

Shikama, N., Chan, H.M., Krstic-Demonacos, M., Smith, L., Lee, C.W., Cairns, W. and La Thangue, N.B. (2000) Functional interaction between nucleosome

assembly proteins and p300/CREB-binding protein family coactivators. *Mol Cell Biol*, 20, 8933-8943.

Simon, H.U., Mills, G.B., Kozlowski, M., Hogg, D., Branch, D., Ishimi, Y. and Siminovitch, K.A. (1994) Molecular characterization of hNRP, a cDNA encoding a human nucleosome- assembly-protein-I-related gene product involved in the induction of cell proliferation. *Biochem J*, 297, 389-97.

Simon, R.H. and Felsenfeld, G. (1979) A new procedure for purifying histone pairs H2A + H2B and H3 + H4 from chromatin using hydroxylapatite. *Nucleic Acids Res*, 6, 689-96.

Smith, R.M. and Rill, R.L. (1989) Mobile histone tails in nucleosomes. Assignments of mobile segments and investigations of their role in chromatin folding. *J Biol Chem*, 264, 10574-81.

Smith, S. and Stillman, B. (1989) Purification and characterization of CAF-I, a human cell factor required for chromatin assembly during DNA replication in vitro. *Cell,* 58, 15-25.

Sobel, R.E., Cook, R.G., Perry, C.A., Annunziato, A.T. and Allis, C.D. (1995) Conservation of deposition-related acetylation sites in newly synthesized histones H3 and H4. *Proc Natl Acad Sci* U S A, 92, 1237-1241.

Sreerama, N. and Woody, R.W. (2000) Estimation of protein secondary structure from circular dichroism spectra: comparison of CONTIN, SELCON, and CDSSTR methods with an expanded reference set. *Anal Biochem*, 287, 252-260.

Stein, A. (1989) Reconstitution of chromatin from purified components. *Methods Enzymol,* 170, 585-603.

Stein, G.S., Van Wijnen, A.J., Montecino, M., Stein, J.L. and Lian, J.B. (1999) Nuclear structure/gene expression interrelationships. *J Cell Physiol,* 181, 240-250.

Strahl, B.D. and Allis, C.D. (2000) The language of covalent histone modifications. *Nature*, 403, 41-5.

Sullivan, S., Sink, D.W., Trout, K.L., Makalowska, I., Taylor, P.M., Baxevanis, A.D. and Landsman, D. (2002) The Histone Database. *Nucleic Acids Res*, 30, 341-2.

Terrell, A.R., Wongwisansri, S., Pilon, J.L. and Laybourn, P.J. (2002) Reconstitution of nucleosome positioning, remodeling, histone acetylation, and transcriptional activation on the PHO5 promoter. *J Biol Chem,* 277, 31038-47.

Thiriet, C. and Hayes, J.J. (2001) A novel labeling technique reveals a function for histone H2A/H2B dimer tail domains in chromatin assembly in vivo. *Genes Dev*, 15, 2048-2053.

Thomas, J.O. and Kornberg, R.D. (1978) The study of histone--histone associations by chemical cross-linking. *Methods Cell Biol*, 18, 429-40.

Tse, C., Fletcher, T.M. and Hansen, J.C. (1998) Enhanced transcription factor access to arrays of histone H3/H4 tetramer.DNA complexes in vitro: implications for replication and transcription. *Proc Natl Acad Sci* U S A, 95, 12169-73.

Tyler, J.K. (2002) Chromatin assembly. Cooperation between histone chaperones and ATP- dependent nucleosome remodeling machines. *Eur J Biochem,* 269, 2268-2274.

Tyler, J.K., Adams, C.R., Chen, S.R., Kobayashi, R., Kamakaka, R.T. and Kadonaga, J.T. (1999) The RCAF complex mediates chromatin assembly during DNA replication and repair. *Nature*, 402, 555-560.

Urnov, F.D. (2002) A feel for the template: zinc finger protein transcription factors and chromatin. *Biochem Cell Biol*, 80, 321-33.

Urnov, F.D. and Wolffe, A.P. (2001) Chromatin remodeling and transcriptional activation: the cast (in order of appearance). *Oncogene*, 20, 2991-3006.

Verreault, A. (2000) De novo nucleosome assembly: new pieces in an old puzzle. *Genes Dev*, 14, 1430-1438.

Verreault, A., Kaufman, P.D., Kobayashi, R. and Stillman, B. (1996) Nucleosome assembly by a complex of CAF-1 and acetylated histones H3/H4. *Cell,* 87, 95-104.

Walter, P.P., Owen-Hughes, T.A., Cote, J. and Workman, J.L. (1995) Stimulation of transcription factor binding and histone displacement by nucleosome assembly protein 1 and nucleoplasmin requires disruption of the histone octamer. *Mol Cell Biol,* 15, 6178-6187.

Wang, X., Moore, S.C., Laszckzak, M. and Ausio, J. (2000) Acetylation increases the alpha-helical content of the histone tails of the nucleosome. *J Biol Chem*, 275, 35013-20.

White, C.L., Suto, R.K. and Luger, K. (2001) Structure of the yeast nucleosome core particle reveals fundamental changes in internucleosome interactions. *Embo J,* 20, 5207-18.

Widlund, H.R., Vitolo, J.M., Thiriet, C. and Hayes, J.J. (2000) DNA sequence-dependent contributions of core histone tails to nucleosome stability: differential effects of acetylation and proteolytic tail removal. *Biochemistry*, 39, 3835-3841.

Wolffe, A.P. (1998) Packaging principle: how DNA methylation and histone acetylation control the transcriptional activity of chromatin. *J Exp Zool*, 282, 239-244. [pii].

Ye, X., Franco, A.A., Santos, H., Nelson, D.M., Kaufman, P.D. and Adams, P.D. (2003) Defective S phase chromatin assembly causes DNA damage, activation of the S phase checkpoint, and S phase arrest. *Mol Cell*, 11, 341-51.

Yoon, H.W., Kim, M.C., Lee, S.Y., Hwang, I., Bahk, J.D., Hong, J.C., Ishimi, Y. and Cho, M.J. (1995) Molecular cloning and functional characterization of a cDNA encoding nucleosome assembly protein 1 (NAP-1) from soybean. *Mol Gen Genet*, 249, 465-73.

Zheng, C. and Hayes, J.J. (2003) Structures and interactions of the core histone tail domains. *Biopolymers,* 68, 539-546.

Zimmerman, Z.A. and Kellogg, D.R. (2001) The Sda1 protein is required for passage through start. *Mol Biol Cell,* 12, 201-219.

Zucker, K. and Worcel, A. (1990) The histone H3/H4.N1 complex supplemented with histone H2A-H2B dimers and DNA topoisomerase I forms nucleosomes on circular DNA under physiological conditions. *J Biol Chem,* 265, 14487-96.